AD-A068 517 FIBER MATERIALS INC BIDDEFORD MAINE F/G 11/4
ADVANCED IMPACT RESISTANT MULTIDIMENSIONAL COMPOSITES.(U)
JAN 79 J W HERRICK N00019-77-C-0430
UNCLASSIFIED FR-79-1-3 NL

1 OF 2
AD
A068517

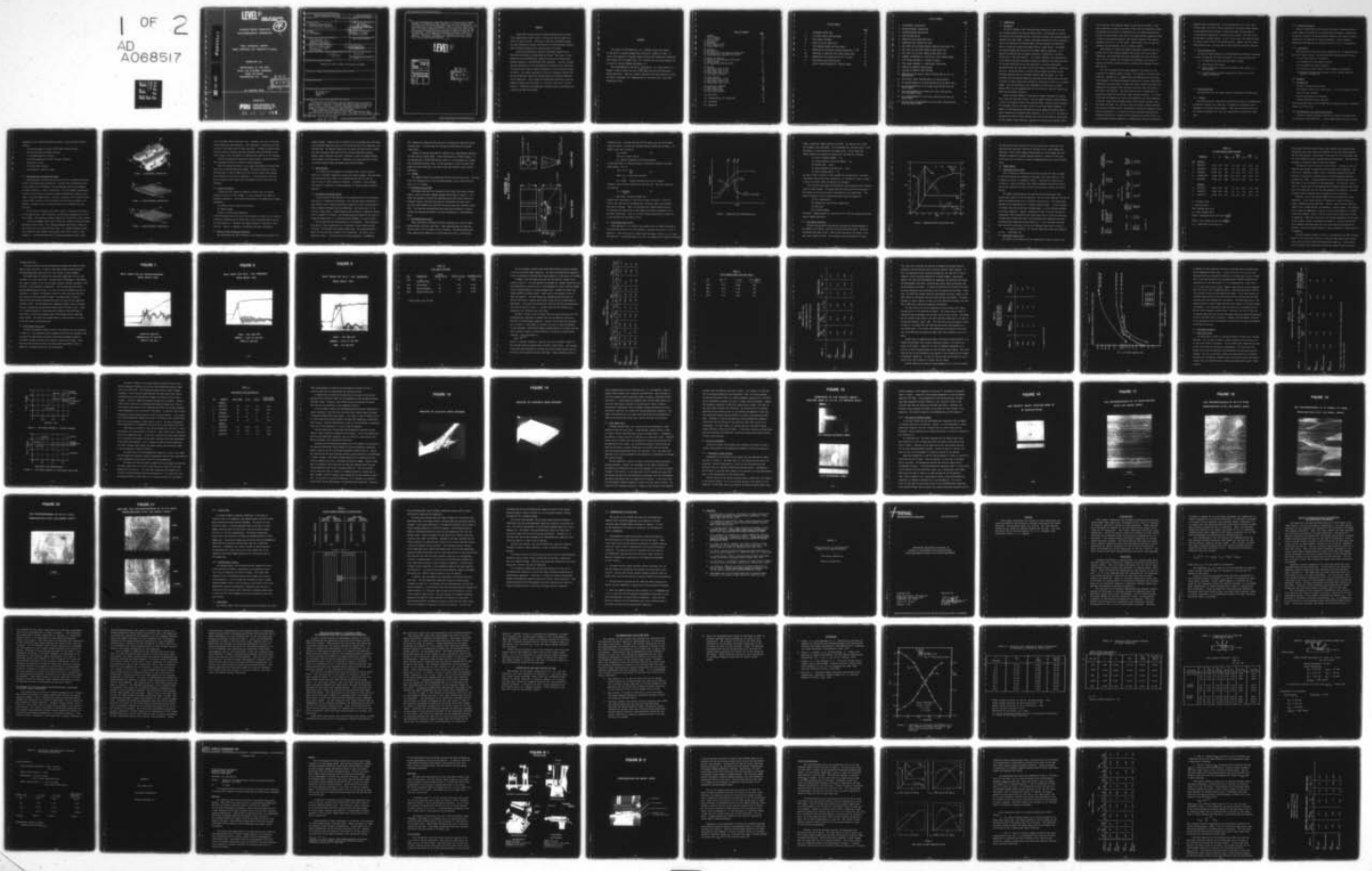

LEVEL II

4

ADVANCE IMPACT RESISTANT MULTIDIMENSIONAL COMPOSITES

FINAL TECHNICAL REPORT

NASC CONTRACT NO. N00019-77-C-0430

SUBMITTED TO:

DEPARTMENT OF THE NAVY
NAVAL AIR SYSTEMS COMMAND
CODE AIR-52032
WASHINGTON, D.C. 20361

30 JANUARY 1979

SUBMITTED BY

FIBER MATERIALS, INC.
BIDDEFORD INDUSTRIAL PARK
BIDDEFORD, MAINE 04005

SECURITY CLASSIFICATION OF THIS PAGE *(When Data Entered)*

REPORT DOCUMENTATION PAGE

READ INSTRUCTIONS BEFORE COMPLETING FORM

1. REPORT NUMBER	2. GOVT ACCESSION NO.
3. RECIPIENT'S CATALOG NUMBER (9)	
4. TITLE *(and Subtitle)* (6) Advanced Impact Resistant Multidimensional Composites.	5. TYPE OF REPORT & PERIOD COVERED Final Report. Oct 1977-Nov 1978
(14)	6. PERFORMING ORG. REPORT NUMBER FR-79-1-3
7. AUTHOR(s) (10) J.W. Herrick	8. CONTRACT OR GRANT NUMBER(s) (15) N00019-77-C-0430
9. PERFORMING ORGANIZATION NAME AND ADDRESS Fiber Materials, Inc. Biddeford Industrial Park Biddeford, Maine 04005	10. PROGRAM ELEMENT, PROJECT, TASK AREA & WORK UNIT NUMBERS
11. CONTROLLING OFFICE NAME AND ADDRESS (11) Naval Air Systems Command Washington, D.C. 20361 Code AIR 52032	12. REPORT DATE 30 January 1979 13. NUMBER OF PAGES
14. MONITORING AGENCY NAME & ADDRESS *(if different from Controlling Office)* (12) 128p.	15. SECURITY CLASS. *(of this report)* Unclassified
	15a. DECLASSIFICATION/DOWNGRADING SCHEDULE

16. DISTRIBUTION STATEMENT *(of this Report)*

Approved for public release; distribution unlimited.

17. DISTRIBUTION STATEMENT *(of the abstract entered in Block 20, if different from Report)*

18. SUPPLEMENTARY NOTES

19. KEY WORDS *(Continue on reverse side if necessary and identify by block number)*

Multidimensional
Composites
Impact

20. ABSTRACT *(Continue on reverse side if necessary and identify by block number)*

Conventional pseudo-isotropic advanced composites may be excessively damaged under certain kinds of low mass and velocity impact conditions on naval aircraft. Therefore, a materials development program has been conducted to evaluate the potential of multidimensional graphite fiber reinforced composites for improved impact resistance.

Several multidimensional graphite fiber-epoxy composites were fabricated and tested as flexure beams and plates. Both types of tests showed

DD FORM 1 JAN 73 1473 EDITION OF 1 NOV 65 IS OBSOLETE

408 254

LB

SECURITY CLASSIFICATION OF THIS PAGE *(When Data Entered)*

that the multidimensional composites possessed increased impact strength compared to two-dimensional (2D) composites. The data indicated that the construction of the multidimensional composite must be designed for the particular type of impact encountered in order to maximize impact resistance. Post impact examination of the test specimens indicated that the multidimensional composites absorbed energy by different mechanisms than 2D composites. The 2D composites delaminated extensively, while the composite fracture was restricted to a relatively small area in the 3D materials. Therefore, multidimensional composites absorb more energy over a smaller area than 2D laminates.

LEVEL II

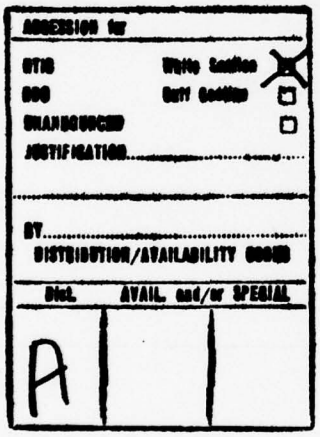

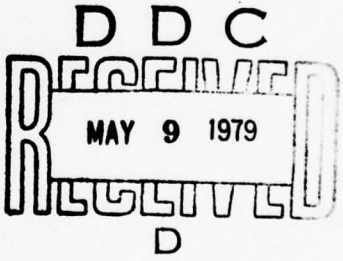

ABSTRACT

Conventional pseudo-isotropic advanced composites may be excessively damaged under certain kinds of low mass and velocity impact conditions on naval aircraft. Therefore, a materials development program has been conducted to evaluate the potential of multidimensional graphite fiber reinforced composites for improved impact resistance.

Several multidimensional graphite fiber-epoxy composites were fabricated and tested as flexure beams and plates. Both types of tests showed that the multidimensional composites possessed increased impact strength compared to two-dimensional (2D) composites. The data indicated that the construction of the multidimensional composite must be designed for the particular type of impact encountered in order to maximize impact resistance. Post impact examination of the test specimens indicated that the multidimensional composites absorbed energy by different mechanisms than 2D composites. The 2D composites delaminated extensively, while the composite fracture was restricted to a relatively small area in the 3D materials. Therefore, multidimensional composites absorb more energy over a smaller area than 2D laminates.

Foreword

This report by Fiber Materials, Inc., Biddeford, Maine was prepared for the Naval Air Systems Command under Contract No. N00019-77-C-0430. It covers work conducted on "Advanced Impact Resistant Multidimensional Composites" from October 1977 to November 1978. Mr. M. Stander was the Project Manager for the Naval Air Systems Command, Washington, D.C.

The Program Manager at FMI was Mr. John Herrick. Mr. James Crawford, Jr., Manager of Woven Products Division at FMI, supervised the multidimensional weaving operations. Materials Sciences Corporation provided analytical services and Effects Technology, Inc. conducted most of the impact tests, both under subcontract to FMI.

Table of Contents

LIST OF TABLES

LIST OF FIGURES

1.0 INTRODUCTION

1.1 Background

The use of graphite fiber reinforced epoxy composites on Naval Aircraft has increased rapidly over the past several years. The increase is primarily the result of this advanced material's excellent stiffness and strength properties combined with light weight. However, the impact resistance of these composites may not be sufficient to withstand some of the anticipated field conditions, such as a hand tool dropped from several feet or runway stones. Furthermore, the problem becomes more severe with the higher modulus composites. It is generally recognized that the impact resistance of composites is inversely proportional to the fiber modulus. It is clear, therefore, that the questions of the impact properties and damage tolerance of graphite fiber composites must be resolved before they can be used extensively in aircraft applications. Considerable work has been done to define the extent of the problem. Adsit and Waszczak studied the effect of various types of impact conditions on both honeycomb supported and rib stiffened graphite composite panels. (1) They concluded that considerable damage was sustained by the laminate even with very low levels of impact energy which resulted in just barely visible or non-visible damage. They also pointed out that interlaminar failure usually occurred between $\pm 45^{o}$ plies and suggested that the use of bias cut cloth for these plies might increase impact resistance.

Several possible methods of increasing the impact resistance of graphite fiber composites have been studied. The most common technique involves adding a second, lower modulus fiber to the graphite fibers, making a hybrid composite. This secondary fiber can be glass, Kevlar or even lower modulus graphite. A number of investigators have reported that hybrid composites possess superior impact strength to all-graphite fiber composites. (2, 3, 4, 5, 6) The extent of the beneficial effect of the secondary fiber varies with composite construction and test method. Some researchers reported that locating the secondary fibers

on the outside of the composite tended to yield the best results. (2,4) Other researchers located the secondary fibers within the composites, either as separate plies or mixed in individual plies, and obtained good results. (3,5,6) The span-to-depth (S/D) ratio of the beam specimens appeared to have an effect on the desired location, with exterior secondary fiber location preferred at high (i.e. 16) S/D ratios. Other factors, such as fiber concentration and orientation, also can influence results.

Other efforts to improve the impact resistance of graphite fiber composites are 1) fiber surface treatment and coating, and 2) resin matrix toughening. Both techniques have been investigated with some limited success. (6,7,8) However, the introduction of different resin systems as coatings on matrices creates properties and fabrication problems for many applications.

The final technique that has been suggested is the effect of fiber orientation on composite impact strength. This approach is also the least developed. Bradshaw et.al. suggested that multidimensional (or 3D) fiber reinforcement be investigated because of potentially increased interlaminar strength and fracture energy. (2) These RAE authors staked conventional two-dimensional (2D) graphite fiber laminates with glass fiber pins normal to the plane of the laminate. They found that the area of delamination was reduced upon impact and the residual shear strength increased. It is noteworthy that the composite was both a multidimensional and hybrid composite. In another study, Novak stitched through plies of boron and glass fibers with Kevlar 49 fibers. (6) Ballistic tests with gelatin spheres indicated that the third direction Kevlar reinforcement increased the composites resistance to delamination. In an analytical study, Greszczuk calculated the threshold velocities to initiate tensile, compressive and shear failures in several pseudo-isotrapic composites, including glass, boron and high modulus

graphite fiber reinforced epoxy. (9) He concluded that for a thick, semi-infinite plate, the initial failure should be by sub-surface shear stresses. If the composite shear strength is sufficiently high, the next mode of failure would be compression or crushing at the surface. The least likely failure mode is surface tension. If this is true, then a 3D composite would be ideally suited to resist the imposed stresses. However, for thin plates where bending occurs, in-plane tensile forces should be much more important.

1.2 Prior Studies at FMI

An earlier program conducted at FMI demonstrated the potential advantages of using 3D composites for impact resistance. (10) It was concluded that:

(1) 3D composites may have increased impact strength,

(2) delaminations were reduced,

(3) impact strength was related to longitudinal fiber volume in a beam specimen,

(4) a Kevlar-graphite 3D hybrid composite was superior to an all-graphte 3D composite.

1.3 Program Objectives

The program plan for the current contract included the following tasks:

1.3.1 Testing

The FMI falling ball tester would be modified according to recommendations by Materials Sciences Corp. (MSC) and, if necessary, be replaced by other equipment or an outside testing company. After some preliminary testing at FMI, Effects Technology, Inc. (ETI) was subcontracted to perform all impact tests.

1.3.2 Design and Analysis

MSC was subcontracted by FMI to perform analyses on optimum multidirectional composite constructions for maximum impact resistance. Another task for MSC was to design a 2D pseudo-isotropic composite that could be directly compared to a 3D composite for impact performance. A major problem in designing the 2D composite was selecting the basis of 2D vs. 3D comparison.

1.3.3 Fabrication

FMI would fabricate multidirectional composites and a 2D comparative composite for impact testing. The multidirectional composites would include:

(1) 3D, 4D and higher D, if possible,

(2) orthogonal and non-orthogonal designs,

(3) all-graphite and hybrid composites,

(4) evaluation of fiber angles for non-orthogonal constructions,

(5) advanced multidimensional concepts, such as combined 3D/2D and automatic loom woven 3D.

2.0 MATERIALS

2.1 Raw Materials

The basic raw materials used were:

T300 graphite fibers (Union Carbide Corp.) - with resin compatible finish

Kevlar 49 fibers (DuPont)

Rigidite 5208 epoxy resin (Hercules)

Rigidite 5208/T300 pre-preg (Hercules)

The Rigidite 5208 epoxy resin and 5208/T300 pre-preg were stored in sealed containers at $0^{o}F$ until use.

2.2 Two-Dimensional (2D) Composite Fabrication

2D control panels were molded according to a design calculated by MSC. The lay-up was $\{ 0_2^{o}/\pm 45_2^{o}/90^{o} \}_s$. Rigidite 5208/T300 pre-preg was cut into

appropriate sizes, stacked according to the MSC lay-up and press molded as follows:

(a) pre-preg heated in press to 135°C under contact pressure,

(b) held 50 minutes at contact pressure,

(c) increased pressure to 90 psi,

(d) raised temperature to 177°C in about 15 minutes,

(e) held for 2 hours,

(f) cooled under pressure,

(g) postcured at 400°F for 4 hours.

2.3 Multidimensional Composite Fabrication

Multidimensional pre-forms were woven with dry yarn (graphite and Kevlar) by FMI's proprietary weaving techniques. The basic woven constructions used in the program were 3D orthogonal, 3D non-orthogonal and 4D non-orthogonal, as shown in figures 1, 2 and 3, respectively. The 3D orthogonal construction, in which all the fibers are located at mutually perpendicular angles to each other, is the most common design. The basic variations in this design are the relative ratio of fibers in the 3 directions and the center-to-center (c-c) spacing. In general, the c-c spacing for most of the composites was near 0.05 inch.

For the sake of convention, the fibers located in the plane of the panel will be taken as the X and Y direction, and the fibers perpendicular will be the Z fibers. The direction of impact loading will be parallel to the Z fibers.

In the non-orthogonal panels, the Z fibers are located at some angle other than 90° to the X-Y plane. For a 3D/non-orthogonal construction (Figure 2), the Z fibers are at an angle θ to this plane. In a 4D/non-orthogonal design, the Z fibers are split equally into Z_1 and Z_2, both at θ° to the X-Y plane (Figure 3). It should be noted that in these non-orthogonal weaves, there

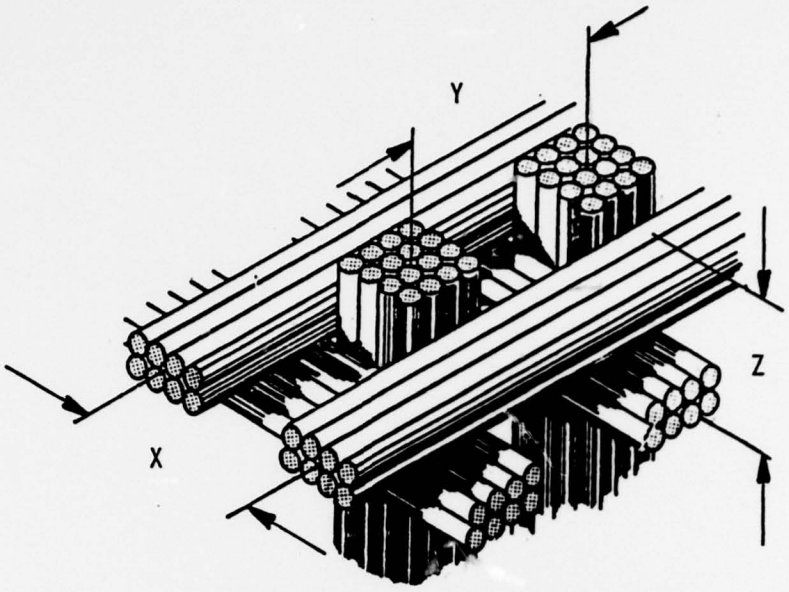

FIGURE 1. 3D/ORTHOGONAL CONSTRUCTION

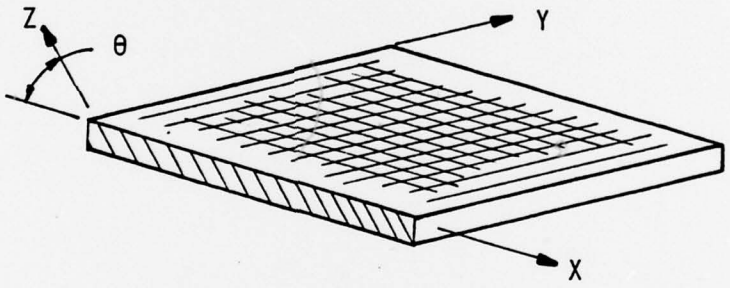

FIGURE 2. 3D/NON-ORTHOGONAL CONSTRUCTION

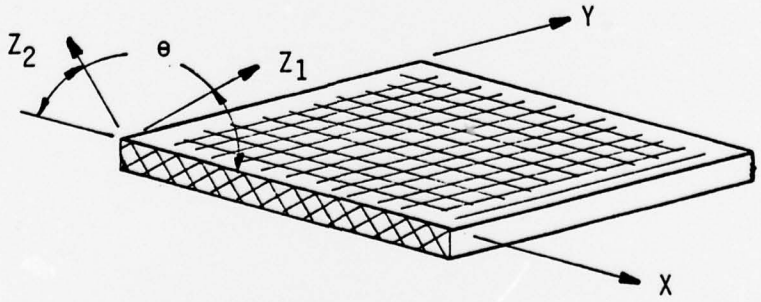

FIGURE 3. 4D/NON-ORTHOGONAL CONSTRUCTION

are no off-angle fibers along the Y axis. Therefore, the X and Y directions cannot possess the same properties. This difference in properties will show up later in the impact data for beams and plates. Although consideration was given to weaving a 6D panel with equal off-angle fiber distribution in the X and Y axes, it was not possible to fabricate this material on this program.

Several 4D preforms were woven with varying angles, ranging from 15^{o} to 60^{o}, to evaluate the effect of angle on impact properties.

After the preform was woven, it was vacuum infiltrated with molten 5208 epoxy resin system and then press molded. The molding conditions closely followed those for the 2D composite so that the resin matrix would possess the same degree of cure for all composites. It was essential to hold the matrix constant so that impact data would depend solely on the fiber reinforcement.

3.0 Design and Analysis

A subcontract was signed with Materials Sciences Corp. to provide analytical services for this program. A copy of the MSC Final Report is attached as Appendix A. MSC treated three aspects of 3D composites for impact performance:

(1) effect of fiber volume and orientation

(2) hybrid systems

(3) 4D vs. 2D equivalent composites

In the MSC analyses the plane of the flat composites is taken as Y-Z, with the Y direction containing the off-angle fibers, and the direction normal to the Y-Z plane taken as X. Therefore, the impact direction is parallel to the X direction. Figure 1 in Appendix A illustrates the fiber orientations.

3.1 Effect of Fiber Volume and Orientation

MSC assumed that the shear properties of the laminate are related to its

impact strength. Composite elastic properties for 2D laminates were calculated by the MSC-CLAM composites code, and for multidirectional (X-D) composites, the MSC-XCAP code. The analyses showed that the impact resistance should increase with both increasing fiber angle and fiber volume through the thickness. However, these conditions also cause a decrease in buckling strength because of the removal of in-plane fibers. Therefore, it was concluded that a trade-off existed between impact performance and buckling strength.

3.2 Hybrid Systems

It is known that the addition of a secondary fiber, such as glass or Kevlar 49, to graphite composites increases the impact strength. MSC calculated that substituting the X fibers in a 4D composite with Kevlar 49 did not greatly reduce in-plane structural properties. Therefore, it was concluded that hybrid X-D composites are good candidates for improved impact resistant materials.

3.3 2D Comparative Laminate Design

A major problem at the beginning of the program that had to be solved was the design of a comparative 2D laminate. This laminate must be comparable in some realistic way to the multidirectional composite so that a true measure of impact strength improvement could be determined. One obvious basis of comparison is equal weight. Another method could be based on a composite property such as strength or stiffness. MSC selected buckling strength as the basis of comparison because this is an important design parameter in aircraft panels.

FMI provided MSC with the properties of a 4D composite. These properties were density, fiber concentration in 4 directions, X-fiber angle and panel thickness. MSC designed a 2D laminate construction that possessed approximately the same buckling strength as the 4D composite. The results are in Appendix A, where a 2D construction of $(0^{o}_{2}/\pm 45^{o}_{2}/90^{o})$ is recommended.

This laminate was molded and forms the basis of comparative impact testing for the beam tests. A similar panel was designed and fabricated for the plate impact tests.

Another 2D laminate was molded for comparison to a 3D/orthogonal composite. The basis here was equal weight. The 2D construction was $0^{o}/90^{o}$ crossply. It was reasoned that a $0^{o}/90^{o}$ laminate was similar to a 3D/orthogonal but without the through-the-thickness fibers. By testing panels of equal thickness (and weight at similar densities), the value of the 3rd direction fibers could be determined.

4.0 TESTING

The composite impact test program was divided into two major parts. The first tests were conducted on 0.5 inch wide beam specimens, and a second series of tests on 5" x 5" plates.

4.1 Preliminary Tests at FMI

Preliminary data were first obtained on FMI's Model 1323 Instron Testing machine, using a one piece aluminum specimen holder shown in Figure 4. This holder was designed to restrain the specimen during rapid center loading and eliminate spurious vibrations that may have interferred with prior tests. The fixed span-to-depth (S/D) ratio was 5 and test speed was 5 feet per second (FPS). The load-time and deflection-time traces were recorded on a digital Nicholet oscilloscope with memory, and then transcribed as a load-deflection curve.

4.2 Beam Impact Tests at ETI

Impact testing was conducted by Effects Technology, Inc. (ETI) on their Dynatup machine using the guide tower. Short beam specimens were machined from the panels with the length in the X direction. The beam specimens were simply supported and impacted in a 3 point bend test with a 1.5 pound mass

FIGURE 4
BEAM SPECIMEN HOLDER

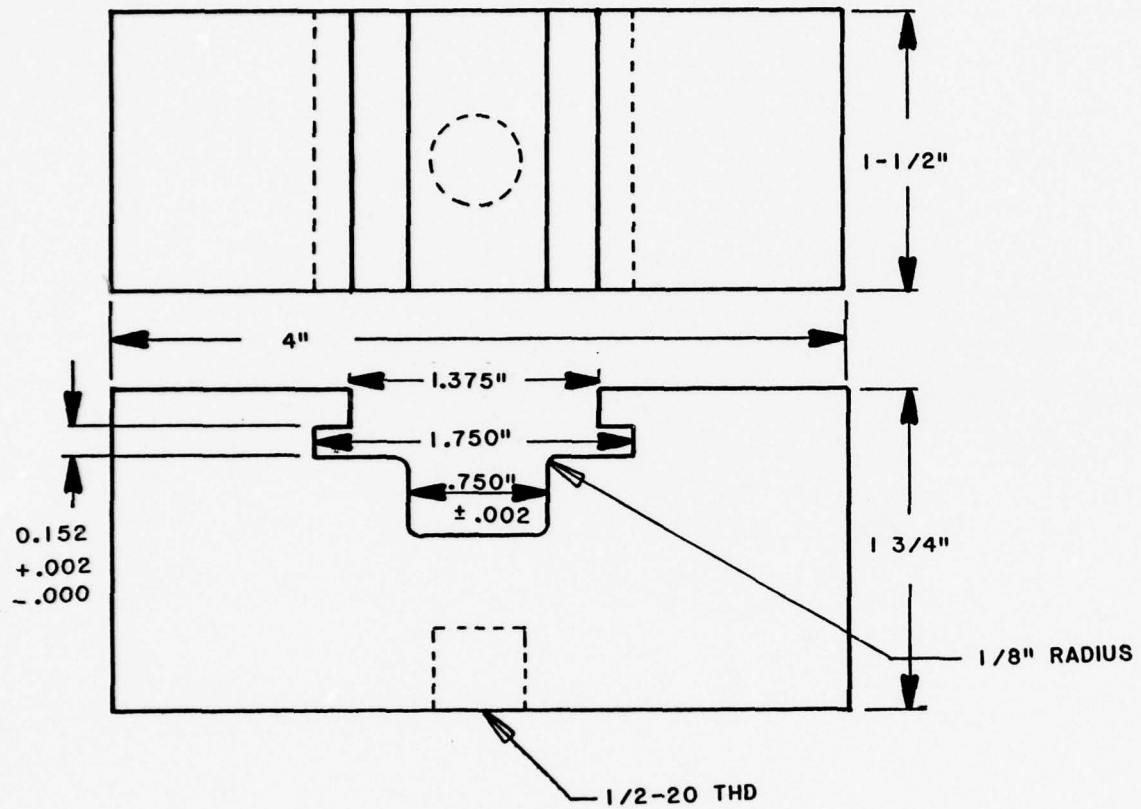

REACTION FRAME

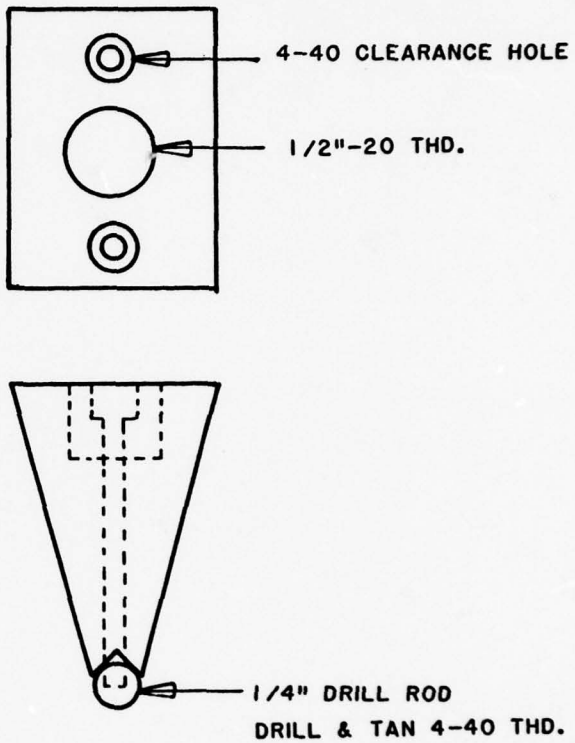

LOADING NOSE

at 10-20 ft./sec. The data obtained form the impact tests are oscilloscope traces of load vs. time and the integrated energy absorbed during impact. The energy at any time is given by:

$$E_a = V_o \int P dt \qquad (1)$$

where V_o = impact velocity

E_a = energy integrated by the Dynatup machine

A correction factor is required because of the velocity change of the head during impact. This is:

$$\Delta E_o = E_a \left(1 - \frac{E_a}{4E_o}\right) \qquad (2)$$

where ΔE_o = actual enery absorbed

$E_o = \frac{1}{2} MV_o^2$ (energy available just prior to impact)

In general, the correction factors were less than 10%. The shear stress was calculated by:

$$\sigma_s = \frac{0.75\ Pmax}{Area} \qquad (3)$$

where Pmax = maximum recorded load

A generalized load-energy vs. time trace is shown in Figure 5. The first break on the load curve is designated Pinc (incipient load), and indicates the onset of fracture. Pmax is the maximum load recorded during the test. Einc and Emax are those points on the energy curve which correspond to Pinc and Pmax, respectively. E_{tot} is the total energy absorbed during fracture up to the time when the load drops to zero.

4.3 Plate Impact Tests at ETI

Plate specimens 5" x 5" square, were tested at ETI for impact performance. A detailed description of the test equipment, procedure and results is given in Appendix B. The flat plate was clamped around the edges, leaving a 3" x 3" area for impacting. A crosshead wieght of 137 lbs. was dropped from a height of three (3)

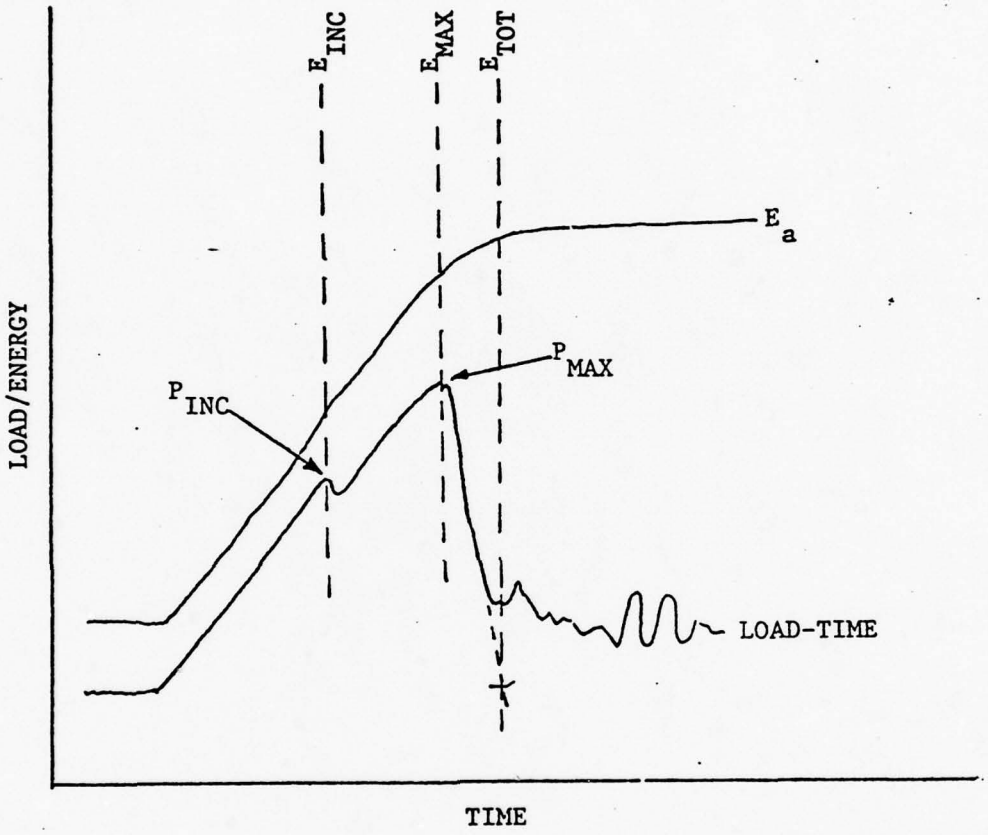

FIGURE 5. GENERALIZED DATA TRACES-BEAM TESTS

inches, yielding an impact velocity of 3.9 FPS. The impactor was a 0.625 inch diameter steel hemisphere. The instrumented tup provided load vs. time and energy vs. time histories of the impact event. The ETI Model 300 System recorded and analyzed the impact data, including the following:

(1) load at incipient damage = P_I

(2) energy absorbed to incipient damage = E_I

(3) maximum load = Pmax

(4) energy absorbed to maximum load = Emax

(5) total absorbed energy = E_T

The type of data is similar to that produced for the beam tests. An actual load-energy trace for the thru -penetration of a 2D plate is shown in Figure 6, where the various loads and energies are indicated.

Four replicate test plates of each material were exposed to four different levels of impact energy. The energy imput was controlled by placing stops in the machine to restrict the depth of penetration by the impact head. The levels of energy in order of decreasing impact energy correspond to:

(1) thru penetrations,

(2) between peak load and thru -penetration,

(3) peak load,

(4) incipient damage.

Therefore, a damage gradient was obtained for each material spanning the entire range of damage mechanisms.

4.4 Post-Impact Evaluation

Selected impacted plate specimens were evaluated by photomicrographs of the damaged cross-section, ultrasonic testing and flexure tests. The photomicrographs were taken at 50X - 160X of cross-sections at the center of the panel where impact occurred. The ultrasonic tests were primarily B-scans.

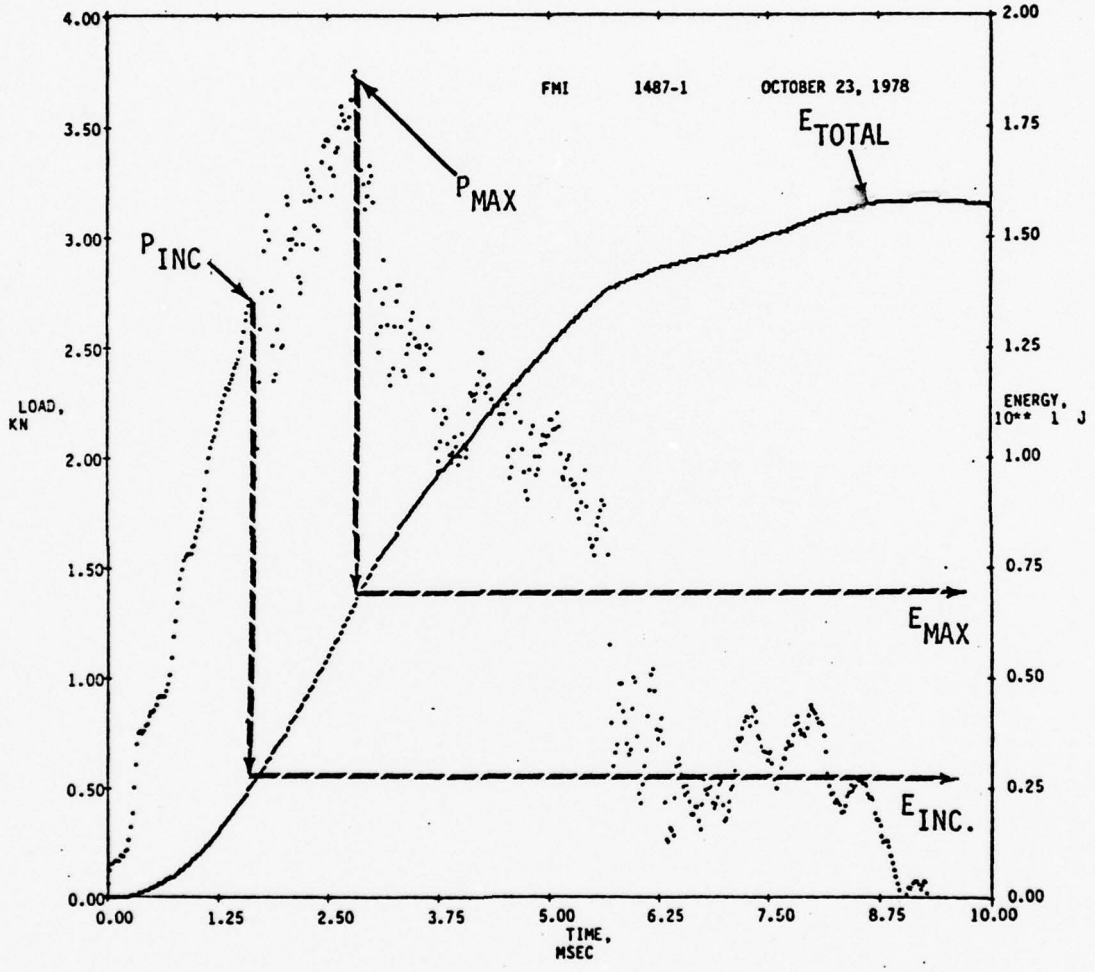

FIGURE 6. GENERALIZED DATA TRACES-PLATE TESTS

The flexure tests were obtained on 0.25 inch wide strips sliced with a diamond saw across the panel, starting at the edge of the visible damage area. Therefore, if non-visible damage occured beyond the visible damage area, the decrease in mechanical strength should be measured. Narrow 0.25 inch wide strips were cut in an effort to identify damage gradients away from the impact point.

5.0 IMPACT RESULTS

5.1 Preliminary Tests at FMI

Four (4) materials fabricated and previously tested for impact strength at FMI were selected for evaluation on the Model 1323 Instron Tester, (10). A summary of results is presented in Table I. The physical properties are in Table Ia. Table Ib contains prior impact strengths along with new flexure impact data reported as initial and final failure stress, modulus and time to failure.

The impact strength data do not show that the multidimensional composites were superior to the 2D composites. One of the 2D composites (P/N 001-37) should be omitted because of its relatively high S/D ratio. This would cause the beam to be loaded primarily in flexure instead of shear. If this specimen is omitted, then the Instron data indicated there is little difference between the various composites. However, inspection of Table Ia reveals that the 2D longitudinal fiber concentration was almost twice that of 3D and 4D composites. If these fiber volumes were equal, the multidimensional composites would have exhibited better comparative impact properties. It was concluded from these data that the Instron Tester did not yield adequate impact data in order to [illegible]te the materials properly. All further impact tests were then conducted by Effects Technology, Inc.

5.2 Beam Impact Tests at ETI

The results of the impact tests are summarized in Table II, which lists

TABLE I

PRELIMINARY IMPACT DATA

Table Ia

Physical Properties

SPECIMEN	CONSTRUCTION	DENSITY (gr/cc)	THICKNESS (in.)	LONGITUDINAL FIBER VOLUME (%)
2270	3D/Hybrid/θ=45^{o}	1.45	0.138	23
001-51	2D (0^{o}/90^{o})	1.55	0.153	37
2271	4D/θ=$\pm$32^{o}	1.47	0.111	20
001-37	2D (0^{o}/90^{o})	1.52	0.078	40

Table Ib

Impact Properties

SPECIMEN	S/D	IMPACT * STRENGTH ft-lb / in 4	FAILURE STRESS (ksi) INITIAL	FINAL	MODULUS 10^6 psi	TIME TO FAILURE (MS.)
2270	5.6	188	60	97	2.3	6.5
001-51	4.9	269	67	91	2.8	5.8
2271	6.8	146	57	82	2.7	5.3
001-37	9.6	400	103	111	4.2	4.6

* From Ref. 10

TABLE II

ETI IMPACT RESULTS-BEAM SPECIMENS

NO.	COMPOSITE	t	ρ	P_{max}	σ_s	$\frac{E_{max}}{A}$	C.V.	$\frac{E_{tot}}{A}$	C.V
	SERIES A								
1.	4D/θ=±32°	0.111	1.47	737	9.5	14.0	4.3	19.4	9.4
2.	2D/PSEUDO-	0.070	1.51	297	6.5	2.6	12.0	6.3	31.6
3.	3D/ORTHO-	0.150	1.47	737	7.3	15.9	15.5	21.7	11.6
4.	2D/CROSS-PLY	0.150	1.55	1070	10.5	12.5	8.9	15.6	9.5
5.	4D/θ=±45°	0.098	1.43	538	8.4	10.4	22.6	17.2	14.3
	SERIES B								
6.	4D/θ=±60°	0.150	1.55	514	5.2	10.5	18.6	15.5	10.9
7.	4D/θ=±45°	0.150	1.59	468	4.7	5.8	9.2	16.8	9.5
8.	4D/θ=± 15°	0.150	1.56	661	6.6	12.0	32.8	22.1	7.6

t = Thickness (inch)

ρ = Density (gr/cc)

P_{max} = Maximum Load (lbs.)

σ_s = Shear Strength (KSI)

E_{max}/A = Maximum Energy per Unit Area $(\frac{ft\text{-}lb}{inch^2})$

E_{tot}/A = Total Energy per Unit Area $(\frac{ft\text{-}lb}{inch^2})$

C.V. = Coefficient of Variation (%)

the maximum load during impact (Pmax), shear strength (σ_s), maximum energy absorbed per unit cross-section area (Emax/A) and the total energy absorbed per unit area (E_{tot}/A). Coefficients of variation (C.V.) for the energy data are also included, as well as specimen density and thickness. Each data point represents a minimum of three (3) tests per material.

The data are listed in two sets, series A and B. In series A, five (5) materials were tested, including two 2D, one 3D and two 4D composites. The first set of composites, numbers 1 and 2, represents comparative 4D and 2D laminates, respectively, and were based on a design prepared by Materials Sciences Corp. (MSC). The beam specimens for the 2D laminates were cut with the length in the 0^o direction of the molded panel. The resulting data in Table II indicate that the multidimensional 4D composite absorbed about 200% more total energy per unit area than the comparative 2D composite. The shear strength of the 4D composite was also higher than the 2D laminate.

Specimens 3 and 4 show another comparison of multidimensional and 2D composites. In this case, the basis of comparison is equal thickness or weight, assuming equivalent densities. Actually, the 2D laminate (specimen number 4) has a higher density, and therefore, a greater weight. The construction of these two composites is similar in that the 2D composite is a $0^o/90^o$ cross-plied laminate, which is similar to the in-plane construction of the 3D composites. About 10% of the fibers are located perpendicular to the plane of the 3D panel, making an orthogonal 3D composite. The data indicate that the 3D composite absorbed almost 40% more total impact energy than the 2D laminate. The shear strength, however, of the 2D laminate is greater than the 3D composite.

The final material tested in series 1, a 4D composite with $\pm 45^o$ off-angle fibers in the Z direction, exhibits a relatively high absorbed total energy value, but less than the other multidimensional composites. Other factors, such as relative fiber volume per direction and composite density may have

influenced the data.

The second series of tests was conducted to evaluate the effect of fiber angle in the Z direction. A trend is seen toward higher absorbed energies with decreasing fiber angle, but with little change in shear strength.

The coefficients of variation for these data ranged from 7.6% to 31.6%, with most C.V.'s near 10% or less. Several actual load-energy vs. time traces are shown in Figures 7-9 for the 2D pseudo-isotropic laminate, the 4D/θ = $\pm$ 32^{o} and 4D/θ = $\pm$ 45^{o} composites, respectively. The load-time trace for the 2D pseudo-isotropic laminate (Figure 7) is seen to be quite different from the 4D composites. In general, 2D composites exhibit a linear load-time trace that falls quickly to near zero after fracture. The data traces in Figure 7 indicate that the specimen is delaminating under low load, but not completely breaking in half. The multidimensional composites normally show an incipient fracture, followed by some additional loading before falling to zero. Figure 9 is a typical example of a multidimensional composite load and energy vs. time history is which the specimen supports the maximum load for some time before failure. The resulting absorbed energy is higher because it is equal to the area under the load-time curve.

5.3 Plate Impact Tests at ETI

The four (4) composites impact tested as flat plates by ETI are described in Table III. The 2D pseudo-isotropic composite (P/N 1487) was designed by MSC to possess the same buckling strength as the 4D/non-orthogonal composite (P/N 4238), assuming a normal resin content of about 35% by weight. Since the actual resin content was 27%, the actual buckling strength of the 2D composite is probably greater than the 4D composite.

FIGURE 7

DATA TRACE FOR 2D PSEUDO-ISOTROPIC BEAM IMPACT TEST

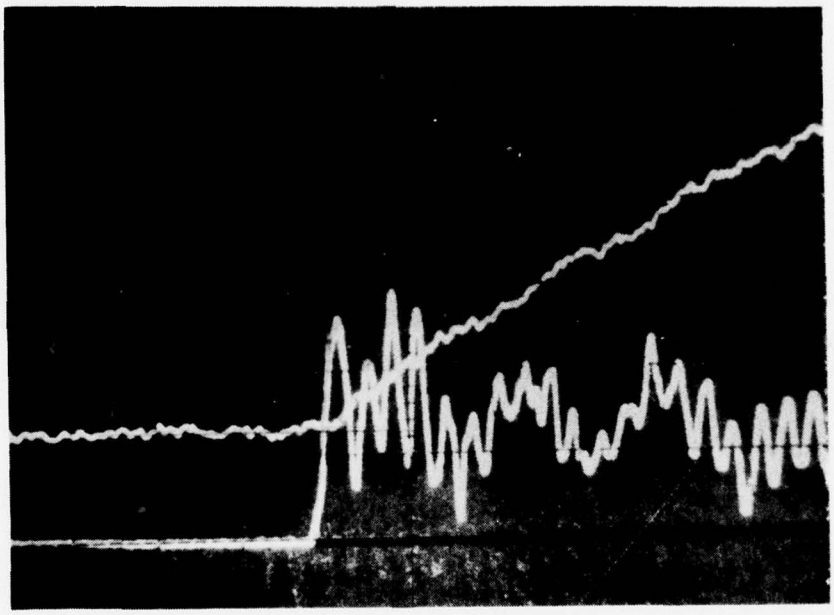

LOAD=100 LBS./DIV.

ENERGY=0.52 FT.-LB./DIV.

TIME=0.2 MS./DIV.

FIGURE 8

DATA TRACE FOR 4D/θ = ±32° COMPOSITE

BEAM IMPACT TEST

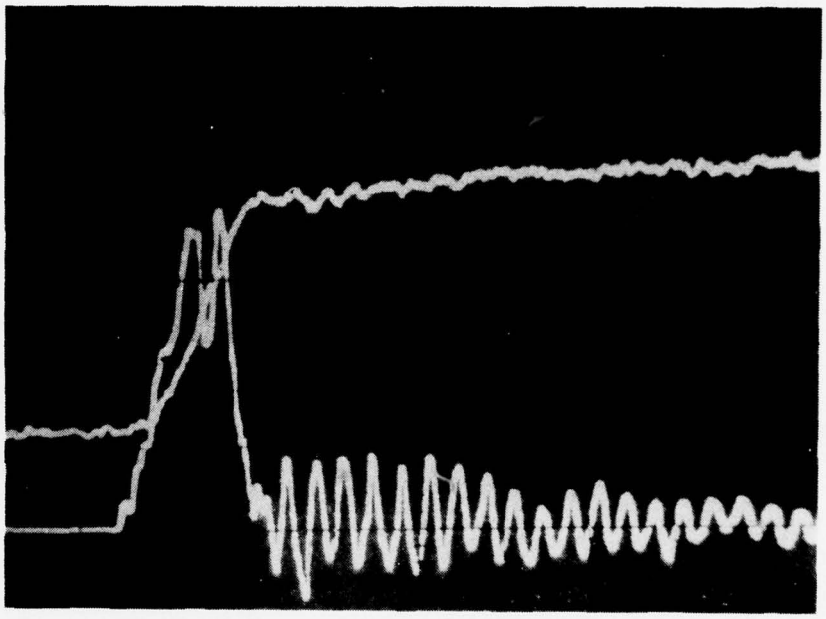

LOAD = 200 LBS./DIV.

ENERGY = 0.48 FT.-LB./DIV.

TIME= 0.2 MS./DIV.

FIGURE 9

DATA TRACE FOR 4D/θ = ±45° COMPOSITE

BEAM IMPACT TEST

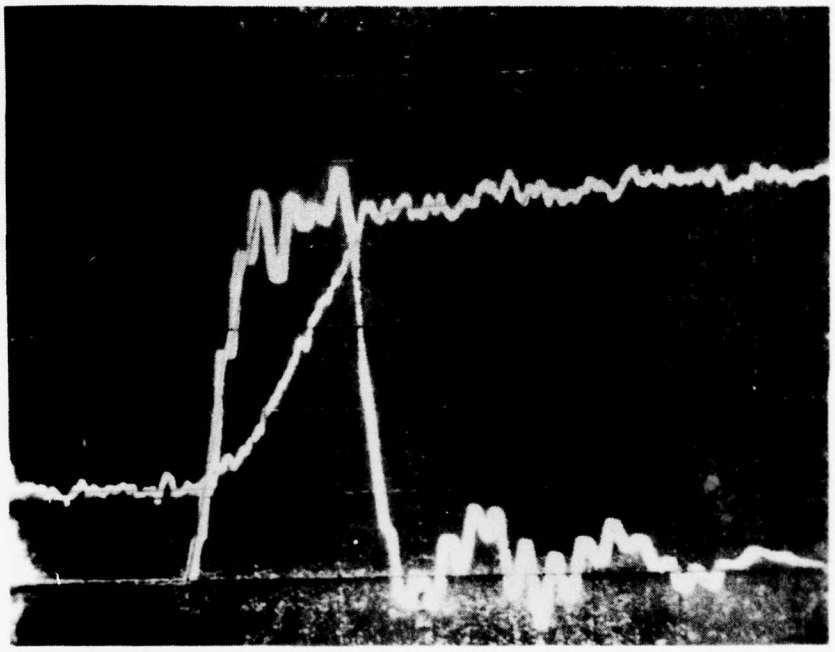

LOAD = 100 LBS./DIV.

ENERGY = 0.46 FT.-LB./DIV.

TIME = 0.2 MS./DIV.

TABLE III

PLATE IMPACT SPECIMENS

P/N	CONSTRUCTION	RESIN CONTENT (WT.%)	DENSITY (gr/cc)	THICKNESS (inch)
1487	2D $(0_2^{\hat{}}{}^{o}/\pm 45_2^{\hat{}}{}^{o}/90^{o})_s$	27	1.52	0.086
4237	3D/orthogonal	35	1.48	0.164
4238	4D/non-orthogonal	43	1.46	0.105
4239	4D/Hybrid*/Non-ortho	34	1.46	0.100

* Kevlar Fibers thru thickness

The test program is based on the calculated equivalent buckling strength of the 2D and 4D (P/N 4238) composites. The other multidimensional composites are to be evaluated by relating their impact behavior to the results of P/N 4238.

A summary of the ETI impact data for the four materials tested is presented in Table IV. For each material the average ($\bar{x}$), standard deviation (S.D.) and coeffiecient of variation (C.V.) are presented for load at incipient damage (Pinc), energy absorbed to incipient damage (Einc), maximum load (Pmax) and energy absorbed to maximum (Emax). These results are averages of four (4) tests per material. The total energy (E_t) absorbed during the tests was omitted from Table IV because these values varied with the allowed depth of penetration. The E_t data for each material obtained from the thru-penetration data trace are given in Table V. The data normalized for thickness E_t/t (energy per unit thickness) are also listed.

The data in Tables IV and V indicate that the energy absorbed by all the multidimensional composites is greater than the 2D composites, especially P/N 4237, the 3D/orthogonal composite. However, the thickness of the panels has, of course, a large effect on stiffness and also on impact performance. ETI has developed a relationship between absorbed energy in an impact test and plate thickness, based on results obtained in a study of 2D graphite-epoxy laminates. This relationship is:

$$E_{INC} = 48t^{1.29}$$

where t is the panel thickness. Table VI lists the "corrected" values for Einc and Emax based on average panel thickness, along with E_t The corrected values were then normalized by dividing the 3D and 4D panel energy levels by the values of the baseline 2D panel (P/N 1487). These normalized values of

TABLE IV

RESULTS OF PLATE IMPACT TESTS

PANEL NO.	P_{INC}			E_{INC}			P_{MAX}			E_{MAX}		
	$\bar{X}$ LBS.	S.D. LBS.	C.V. (%)	$\bar{X}$ FT. LBS.	S.D. FT. LBS.	C.V. (%)	$\bar{X}$ LBS.	S.D. LBS.	C.V. (%)	$\bar{X}$ FT. LBS.	S.D. FT. LBS.	C.V. (%)
1487 (2D)	500	90	18	1.43	0.39	27	830	17	2.0	4.73	0.15	3.2
4237 (3D/Orthog.)	1050	19	1.8	5.35	0.70	13	1358	54	4.0	28	5.34	19
4238 (4D/Non-orthogonal)	498	77	15	1.93	0.40	21	596	82	14	5.37	0.64	12
4239 (4D/Hybrid)	566	51	9.0	2.57	0.25	9.7	710	39	5.5	6.87	1.27	18

$\bar{X}$ = Average

S.D. = Standard Deviation

C.V. = Coefficient of Vaviation

TABLE V

TOTAL ABSORBED ENERGY FOR PLATE IMPACT

P/N	MAX. E_T	t (inch)	$E_{T/t}$ ($\frac{ft\text{-}lb}{inch}$)
1487	11.6	0.093	125
4237	48.2	0.165	292
4238	10.3	0.103	100
4239	17.3	0.101	171

TABLE VI

COMPARISON OF DATA USING

THICKNESS CORRECTION ($t^{1.29}$)

(Panel 1487 Used as Baseline)

PANEL NO.	ENERGY VALUES WITH THICKNESS CORRECTION			NORMALIZED VALUES		
	E_{INC} AVG. (FT. LBS.)	E_{MAX} AVG. (FT. LBS.)	E_T (FT. LBS.)	E_{INC}	E_{MAX}	E_T
1487 (2D)	1.43	4.73	11.6	1.0	1.0	1.0
4237 (3D/Orthog.)	2.27	12.0	20.5	1.6	2.5	1.8
4238 (4D/Non-orthogonal)	1.38	3.85	7.4	1.0	0.81	0.64
4239 (4D/Hybrid)	2.10	5.64	14.2	1.5	1.2	1.2

Einc, Emax and E_t indicate now that the 4D composite with equal buckling strength to the 2D composite does not possess superior impact behavior. In fact, the maximum and total energies absorbed are less than that of the 2D composite, while the energy absorbed to incipient damage is about equal. However, the other two multidimensional composites, the 4D hybrid (P/N 4239) and 3D/orthogonal (P/N 4237), exhibited much better impact performance than the 2D comparative laminate. It should be noted that the 4D hybrid has about the same construction and thickness as the all-graphite 4D (P/N 4238). Therefore, this buckling strength should be approximately the same, except for the small effect of the Kevlar fibers which MSC considers negligible. The impact strength is clearly superior to that of the 2D comparative laminate, and from 50% to 100% better than the all-graphite 4D composite.

The test results can also be compared on an equal weight basis (equal thickness basis if the densities are equal). The values shown in Table VII compare the energy parameters for the four types of panels tested. The energy per unit weight values shown in the table have been normalized to the data for the baseline material, panel 1487. This table shows the same general trends as Table VI but panels 4237 and 4239 seem even better when compared on a unit weight basis. This results from normalizing with respect to the thickness (since densities are about the same) rather than thickness to the 1.29 power.

Another means of comparing the impact resistance of these materials is to compare the permanent front surface indentation induced in the panels as a result of the impact. Figure 10 is a plot of permanent indentation as a function of total absorbed energy for the four panel types tested. The curves show that the 3D and 4D materials are superior to the 2D material with respect to permanent indentation. The data for the two types of 4D panels are quite similar while the 3D material is better than all others.

Besides comparing the materials among themselves, it is also of interest

TABLE VII

COMPARISON OF COMPOSITES
ON AN EQUAL WEIGHT BASIS
(Normalized to 2D Panel)

PANEL NO.	$\frac{E_{INC/W}}{(E_{INC/W})_{1487}}$	$\frac{E_{MAX/W}}{(E_{MAX/W})_{1487}}$	$\frac{E_{T/W}}{(E_{T/W})_{1487}}$
1487	1.0	1.0	1.0
4237	2.1	3.3	2.3
4238	1.1	1.0	.75
4239	1.7	1.4	1.4

W = Weight of Test Panel

FIGURE 10

PERMANENT DEFORMATION AS A FUNCTION OF TOTAL ABSORBED ENERGY

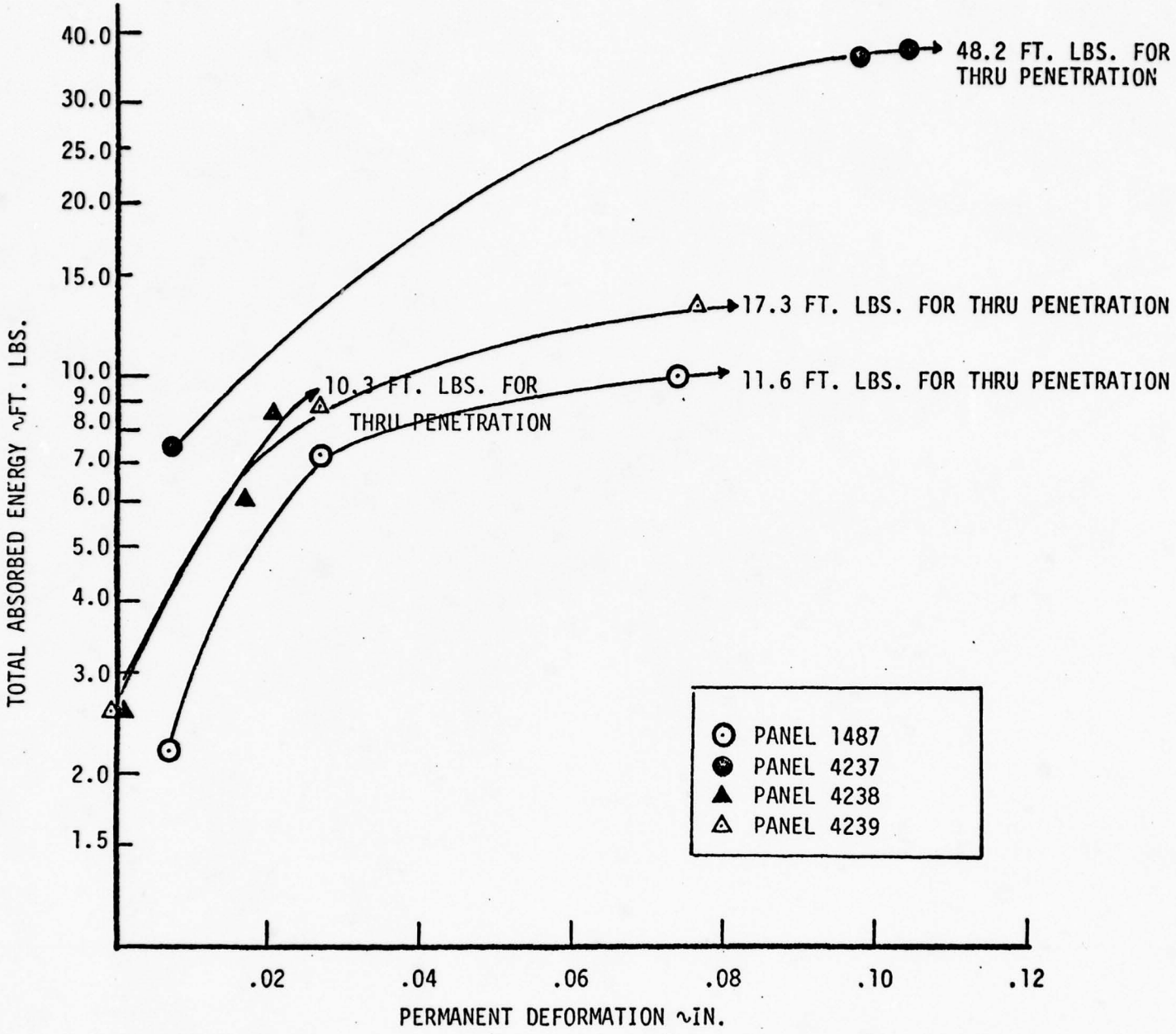

to compare all these materials with the existing data base on graphite epoxy panels subjected to impact tests. In order to do this, not only must the thickness effect be evaluated but specimen size effects must also be included. Most of the existing data on 16 ply graphite epoxy (AS3501-5) materials was generated with a specimen having a 5" x 5" unsupported area, rather than a 3" x 3" area, used in this section. However, data do exist on 8 ply graphite epoxy for both 3" and 5" unsupported areas. These data were used to obtain a size correction factor for the present test series. Table VIII compares the incipient energy levels for the FMI panels with the existing data base after accounting for both thickness and size effects. The table shows that all the present materials are more impact resistant (with respect to incipient damage) than AS3501-5. The improvements range from 13% for the 4D graphite epoxy to 86% for the 3D orthogonal graphite epoxy. Obviously, the scaling laws used to generate these data have not been thoroughly tested and therefore differences of 10% to 20% might not be significant. However, the improvements indicated in the performance of the 3D orthogonal and 4D with Kevlar epoxy reinforcement are believed to be real.

6.0 DISCUSSION OF RESULTS

6.1 Beam Impact Tests

The impact data in Table II have been plotted in Figure 11 vs. specimen thickness. This is done to present a clearer picture of the results as well as look at the effect of thickness. The two dotted lines connect the two sets of data points that are related by an equivalency. The line on the left connects the 2D and 4D composites that theoretically possess equal buckling strength. The line on the right connects the impact data for a 2D ($0^{o}/90^{o}$ crossply) and 3D orthogonal composites that have equal thickness (and weight). In both cases, the multidimensional composite possessed much superior impact strength.

TABLE VIII

COMPARISON OF FMI COMPOSTIES WITH 16 PLY AS3501

PANEL NO.	E_I~ FT. LBS.	SIZE CORRECTION FACTOR * (SCF)	THICKNESS CORRECTION FACTOR ** (TCF)	$E_{I_{CORR.}} = \frac{E_I * SCF}{TCF}$	PERCENT IMPROVEMENT OVER 16 PLY AS3501 WITH 5" UNSUPPORTED AREA E_I = 2.24 FT. LBS.
1487 (2D)	1.43	1.74	.94	2.65	18
4237 (3D/Orthog.)	5.35	1.74	2.21	4.21	88
4238 (4D/Non-orthogonal)	1.93	1.74	1.32	2.54	13
4239 (4D/Hybrid)	2.57	1.74	1.15	3.89	74

* Based on impact tests on AS3501 Gr/Ep with 3" and 5" Square Unsupported Areas

** Based on 16 Ply (.088") Gr/Ep

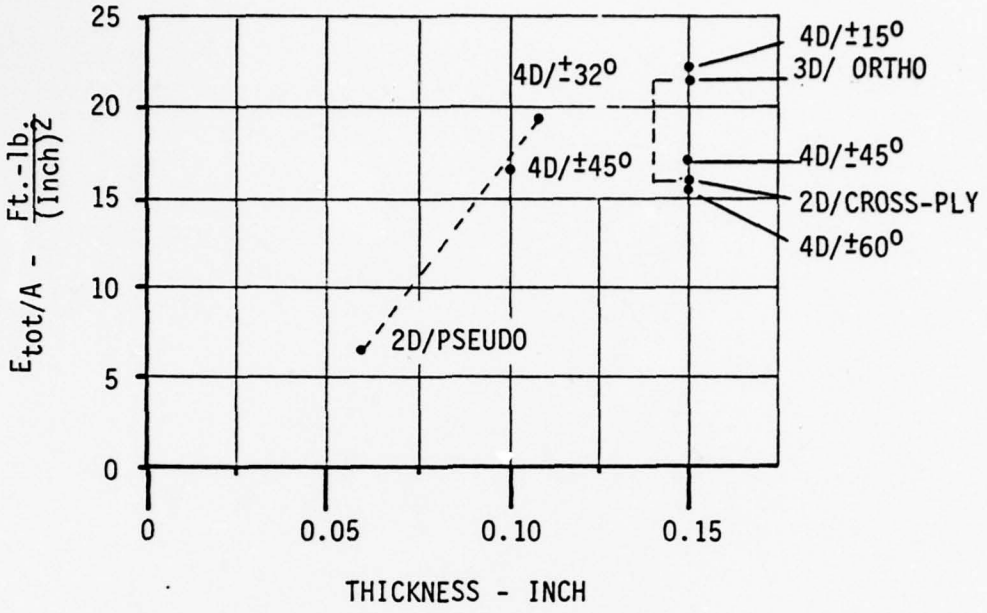

FIGURE 11. TOTAL ENERGY ABSORBED VS. SPECIMEN THICKNESS

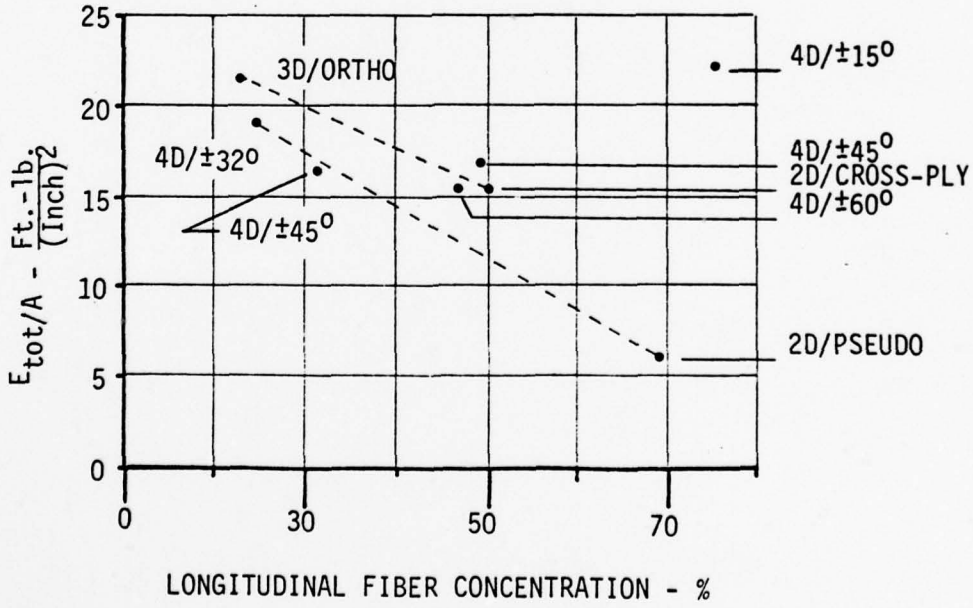

FIGURE 12. TOTAL ENERGY ABSORBED VS. LONGITUDINAL FIBER VOLUME

The data in Figure 11 also present impact strength of three 4D composites with equal thickness, but with varying through-the-thickness angles θ of $\pm 15^{o}$, 45^{o} and 60^{o}. With decreasing fiber angle the impact strength increased. It was originally theorized that the lower angle fibers should contribute more to the longitudinal strength, and thereby increase impact strength. Initially, these data tended to support that conception. However, another factor that must be considered when evaluating these data is the relative fiber concentration in the longitudinal direction of the beam specimen, which corresponds to the X direction of the panels. In Table IX, the in-plane longitudinal fiber concentrations are listed for each material. Also listed for the multidimensional composites are the Z (off-angle) fiber concentrations, and the in-plane component of these fibers, Z cos θ. The total longitudinal fiber concentration is, therefore, the sum of the in-plane fibers and Z cos θ.

These data are plotted as total energy absorbed per unit area vs. total longitudinal fiber concentration in Figure 12. Again, dotted lines connect the two sets of comparative data. In this plot, materials with good impact behavior are in the upper left quadrant of the graph, and those with poorer performance in the lower right quadrant. This is because the most efficient composites for impact strength should absorb the highest energy with the minimum fibers in the longitudinal direction of testing.

The superiority of the multidimensional composites is seen, even though both 2D comparative laminates possessed considerably greater fiber concentrations in the longitudinal direction than their 3D or 4D counterparts.

The reasons for the high impact strength for the 4D composite containing the lowest angle fibers ($\theta = \pm 15^{o}$) is now seen to be a result of very high longitudinal fiber volume. This high fiber volume was not intended, but is a result of multidimensional weaving characteristics. It is seen, now, that the apparent effect of fiber angle θ is in reality an effect of longitudinal

TABLE IX

LONGITUDINAL FIBER CONCENTRATION

NO.	MATERIAL	LONG. FIBER	Z (%)	Z COS θ	TOTAL FIBER CONCENTRATION
	SERIES 1				
1.	4D/θ=±32°	20	5.3	4.5	24.5
2.	2D/PSEUDO-	29	57	40.5	69.5
3.	3D/ORTHO-	22	3.7	0	22
4.	2D/CROSS-PLY	60	60	0	60
5.	4D/θ=±45°	26	6.1	4.3	30.3
	SERIES 2				
6.	4D/θ=±60°	42	10.6	5.3	47.3
7.	4D/θ=±45°	42	10.6	7.5	49.5
8.	4D/θ=±15°	72	4.5	4.3	76.3

fiber volume because in Figue 12, an approximately straight line with a positive slope could be drawn between the three data points.

It should also be noted that two data points are shown for two 4D composites with $\theta = \pm 45^{o}$ which appear to be independent of both specimen thickness and fiber volume. Obviously, other factors must be influencing the impact data that are not considered in this elementary analysis.

One of the major reasons for investigating multidirectional composites for impact resistance is that the third direction fibers should reduce the amount of composite delamination during impact. This effect is seen in Figures 13 and 14, which show the 2D pseudo-isotropic and $4D/\theta = \pm 32^{o}$ composites, respectively, after testing. Extensive delamination is seen for the 2D laminate, as expected, while very little delamination is seen for the 4D composite.

The beam impact data indicate that multidimensional composites possess superior impact strength to comparative 2D laminates. It was also demonstrated that the multidimensional composites restrict failure to a much smaller area than 2D laminates, which delaminated extensively.

The reason for the improved performance was first thought to be related to the improved interlaminar shear strength of the multidimensional composites. However, this may not be a satifactory explanation because Table II contains data showing that the shear strengths probably cannot account for the differences in impact strength. Good impact strength appears to be related more to how long the composite can carry a load after the onset of damage. Figure 9 shows that a 4D composite carried the load for some time, whereas the 2D specimen failed immediately after initial fracture (Figure 7). This load carrying ability after the onset of fracture is probably related in a complex way to shear strength, tensile strength, crack propagation and other material properties. On the basis of available information, it is impossible to identify a single reason for the good behavior of multidimensional composites. Certainly

FIGURE 13

IMPACTED 2D COMPOSITE BEAM SPECIMEN

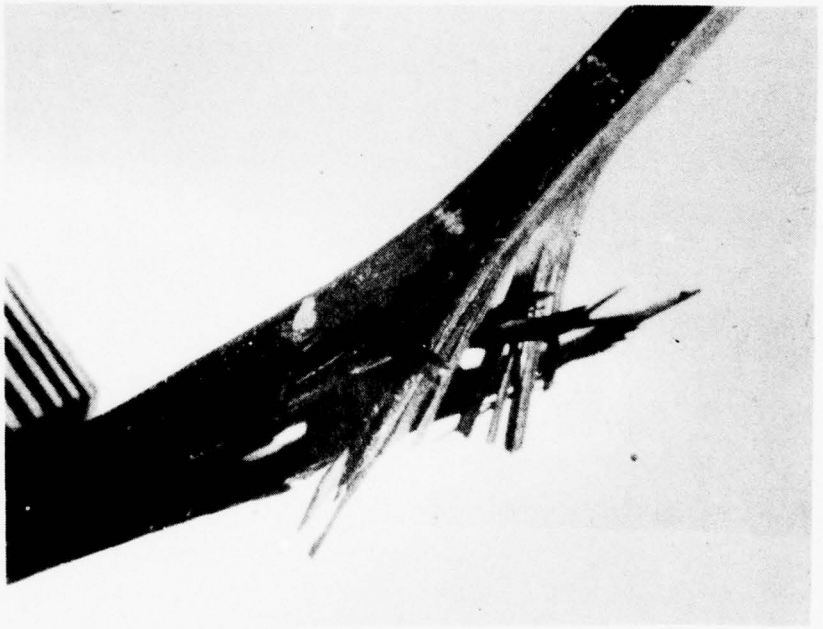

FIGURE 14

IMPACTED 4D COMPOSITE BEAM SPECIMEN

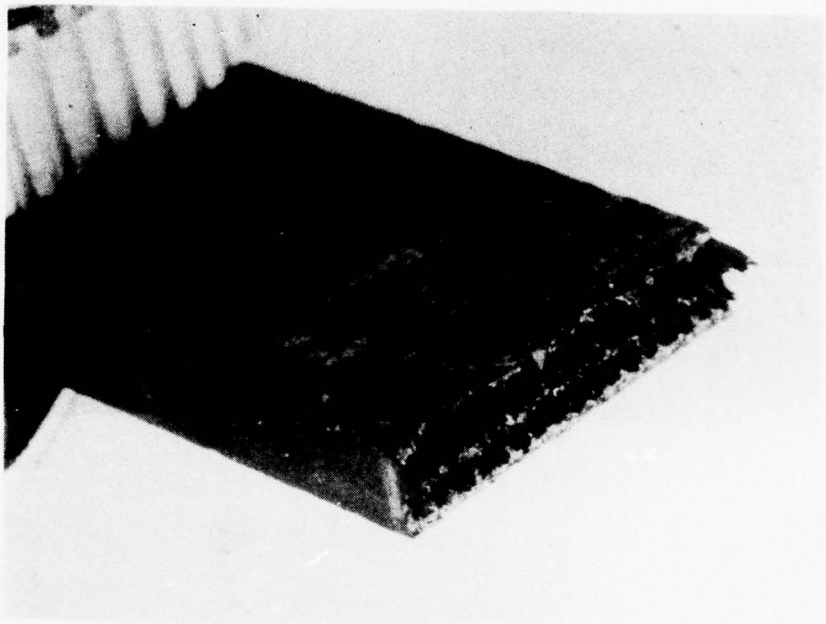

crack propagation must play an important role. In a 2D composite, planes of weakness exist between plies, especially the $\pm 45^{o}$ plies. Once initiated, a crack can progress rapidly along these planes, assuming a relatively brittle resin matrix. A multidimensional composite does not have these planes, and cracks are more readily arrested by the multitude of fibers in various orientations. Furthermore, there is probably a denser distribution of multi-directional cracks per unit volume with the multidimensional composite. This higher crack density per unit volume could explain how the multidimensional composite can absorb more energy over a smaller area than a 2D laminate.

6.2 Plate Impact Tests

Although the beam impact test results were quite encouraging, a major problem existed with these tests. A beam specimen, whether tested in shear or flexure, suffers from directional stresses and edge effects. Furthermore, the material in actual use will be used more as a plate than a beam. Therefore, another series of impact tests was conducted on several multidirectional and 2D composites as flat plates. By restraining the edges of these plates and impacting the center, a better distribution of stresses could be achieved that more closely approximated actual use conditions. Also, the impact data generated by ETI could be compared to data obtained on conventional 2D laminates from another program.

The data reported in section 5.3 tend to confirm the results obtained on the beam specimens. However, the improvement in the impact strength with multidimensional composites over that of 2D laminates is not quite as dramatic although it still exists. In the beam tests, the 4D specimen was about 200% more impact resistant than the comparative 2D laminate, while the 3D/orthogonal specimen was 40% better than its comparative 3D laminate. In the plate tests, the 3D/orthogonal composite appeared to possess the best impact strength. The reason for this difference probably is related to the isotropy of the composite

and the stress distribution resulting at impact. The stresses in a beam test will be resisted primarily by the longitudinal fibers in the beam specimen. The thru-the-thickness fibers in a 4D/non-orthogonal composite will contribute to the longitudinal strength, and result in better impact performance. However, the transverse properties (Y direction) should not be as good. The plate impact tests tend to support this reasoning. The anisotropic 4D all-graphite composite did not perform as well as the isotropic 3D composite in the plate test, where the stresses were distributed in a polar array around the impact point. Therefore, it may be concluded that the multidimensional composite construction must be tailored for the particular type impact stress to be encountered. For plate impact, an isotropic design is required to absorb energy uniformly at the point of impact. If the impact stresses are directional, then the anisotropic multidimensional construction should have fibers oriented to absorb these stresses.

6.3 Post-Test Evaluation

Several post impact test analyses were conducted in an effort to obtain a better understanding of the mechanisms of damage for the various materials.

6.3.1 Photographs of Back Surfaces

Photographs of the backface of two plates after thru-penetration impacts are shown in Figure 15. The upper panel is a 2D laminate and the lower a 3D composite. Extensive delaminations is seen for the 2D laminate with the horizontal back ply completely delaminated from the surface. The damage to the 3D plate, on the other hand, appears to be confined to an area approximately equal to the projected area of the indentor head.

Another feature of the impacted 3D panel shown is Figure 15 in the symmetry of the fracture pattern. This is as expected because of the isotropy of the composite. On the other hand, an anisotropic 4D composite should exhibit less

FIGURE 15

COMPARISON OF LOW VELOCITY IMPACT FRACTURE MODE OF 2-D VS. 3-D GRAPHITE EPOXY

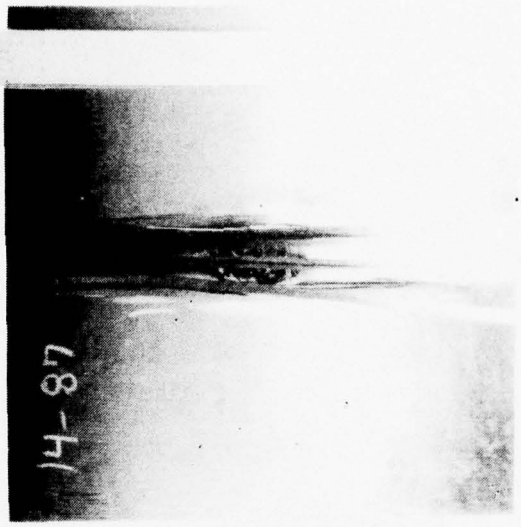

2-D PSEUDO-ISOTROPIC PANEL

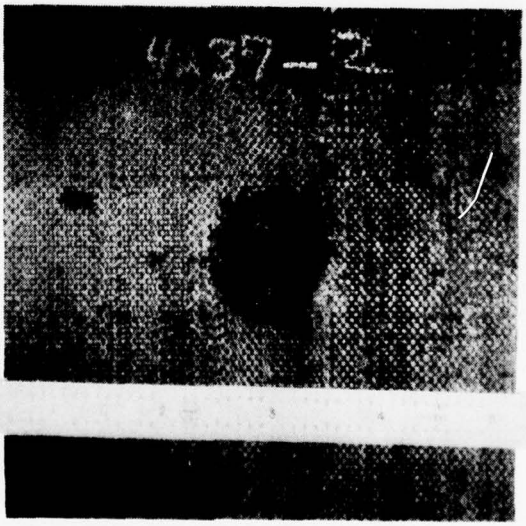

3-D ORTHOGONAL PANEL

fracture symmetry if the hypothesis of isotropy vs. anisotropy as expressed above is correct. Figure 16 is the backface photograph of a 4D all graphite composite (P/N 4238). Close examination of the fracture pattern indicates that there appeared to be more fracture in the Y direction, which is the direction that does not contain any off-angle (θ) fibers. Therefore, the fracture pattern supports the theory on the effect of fiber isotropy in the composite. The 4D hybrid composite (P/N 4238) exhibited similar behavior.

6.3.2 Cross-Section Photomicrographs

It has been claimed that the multidimensional composites restrict damage to a smaller area than a 2D laminate. Further, it is believed that in a multidimensional composite, the total fracture area is visible, while with 2D laminates, interior damage may occur beyond that which is visible, as reported in the literature (1).

To investigate this, the plates impacted with the lowest energy levels were carefully cut with a diamond saw across the center of the plate at the point of impact. Specimens at the impact point were then mounted, polished and low power photomicrographs obtained. Several are shown in figures 17-21, where the top of the photograph is oriented to the top of the specimen.

Extensive delamination is seen for the 2D laminate in Figure 17, especially toward the back of the panel. Some ply fracture is also seen in the upper half of the panel. The delamination extends away from the impact point a considerable distance. In the multidimensional composites shown in Figures 18-20, it was difficult to find significant cracks, and no delamination was evident. Some cracks are seen in Figure 21 at 100x and 160x for the 3D composite. Fiber fracture appears to be a major mode of failure in the multidimensional composites, as opposed to delamination in the 2D composite. No cracking could be found away from the impact point for the multidimensional composites. These photomicrographs tend to support the fracture mechanisms expressed earlier.

FIGURE 16

LOW VELOCITY IMPACT FRACTURE MODE OF

4D GRAPHITE/EPOXY

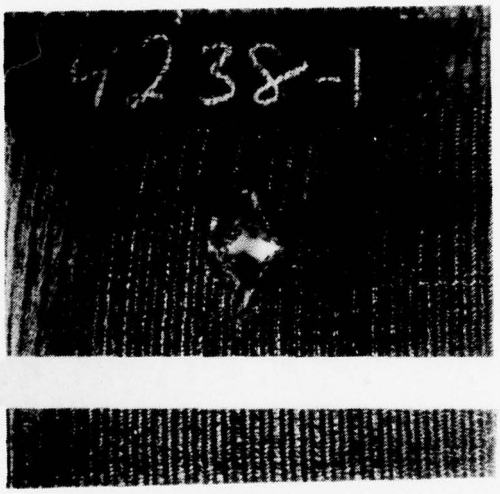

FIGURE 17

50X PHOTOMICROGRAPH OF 2D CROSS-SECTION

AFTER LOW ENERGY IMPACT

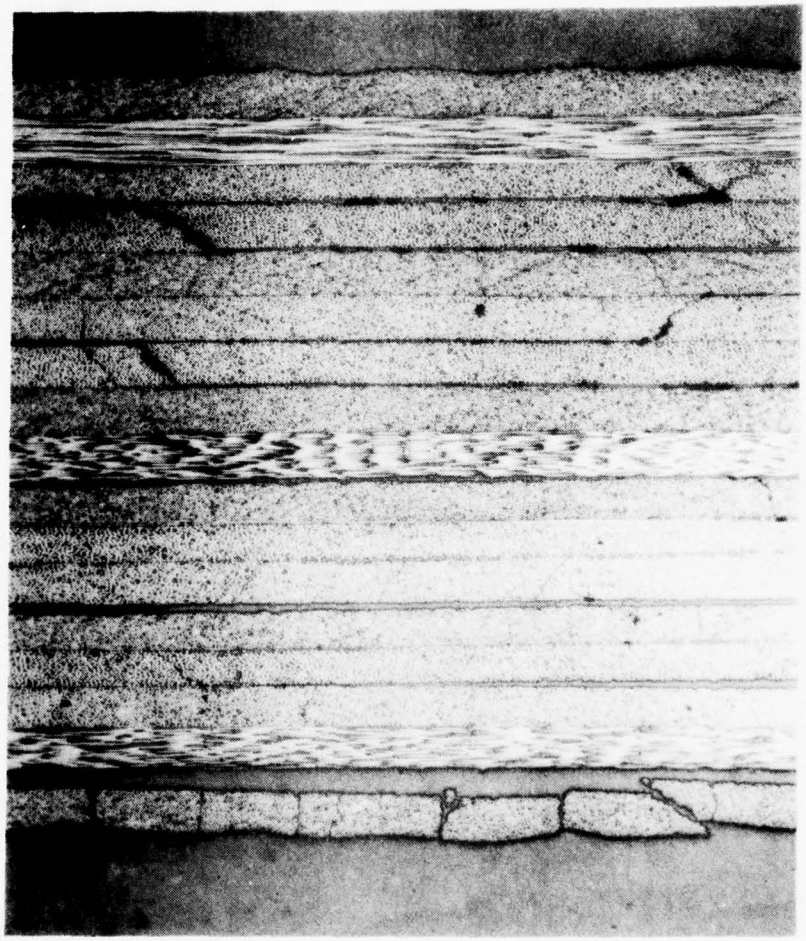

0.020

FIGURE 18

50X PHOTOMICROGRAPH OF 4D (P/N 4238)

CROSS-SECTION AFTER LOW ENERGY IMPACT

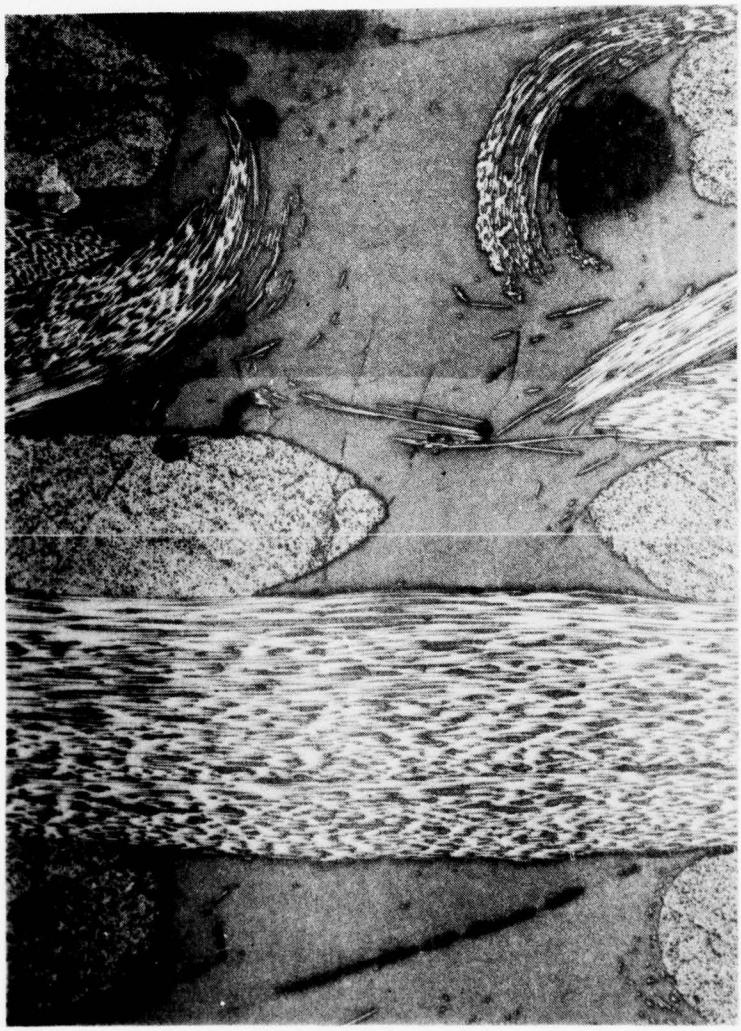

0.020"

FIGURE 19

50X PHOTOMICROGRAPH OF 4D HYBRID (P/N 4239)

CROSS-SECTION AFTER LOW ENERGY IMPACT

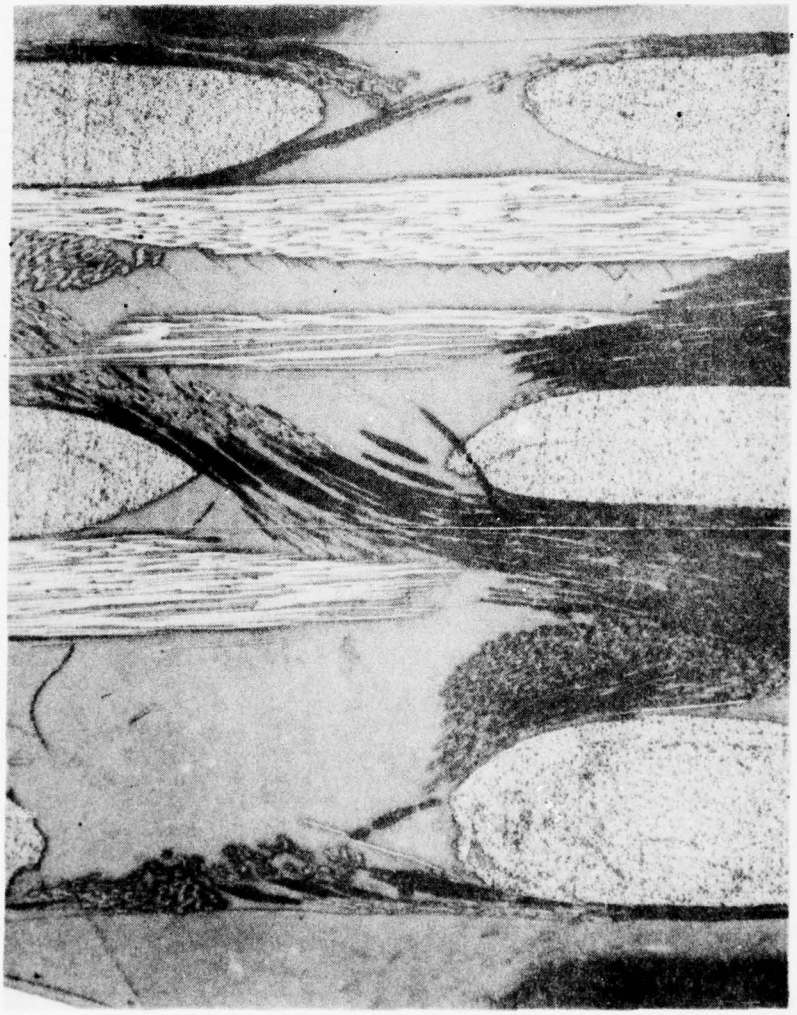

0.020"

FIGURE 20

50X PHOTOMICROGRAPH OF 3D (P/N 4237)

CROSS-SECTION AFTER LOW ENERGY IMPACT

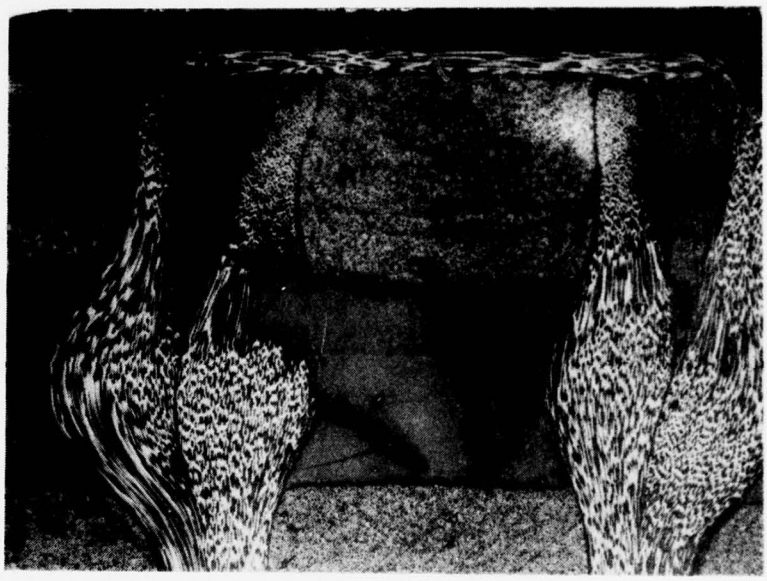

0.020"

FIGURE 21

100X AND 160X PHOTOMICROGRAPHS OF 3D (P/N 4237) CROSS-SECTIONS AFTER LOW ENERGY IMPACT

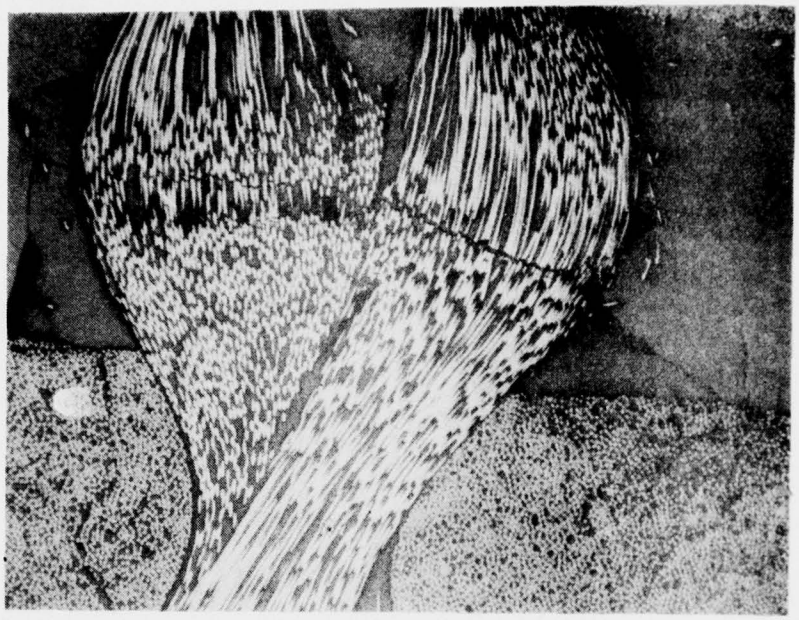

100X

0.010"

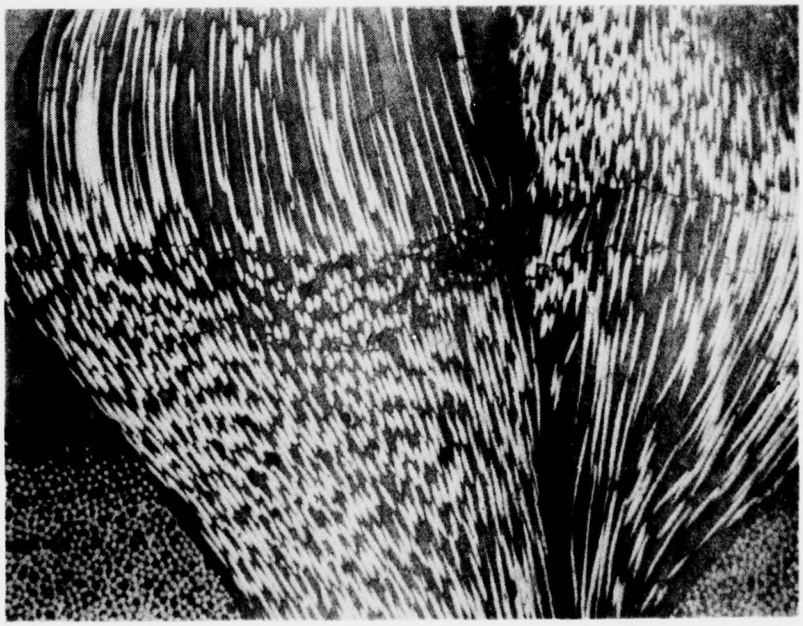

160X

0.006"

6.3.3 Flexure Tests

In another attempt to determine differences in the extent of fracture of 2D vs. 4D composites, two impacted panels (P/N 1487 & 4238) were sectioned into narrow flexure specimens. The results are summarized in Table X. The test specimens start at the edge of visible damage, which was wider for the 2D panel than the 4D panel (roughly 5/8" dia. vs. 1/2" dia., respectively). The flexure strength and modulus data indicate that the 2D panel was damaged beyond the visible damage area. These results support the conclusion that the 2D composites delaminated more extensively during impact than multi-dimensional composites. Furthermore, the residual strength of the 2D composite was decreased over a wider area by non-visible damage than the 4D composite, where actual damage appeared to be restricted to the visible damage area.

6.3.4 Non-Destructive Testing

Two impacted panels, the 2D laminate and the comparative 4D composite (P/N 1487-2 & 4238-2, respectively), were examined by ultrasonic B-scan to determine the extent of damage. Both panels were impacted at ETI at intermediate energy levels between peak load and thru-penetration. It was concluded that although the area of damage appeared somewhat larger in the 2D composite, the extent of non-visible delamination could not be determined. Apparently, the test was insensitive to the relatively small dimensions of composite delamination so that only the visibly damaged areas could be detected by the ultrasonic B-scans.

7.0 CONCLUSIONS

Low velocity impact tests on both beam and plate specimens have shown

TABLE X

FLEXURE STRENGTH GRADIENTS OF IMPACTED PANELS

	1487 (2D)		4238 (4D)	
	STRENGTH ($\times 10^3$ PSI)	MODULUS ($\times 10^6$ PSI)	STRENGTH ($\times 10^3$ PSI)	MODULUS ($\times 10^6$ PSI)
1A	121	8.6	94	4.9
2A	163	10.6	98	4.7
3A	159	10.5	104	5.0
4A	162	10.1	101	5.2
5A	145	9.9	89	5.0
1B	124	8.9	74	4.1
2B	159	10.9	77	4.1
3B	165	10.6	82	4.4
4B	154	10.3	86	5.2
5B	133	10.6	95	5.7
W	5/8"		1/2"	

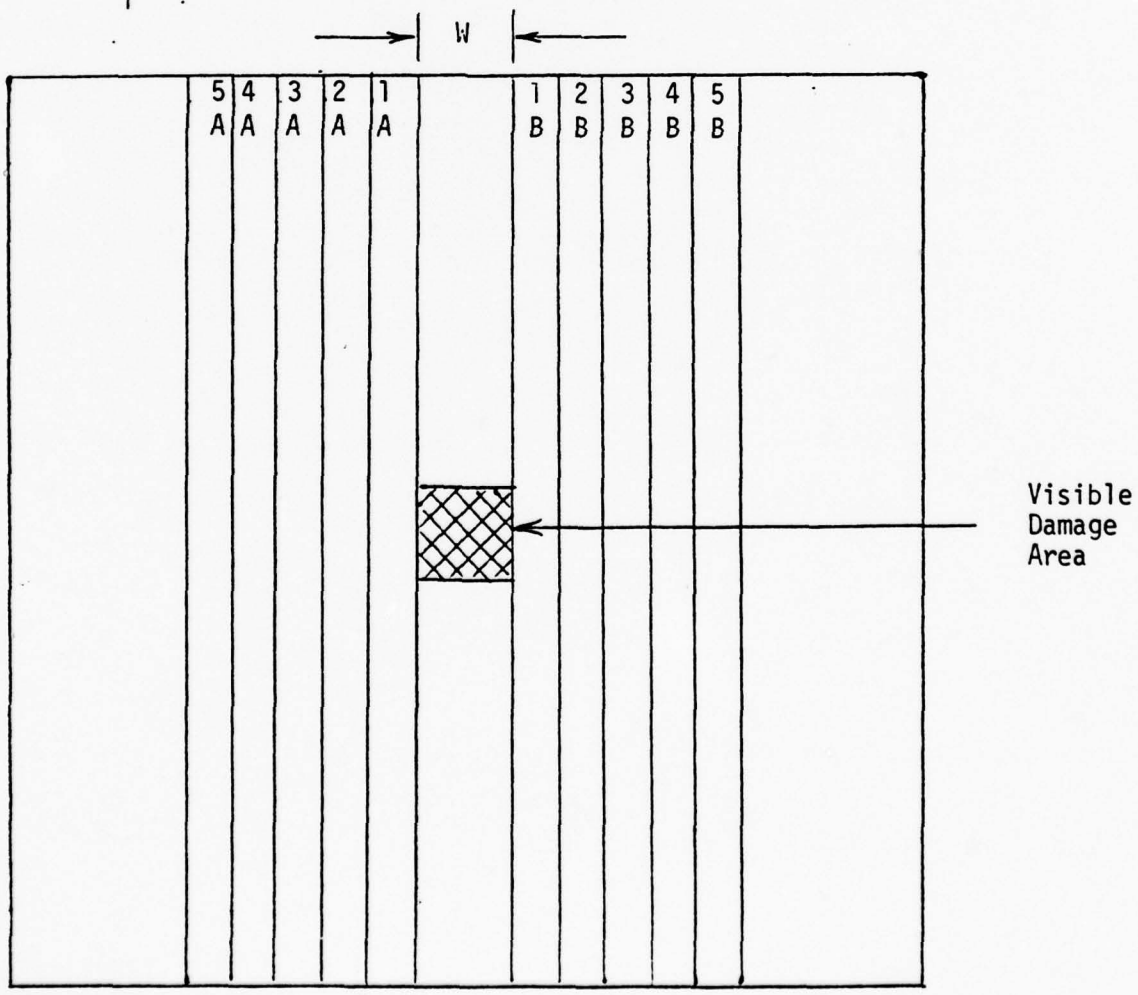

that multidimensional fiber reinforced composites possess superior impact resistance to conventional 2D composites.

The beam tests indicated that the impact strength of a 4D composite was 200% better than a 2D pseudo-isotropic laminate possessing equivalent buckling strength. On an equal weight basis, a 3D composite exhibited a 40% increase in impact strength compared to a $0^{o}/90^{o}$ 2D laminate. The 2D pseudo-isotropic composite delaminated extensively while the multidimensional (3D & 4D) composites did not. Impact resistance did not appear to be related to thru-the-thickness fiber angle (Z direction). Analyses of the data indicated that the impact properties of composites were related to how long the specimen carried a load until complete failure occurred. The 2D pseudo-isotropic laminate failed immediately upon reaching the maximum load, while the multidimensional composites supported the peak load for significant periods of time before failure. The area under the load-time curve increased, resulting in a corresponding increase in absorbed energy. This ability of multidimensional composites to carry loads may be related to several composite properties, including shear strength, tensile properties, crack propagation behavior and other materials characteristics. The result is that the multidimensional composites absorbed more energy in a smaller volume of material than a 2D laminate.

In general, the plate impact tests supported the conclusions from the beam tests. The multidimensional composites possessed increased impact strength over that for a 2D laminate, but the improvement was less than for the beam specimens. The anisotropy of the 4D construction may have degraded the impact strength in a plate test, where stresses are distributed in a polar array around the impact points. The more isotropic 3D orthogonal composite appeared to be superior to the anisotropic 4D composite in plate tests. A Kevlar-graphite hybrid 4D composite absorbed at least 50% more impact energy than an all-graphite 4D composite of similar construction. The data also

indicated that all the multidimensional composites tested in this program possessed superior impact resistance to a 16 ply pseudo-isotropic laminate evaluated by ETI in another program.

As with the beam specimens, the 2D plates showed much more evidence of delamination than the multidimensional composites, especially at the back surface. The interior delamination in the 2D panels extended beyond the visibly damaged area. The damage to the multidimensional panels was restricted to the area of impact and did not include any delamination. Therefore, it is concluded that the residual strength of the multidimensional composites after impact was superior to that of the 2D laminate.

The data also indicate that the multidimensional composites should be designed for specific impact conditions in order to maximize the energy absorbed.

The combined results of the beam and plate tests show that multidimensional composites possess greater impact strength than 2D laminates, coupled with much less composite damage. Therefore, multidimensional composites absorb more energy over a smaller area than 2D composites.

This program has demonstrated the excellent potential for the use of multidimensional composites in solving the impact resistance problem with 2D graphite/epoxy composites. Future work is required to develop relationships between multidimensional composite design and specific impact conditions. Then, prototype composite aircraft components should be constructed and tested for impact performance against conventional 2D pseudo-isotropic composites.

8.0 RECOMMENDATIONS FOR FUTURE WORK

The results of this program have shown that multidimensional graphite fiber reinforced composites can be applied to aircraft structures where improved impact resistance is required. In order to take advantage of this material's potential, the following program is recommended.

1. Multidimensional composite test panels should be designed and fabricated based on the data generated in the current report. These larger panels should include hybrid constructions of combined graphite and Kevlar fibers as well as combinations of 2D and multidimensional composites. The objective would be to determine the most effective multidimensional composite design for particular impact conditions. Materials Sciences Gorp. would assist in the composite design based on their analyses.

2. The panels would be impact tested by Effects Technology, Inc. and the data compared to conventional 2D laminates now being used on naval aircraft. Testing would include residual strength evaluation after low energy impact and fracture analyses to establish impact failures mechanisms.

3. The date would be analyzed and the composite designs selected that possess the best combination of impact and in-plane structural properties.

4. After the composite design has been optimized, it is recommended that a full or sub-scale aircraft component be designed and fabricated of both the multidimensional and conventional 2D composites. Impact and other physical properties should be determined and a final evaluation made of the impact performance of multidimensional composites.

9.0 REFERENCES

1. N.R. Adsit and J.P. Waszczak, "Investigation of Damage Tolerance of Graphite/Epoxy Structures and Related Design Implications." Final Report, NDAC-76387-30 (Dec. 1976).

2. F.J. Bradshaw, G. Dorey and G.R. Sidey, "Impact Resistance of Carbon Fibre Reinforced Plastics", Royal Aircraft Establishment Technical Report 72240 (January 1973).

3. L.J. Broutman and A. Rotem, "Impact Strength and Toughness of Fiber Composite Materials," Foreign Object Impact Damage to Composites, ASTM STP 568, American Society for Testing and Materials (1975).

4. P.W.R. Beaumont, P.G. Riewald and C. Zweben, "Methods for Improving the Impact Resistance of Composite Materials", Foreign Object Impact Damage to Composites", ASTM STP 568, American Society for Testing and Materials (1975).

5. K.W. Hofer, Jr. and L.C. Bennett, "The Effects of Moisture on the Performance of T300 Graphite/Glass/Epoxy Hybrid Composites", Final Report to NASC on contract no. N00019-75-C-0113 (Dec. 1975).

6. R.C. Novak, "Materials Variables Affecting the Impact Resistance of Graphite and Boron Composites -II", AFML-TR-74-196, Part II (June 1975)

7. P.J. Cavano and W.E. Winters, "Composite Impact Strength Improvement Through a Fiber/Matrix Interphase",NASA CR-134887 (Oct. 1975).

8. J.H. Williams, Jr. "Improvement of Composite Fracture Through Toughness by Fusible Fibers and Coatings", NASA Grant No. NSG-1217 (Dec. 1976).

9. L.B. Greszczuk, "Response of Isotropic and Composite Materials to Particle Impact", Foreign Object Impact Damage to Composites, ASTM STP 568, American Society for Testing and Materials (1975)

10. "Multidimensional Fiber Reinforced Composites for Improved Impact Resistance", Final Report on NASC Contract No. N00019-76-C-0411.

APPENDIX A

Design and Analysis of Multidimensional Composities for Impact Resistance.

Final Report Submitted by

Materials Science Corp.

Materials Sciences Corporation

MSC/TFR/810/4704

CONSULTING ENGINEERING SERVICES IN SUPPORT OF EVALUATION OF MULTIDIRECTIONAL FIBER-REINFORCED PLASTICS FOR IMPACT RESISTANCE

Prepared for:

Fiber Materials, Incorporated
Biddeford Industrial Park
Biddeford, ME 04005

Under P.O. #13153

October, 1978

Approved by:

B. Walter Rosen
President

Blue Bell Office Campus, Merion Towle House, Blue Bell, Pennsylvania 19422 • 215 542-8400

PREFACE

This report summarizes the results of the engineering services provided by the Materials Sciences Corporation for Fiber Materials, Incorporated under P.O. #13153. Mr. John Herrick served as the technical contact between FMI and MSC. The work described herein was performed by Dr. R. L. Ramkumar with assistance from Dr. J. J. Kibler.

INTRODUCTION

This report summarizes the periodic consulting services provided under Fiber Materials, Incorporated P.O. 13153 in response to specific technical requests by FMI personnel. These services were performed in support of the FMI study of the impact resistance of 3-D composites. This report describes the various tasks undertaken. The first section treats the effects of fiber volume fraction and orientation upon the structural properties of 4-D materials. The second section provides a comparison of several hybrid material systems. The third section describes the equivalent laminate materials which were designed to provide a direct comparison of impact resistance of the 2-D and 4-D materials. This is followed by a brief discussion of the test results. The final section discusses recommendations for future test programs.

BACKGROUND

Interply disbonding or delamination is a failure mode which has been observed in structural composite laminates subjected to lateral impact. This is a major motivation for the use of laminates having fibers through the thickness to improve impact resistance. These so-called 3-D laminates are the subject of this report. It is to be expected that the resistance of 3-D laminates to in-plane structural load will be less than that of equal weight 2-D laminates. Hence, a rational comparison of the relative merits of conventional 2-D structural laminates with various types of 3-D laminates requires a comparison between impact properties and between structural properties.

The criteria for structural equivalence may require consideration of stiffness or strength properties depending upon the particular application being considered. Since a major problem is impact damage to aircraft structural skins, an appropriate criterion is the buckling strength of the laminate. This criterion involves both the longitudinal and transverse laminate stiffnesses as well as its in-plane shear stiffness. Buckling

strength is chosen as the structural parameter for comparison of impact strength of 3-D and 2-D materials. If one were to replace a 2-D panel with a material with improved impact resistance, it is likely that the improved material would have to meet or exceed the buckling strength of the 2-D material. Thus, for material comparison purposes, the impact resistance of the 3-D materials studied herein were compared to the impact resistance of 2-D laminates possessing the same buckling characteristics.

The stiffnesses of all the panels were computed using the MSC laminate analysis computer code (CLAM) and the MSC X-D composite analysis computer program (XCAP). The ultimate stresses were then evaluated knowing the fiber bundle strength and the laminate-to-bundle stiffness ratios. The buckling strength is obtained using the formula:

$$N_{x_{cr}} b^2/\pi^2 = 2(\sqrt{D_{11}D_{22}} + D_{12} + 2D_{66}) \doteq K_{ff}D_{22}$$

where the D_{ij}'s are the bending stiffnesses.

The parameter K_{ff} is a measure of the resistance to buckling under in-plane loads as well as a measure of the natural frequency of the panel.

Another structural parameter which has been considered is the transverse shear stiffness, G_{xy}, which is a measure of transverse shear strength. Since impact damage in laminates is related to low transverse shear and tensile strength, it is assumed that improvements in shear strength will result in improved impact resistance. Shear strength for these materials generally increases when shear modulus does, and hence shear modulus, which is easily predicted, is an appropriate measure of shear strength and hence impact resistance.

RELATION BETWEEN MATERIAL CONFIGURATION AND STRUCTURAL PERFORMANCE

The materials treated initially were all T-300 fibers in an epoxy matrix. As was discussed in reference 1, the shear characteristics of the laminate are expected to have a primary influence upon impact resistance. Thus, the shear modulus has been selected as the convenient measure of these properties. The basic 4-D material which was considered for this study consisted of in-plane fibers oriented along the axis of the beam (Y-direction), transverse in-plane fibers located in the Z-direction of the plane, and a pair of out of plane fibers oriented in the XY plane, labelled directions X1 and X2. The out of plane fibers make an angle of θ with the Y axis. This initial study considered increases in the out of plane fiber volume fraction, which were made with compensatory decreases in the fiber volume fraction in the Y-direction, the fiber content in the Z-direction was held constant. The inset in figure 1 shows the orientation angles and fiber directions considered.

Composite elastic properties for laminated materials were computed using the MSC-CLAM code. In the case of X-D materials composite elastic properties were computed using the MSC-XCAP code, reference 2. The XCAP code can model materials which are reinforced in up to 13 fiber directions. For the current material two-edge bundles represented the Y- and Z-directions of reinforcement and a pair of face diagonal bundles were utilized to represent the X1, X2 fibers penetrating through the thickness of the plate. Both the relative amounts and orientation of these fibers can be controlled directly through input to the code.

The variations of the structural performance with orientation angle of the fibers is shown in figure 1 along with the corresponding changes in the impact resistance parameter, K_{ff}. The decrease in in-plane structural performance, G_{xy}, is accompanied by an increase in the transverse shear modulus and impact resistance. From these results, the effect of orientation angle, θ,

on a measure of the impact resistance to structural performance ratio can be obtained and is shown in table 1. This arbitrary but quantitative measure shows that an increase in orientation angle results in an improvement in the impact performance. Table 1 and figure 1 show the effects of changing the orientation of the diagonal fibers while holding the fiber volume fraction constant. If the diagonal fiber volume fractions are increased (at the expense of the Y fiber volume fraction) the results indicate a decrease in the buckling strength of the panel, a corresponding increase in the shear modulus, and therefore an improvement in the relative impact performance, see table 2. A trade-off exists here however, if the X-D panel is to have the same buckling strength as the currently used panels, then increasing the amounts of diagonal fibers will require a thicker and hence heavier X-D material to be defined as a replacement. Since it is desired to keep the weight penalties to a minimum one must attempt to utilize the smallest amount of diagonal fiber directions as possible, consistent with improving the impact performance. From these results it can be seen that it is desirable to keep the diagonal fiber bundle orientation as large as possible as well as the amounts of diagonal fibers.

THE EFFECTS OF UTILIZING HYBRID MULTIDIRECTIONAL COMPOSITES TO IMPROVE IMPACT RESISTANCE

The relatively low strain to failure capability of T-300 fibers limits the amount of energy which these fibers can absorb during an impact. This, coupled with the low transverse shear strength of laminates, is directly responsible for low energy impact damage of these materials. Several recent studies, references 2,3, have shown that by hybridizing graphite with Kevlar or glass fibers, the impact resistance of laminated composites can be increased substantially without severe penalties relative to structural performance capability of the hybrid material. The study by Dorey, reference 2, has shown that a hybrid laminate of

Kevlar/Graphite/Kevlar can result in better than a factor of 2 energy absorption during impact tests with only a 20% reduction in mechanical properties as compared to an all Graphite laminate. Since the impact resistance of any composite will be directly related to the energy absorption capability of the individual constituents, a hybrid of T-300 and Kevlar or glass, woven in an X-D configuration, could perhaps result in even further improvements in the impact properties of the composite.

In an attempt to demonstrate the relative merits of a hybrid of T-300 and Kevlar and a hybrid of T-300 and glass fiber the current 4-D weave configuration was modeled to determine the buckling strength and shear modulus. The basic material modeled was similar to FMI's panel #2271, which consisted of a fiber volume fraction of 20% in the Y-direction, 18% in the Z-direction, and 6% in the combined X1, X2 direction, which are oriented at 32° relative to the Y axis. It was assumed that Kevlar and/or glass fibers could be substituted directly into the X1 and X2 directions, thereby providing a minimum impact on the in-plane properties of the panel. In order to demonstrate the effects of these families of hybrids, diagonal fiber orientations of 20, 32, and 45° were modeled. The results for 0.1 inch thick plates are shown in table 3. For hybrids fabricated in this fashion there is roughly a 10% change in Y-direction modulus, essentially no change in the Z-direction modulus, and relatively minor changes in the shear moduli for the panel. This is due to the fact that the X1, X2 fiber bundles are both relatively small in fiber concentrations and have a small contribution to the in-plane properties. Likewise the buckling parameters show only minor changes from the all T-300 to the T-300 hybrid configurations and relatively consistent changes as the orientation angle of X1, X2 fiber bundles are changed. The structural performance parameter, G_{yz}/K_{ff} indicates a slight reduction in performance of the T-300/Kevlar hybrid over an all T-300 hybrid, and a slight improvement in the T-300/Glass hybrid over the all T-300 material. Quite

obviously the contribution of the diagonal fibers in absorbing impact energies due to deformations through the thickness and in shear deformation are not accounted for in the structural performance parameters listed in table 3. Since the performance parameters in table 3 each show only minor changes, and it is known that the through the thickness performance relative to energy absorption will be better for the hybrid composites, it is to be expected that hybrid panels would show significant improvements over an all T-300 panel, while the in-plane structural modulus, strength, and buckling stiffness would be essentially the same as an all T-300 material. The fact that a hybrid material can offer further improvements in impact resistance without sacrificing in-plane structural properties, indicates that hybrid materials should be pursued further. The hybrid materials could be substituted for current laminates with weight penalties similar to the all T-300 for the materials, but better impact resistance.

DESIGN OF EQUIVALENT 2-D LAMINATE PANELS FOR COMPARISON WITH THE 4-D CONSTRUCTED MATERIALS

As part of FMI's material development program 4-D panels were constructed and densified utilizing T-300 fibers and the 5208 resin system. These panels were sectioned and tested for structural properties and energy absorption capabilities. In order to evaluate the performance of the X-D material, it was desired to fabricate an equivalent 2-D laminate configuration which could be tested as part of the testing program to provide a direct correlation between the energy absorption capability of a typical laminate and its equivalent 4-D construction. As stated previously, since the buckling strength of aircraft panels is considered to be a significant design parameter, laminate constructions were designed which would provide the same buckling strength as the fabricated 4-D materials.

The initial 4-D panel which was considered was FMI's panel #2271. The construction of this panel is listed in table 4. Also listed in table 4 is the design of an equivalent 2-D laminate which would have the same buckling strength as panel #2271. It was found, however, that the fiber volume fractions were incorrectly modeled for panel #2271 and that the buckling strength of this panel was underestimated. This error was not identified until after the equivalent laminate had been fabricated and tested. The implication of this error is that the 4-D panel could have been reduced in thickness from .113 inches to .091 inches to have the same buckling strength as the laminates which were tested. If the energy per unit cross section area is independent of the specimen thickness, the comparison of the 4-D and the 2-D material remains valid. Also, the differences between the two specimen weights is lessened due to the fact that the 4-D material could have been manufactured in a thinner configuration.

Panel #2271 was sliced into thin sections and tested in beam configurations along with its equivalent laminate construction.

The results of these tests are discussed in the following section.

The second FMI panel which was modeled was also a 4-D configuration which is similar to panel #2271. This panel was originally woven .151 inches thick with densities and fiber volume fractions as shown in table 5. After densification the panel thickness was reduced to 0.112 inches, thus there were several options relative to attempting to define the as fabricated fiber volume fraction, as discussed below. The fiber distribution in the preform was 45% of the fibers in the Y-direction, 45% of the fibers in the Z-direction, and 5% of the fibers in each of the X1, X2 directions. The total fiber volume fraction in the panel after densification indicated that the fibers occupied 40% of the volume of the panel. The original orientation of the diagonal fibers in the preform was at ±32° relative to the Y axis of the panel. After densification, since the panel thickness was reduced from .15 to .11 inches, it was not clear that the diagonal fibers remained at ±32° to the Y axis. The initial calculations of the panel properties assumed that the fibers were remained oriented at 32°. Subsequent inspection of the panel indicated that the fibers had been compressed and a 27° orientation was more representative of the direction of the diagonal fibers in the panel. Consequently additional calculations were made to determine the panel properties for this final fiber orientation.

As seen in table 5, the change in orientation from 32 to 27° of the diagonal fibers has only a very small effect upon the panel properties. The properties of an equivalent laminate utilizing the basic 0/±45/90 configuration are also shown in table 5. The buckling strengths of laminates utilizing this small number of layers is extremely sensitive to the actual layup of the laminate. Therefore the 3% difference between the buckling strength of the panel and the buckling strength of the equivalent laminate is very small, and these two materials can be compared directly. It should be pointed out that most of the in-plane properties of the equivalent laminate compare rather well with those of the panel with the exception of a 20% difference in Z-direction

modulus. However, there is a substantial difference (a factor of 4) between the in-plane shear moduli of the two materials. This difference in shear moduli is directly related to the fact that the 4-D panel contains only 0° and 90° direction fibers in the plane, thus resulting in a very low shear modulus material for the panel.

These current materials are to be sectioned into five-inch square plates and tested as plates with center impact conditions. It will be important, in reviewing the impact energies absorbed for the 4-D panel, to attempt to define how much of the impact damage is related to the lack of diagonal fibers in the X-Z-direction plane of the material.

DISCUSSION OF THE TEST RESULTS TO DATE

The results of the tests conducted on 2-D, 3-D, and 4-D materials have been presented in reference 4. The tests measured total energy absorbed, rather than the recommended measurement of energy required to initiate damage. As a result, the test data cannot be compared directly with the analytical results obtained. Evaluation of total energy absorption under impact loads is a complex problem. Such analysis is beyond the scope of the present effort.

RECOMMENDATIONS FOR FUTURE WORK

The results of the initial test program have indicated that X-D materials provide significant advantages over 2-D materials for impact resistance. However, the initial testing was on simple beam specimens and further work is required to obtain a better understanding of the behavior of X-D materials in panel configurations. Additionally the recommendations from reference 1 pointed out that the test conditions themselves must be very carefully evaluated to understand the effects of striker mass and boundary conditions on the panels being tested. Furthermore, the response of the 2-D laminates and the 3-D panels must be carefully evaluated to define if the failure modes are dominated by shear mechanisms or bending mechanisms for the various boundary conditions and test specimen sizes. It is recommended that further testing be performed to evaluate the following different phenomena:

1. The response of 2-D and X-D materials at low energy levels should be evaluated with the purpose of defining the threshold energy required to initiate damage in the material and the resulting residual strength remaining in the material after initial damage has occurred.

2. The effects of boundary conditions, plate thickness, and weave spacing should be evaluated through a series of carefully planned tests.

3. Previous studies and current initial analyses have shown that hybrid materials may provide improved shear strength and hence improved impact resistance without significant effects upon the in-plane panel properties. Various hybrid material configurations should be analyzed, resulting in material specifications to be fabricated and tested.

4. Other X-D configurations should be assessed in order to provide improved shear strength of the panel in all directions. The current 4-D material has high shear strength in the XY plane, but poor properties in the X-D plane as well as the YZ plane. Other X-D material configurations can be evolved which will provide improved shear properties of nearly all of the planes of the panel. These materials should be less susceptible to preferred damage orientation for panels under impact.

REFERENCES

1. Rosen, B. W. and Ramkumar, R. L., "Engineering Services in Support of Evaluation of Multidirectional Fiber-Reinforced Plastics for Impact Resistance", MSC/TFR/706/2471, prepared for Fiber Materials, Incorporated, June, 1977.

2. Dorey, G., Sidney, G. R. and Hutchings, J., "Impact Properties of Carbon Fibre/Kevlar 49 Fibre Hybrid Composites", Composites, Vol. 9, No. 1, pp. 25-32, January, 1978.

3. Murphy, G. C. and Salemme, C. T., "Low-Cost Fod-Resistant Organic Matrix FAN Blades", General Electric Interim Technical Reports 11, 12, 13, 14, prepared for AFML under Contract F33615-74-C-5072, 1976-1978.

4. Herrick, J., "Advanced Impact Resistant Multidimensional Composites", Quarterly Progress Report No. 3, Contract N00019-77-C-0430, July, 1978.

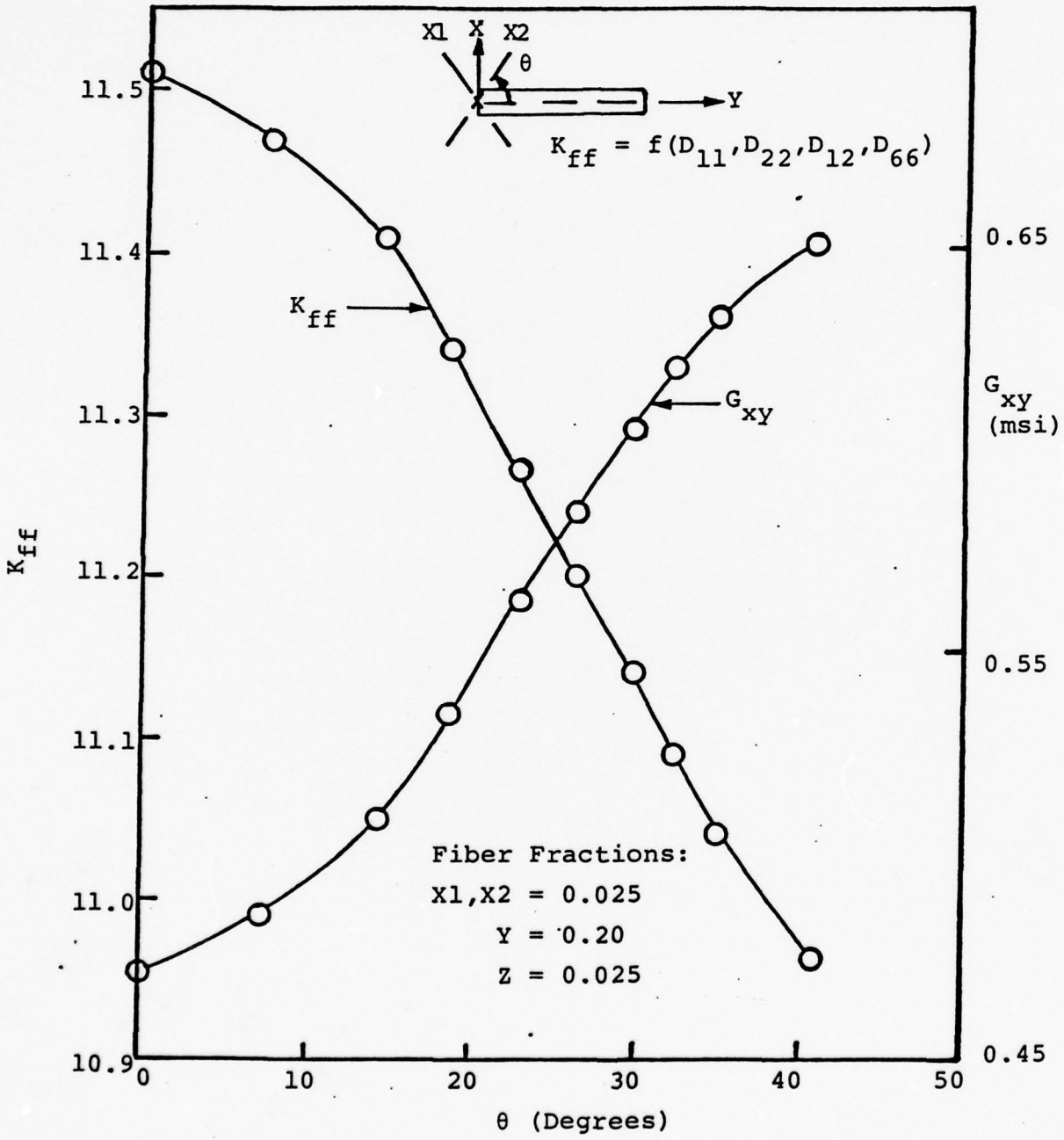

Figure 1. Variation of Structural Performance (K_{ff}) and a Measure of Impact Resistance (G_{xy}) with θ for a Fixed Fiber Volume Fraction

Table 1.* Variation of a Measure of Impact Resistance-to-Structural Performance Ratio with θ.

θ degrees	K_{ff}	G_{xy} (msi)	G_{xy}/K_{ff} (ksi)
5	11.51	0.471	40.92
9.8	11.47	0.487	42.46
14.5	11.41	0.510	44.70
18.9	11.34	0.536	47.27
22.9	11.27	0.563	49.96
26.6	11.20	0.587	52.41
29.8	11.14	0.607	54.49
32.7	11.09	0.622	56.09
35.3	11.04	0.634	57.43
40.9	10.96	0.651	59.40

*Fiber volume fraction in the X1, X2 directions = .025
Fiber volume fraction in the Y-direction = .20
Fiber volume fraction in the Z-direction = .025
Matrix volume fraction = 0.75
Thickness of 4-D panel = 0.1 inch
K_{ff} is the buckling coefficient for an infinitely long plate, fixed on all sides (see text).

Table 2.* Effect of Fiber Volume Fraction on Panel Properties

Fiber volume fractions in the various directions

X1, X2	Y	Z	K_{ff}	G_{xy} (msi)	G_{xy}/K_{ff} (ksi)
.015	.200	0.025	11.51	0.471	40.92
.0375	.1875	0.025	11.50	0.474	41.22
.050	.1750	0.025	11.49	0.476	41.43
.0625	.1625	0.025	11.49	0.479	41.69
.075	.1500	0.025	11.48	0.482	41.99

*θ = 5°

Matrix volume fraction = .75

Table 3. Properties of All T-300 and T-300 Hybrid Panels

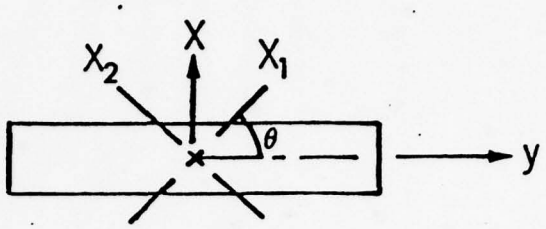

Fiber Volume Fractions = 20%, Y
18%, Z
6%, X1, X2

Material	θ	E_y (ksi)	E_z (ksi)	G_{yz}	K_{ff}	K_{ff}/D_{22}	G_{yx}/K_{ff}
All T-300	20	8.98	7.15	0.78	5.88	3519	132.5
	32	8.36	7.18	0.77	5.68	3411	136.3
	45	7.88	7.22	0.77	5.54	3344	138.7
T-300/ Kevlar	20	8.32	7.08	0.73	5.70	3372	128.3
	32	7.97	7.09	0.73	5.58	3310	130.8
	45	7.69	7.12	0.73	5.50	3260	132.8
T-300/ Glass	20	8.14	7.24	0.79	5.65	3425	140.4
	32	7.97	7.24	0.79	5.60	3392	141.9
	45	7.83	7.26	0.79	5.55	3372	143.2

Table 4. Equivalent 2-D/4-D Panel Designs for FMI Panel #2271

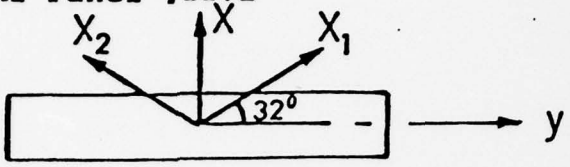

Panel #2271

Fiber Volume Fractions; Y = 0.20, Z = 0.18,
X1, X2 = 0.06

Panel Thickness = 0.113"

Panel Properties

E_x = 1.65 msi G_{xy} = .97 msi

E_y = 8.47 msi G_{xz} = .58 msi

E_z = 7.19 msi G_{yz} = .69 msi

$K_{ff}D_{22}$ = 4885 lb/in

If Thickness Reduced to 0.091 then $K_{ff}D_{22}$ = 2580 lb/in

Equivalent 2-D Laminate

$(0_2/\pm45_2/90)_s$ Thickness = 0.077

E_y = 9.03 msi

E_z = 6.55 msi

G_{yz} = 3.54 msi

$K_{ff}D_{22}$ = 2580 lb/in

Table 5. Properties and Equivalent Laminates for Current FMI Panel.

Panel Geometry

Fiber Volume Fractions: 18%, Y and Z
2%, X1 and X2

Total Fiber Content = 40%

Thickness = 0.151 as woven
= 0.112 after densification

Fiber orientation, θ = ±32° as woven
±27° after fabrication

Properties	$\theta = \pm 32^0$	$\theta = \pm 27^0$	Equivalent* Laminate
E_y	7.53	7.70	10.19
E_z	7.10	7.10	6.98
G_{yz}	0.74	0.74	3.08
h	0.112	0.112	0.0935
$K_{ff}D_{22}$	4554.7	4597.0	4495.7

*Equivalent Laminate Layup:

$(0/90/\pm45/0/\pm45/0/90_{1/2})_s$

APPENDIX B

Plate Impact Tests

Final Report Submitted by

Effects Technology, Inc.

EFFECTS TECHNOLOGY, INC.
A SUBSIDIARY OF FLOW GENERAL INC.
5383 HOLLISTER AVENUE • SANTA BARBARA, CALIFORNIA 93111 • TELEPHONE (805) 964-9831 • TELEX NO. 658 440

6 November 1978

Fiber Materials, Incorporated
Biddeford Industrial Park
Biddeford, Maine 04005

Attention: Mr. John Herrick

Subject: Results of Instrumented Impact Testing on Advanced Composite Materials, P.O. 14815

By: R. Globus

This report reviews the results of sixteen (16) impact tests conducted on panels made of composite materials using advanced fabricational techniques.

Materials

Four different fabrication processes were investigated during this program. Panels 1487 were constructed with a conventional two dimensional (2D) layup of graphite epoxy and served as the basis of comparison for the other fabricational techniques. Panels 4237 were fabricated with a three dimensional (3D) layup of graphite epoxy with the fiber directions mutually perpendicular. Panels 4238 were fabricated with a four dimensional (4D) layup of graphite epoxy with the graphite fibers oriented in the thickness direction at angles of $\pm\theta°$ to the direction normal to the plane of the panel. Panels 4239 were fabricated the same way as panels 4238 except that the fibers in the $\pm\theta°$ directions were Kevlar instead of graphite.

Four panels, each approximately 4.75 inches square, were tested for each fabrication process to obtain a damage gradient in the materials. Panel thicknesses were not uniform, (panels 1487 were approximately 0.084 inches thick, while panels 4237 were approximately 0.163 inches thick) and therefore comparisons among the different fabrication processes had to account for thickness variations by normalizing the data to a thickness parameter.

Summary

The 3D orthogonally fabricated panels were the most impact damage resistant of all the panels tested. With the data normalized to reflect equivalent material thicknesses, these panels required 60% more energy to cause incipient damage, and 80% more energy to cause total panel penetration than the baseline 2D graphite epoxy. The next most effective, damage resistant material was the 4D material having Kevlar as the reinforcement in the off axis thickness directions. Again, with the thickness effect normalized, these panels absorbed 50% more energy to initiate incipient damage and 20% more energy to cause total panel penetration than the baseline material. Panels 4238 did not provide the energy absorbing improvements as the other two groups of advanced panels. The normalized incipient energy level was the same as the baseline material and its through penetration energy level was 36% less than the baseline panel.

In addition to comparing the tested panels among themselves, the results were also compared with published data* on the impact behavior of 16 ply AS3501-5 graphite epoxy. This comparison, after accounting for size and thickness variations, indicates that all panels appear to be more impact resistant than AS3501-5. The improvement in energy required to cause incipient damage ranged from 13% for panels 4238 to 86% for panels 4237.

Another measure of impact performance is the ability of the material to contain damage within a localized region. Damage containment is important because of ease of repair considerations. In this regard, all of the multidimensional (3D and 4D) panels performed very well. Whereas, the 2D panels, 1487, had extensive crack growth at the rear surface of the panel under severe impact conditions, the other panels, because

*Aleszka, J. C. and R. Globus, "Service/Maintainability of Advanced Composite Structures (SMACS), Testing and Evaluation", Effects Technology, Incorporated, 31 March 1978.

of the reinforcement in the thickness direction contained the damage to an area approximately the size of the impactor. It should be noted that conventional 2D graphite epoxy material, when fabricated with woven plies in place of unidirectional tape also exhibits excellent damage containment properties.

Test Setup

The drop tower system shown on the left hand side of Figure 1 was used for these tests. The test fixture, shown in Figure 2, was used to clamp the panels in place during the tests. "C" clamps were used around the perimeter of the fixture to sandwich the panels in the fixture. The fixture dimensions yielded an unsupported, three (3) inch square area in the middle of the panels. All impacts were at the center of the three inch square area.

A crosshead weight of 137 lbs. was used in the drop tower except for the thru penetration test on panel 4237 where a 270 lb. crosshead weight was needed to assure complete panel penetration. For all tests the crosshead was dropped from a height of three (3) inches yielding an impact velocity of 3.9 ft/sec. A braking system was employed to ensure a single impact of the impactor with the specimen.

The impactor used in these tests was a 0.625 inch diameter steel hemisphere. The shank of the impactor fits into a specially instrumented tup which provided load vs. time and energy vs. time histories of the impact event. The ETI Model 300 System was used to record and analyze the test data. This system automatically digitizes, analyzes and prints hard copy records of the impact test.

Test Procedure

Four (4) panels of each construction type were supplied by FMI, for a total of sixteen (16) panels. Each panel was subjected to one impact test at its center point. The first impact test for each type of panel construction was a thru penetration test (panel 4237-1 was an exception since there was not enough energy available in the drop tower

FIGURE B–1

DROP WEIGHT SYSTEMS

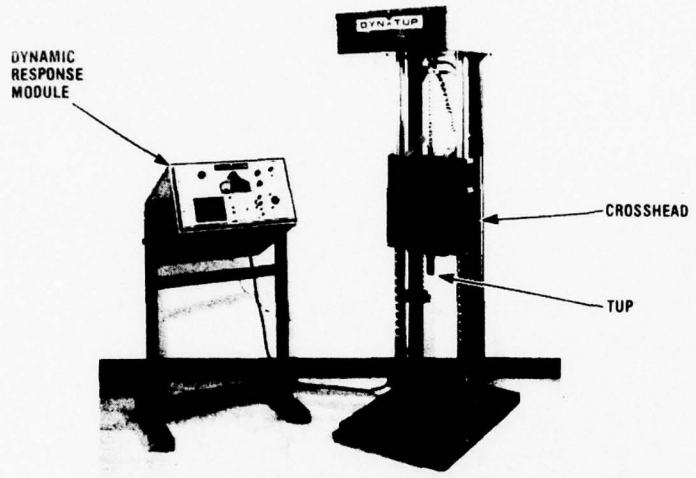

DROP TOWER WITH DYNAMIC RESPONSE MODULE

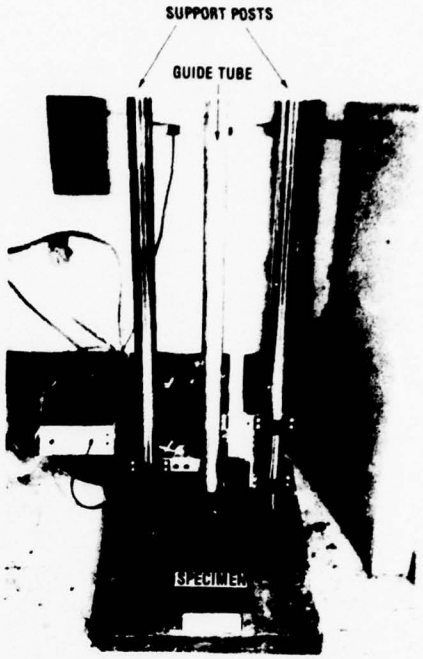

LOWER PORTION OF GUIDE TUBE

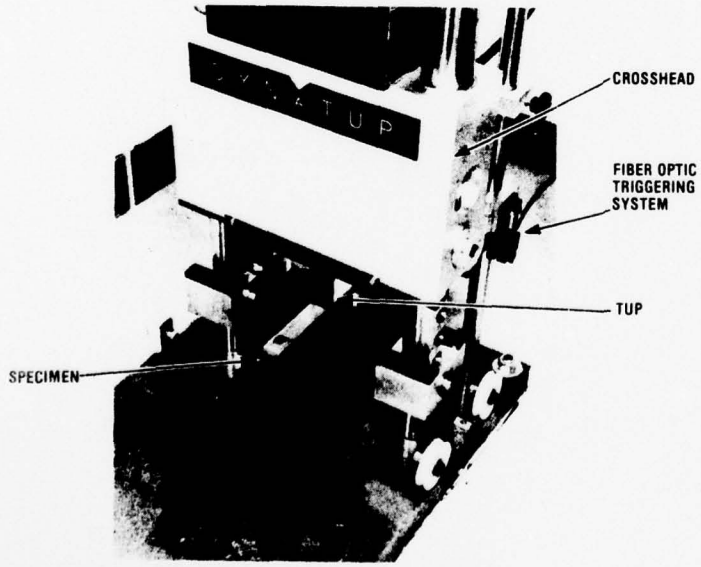

LOWER PORTION OF DROP TOWER

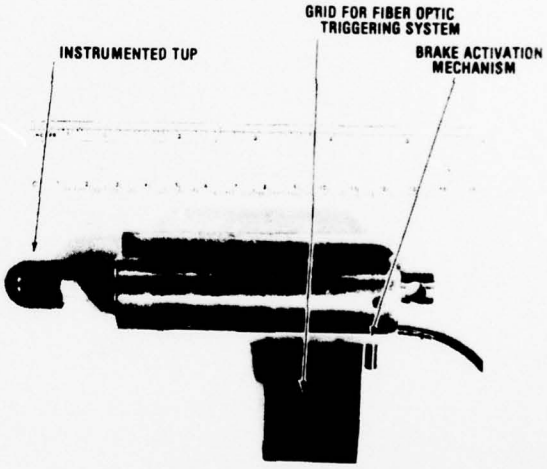

GUIDE TUBE INDENTER

DROP TOWER CAPABILITIES

DROP WEIGHT: 73 LBS. TO 1000 LBS.

DROP HEIGHT: 0.1 IN. TO 3 FEET (0.7 FT./SEC. TO 12.6 FT./SEC.)

DELIVERED ENERGY: 0.5 FT. LBS. TO 2000 FT. LBS.

MAXIMUM WIDTH OF SPECIMEN: 24 INCHES

GUIDE TUBE CAPABILITIES

DROP WEIGHT: 0.5 LBS TO 10 LBS.

DROP HEIGHT: 0.1 IN. TO 9.5 FEET (0.7 FT./SEC. TO 22 FT./SEC.)

DELIVERED ENERGY: 0.05 IN. LBS. TO 75 FT. LBS.

MAXIMUM WIDTH OF SPECIMEN: 20 INCHES

FIGURE B-2

CONFIGURATION FOR IMPACT TESTS

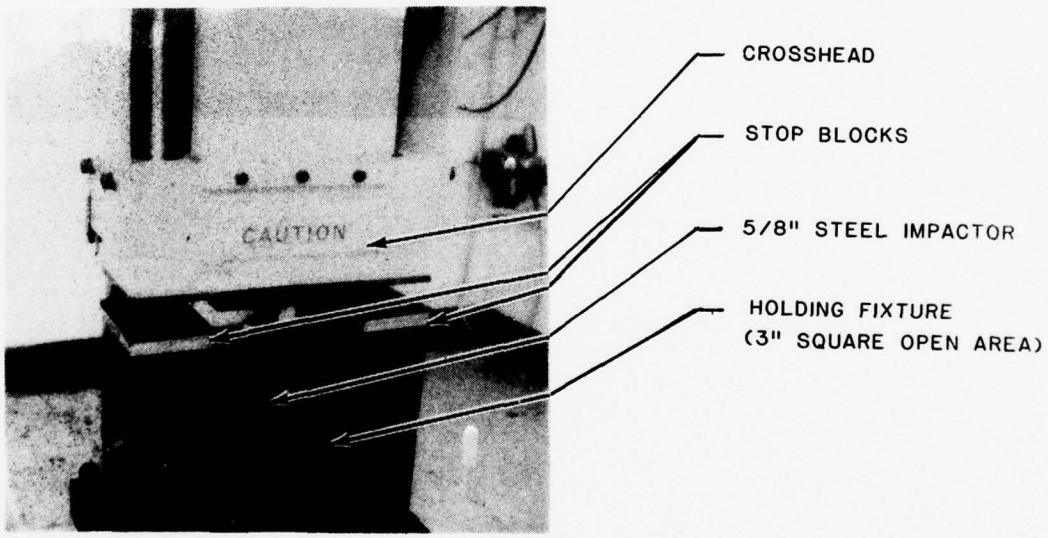

to totally penetrate the panel; therefore, the crosshead weight was increased to 270 lbs and the test on panel 4237-2 was the thru penetration test for this material). Evaluation of the load and energy versus time histories produced by the thru penetration test allowed a determination of incipient damage information to be made. Specifically, the first discontinuity on the load versus time trace has been shown to correspond to incipient visible damage in composite panels. This incipient damage usually corresponds to matrix cracking (crazing on the rear surface) or interlaminar failure in the plies. The peak load point has been shown to correspond to the beginning of significant fiber breakage in conventionally laminated graphite epoxy.

Part of the automatic data reduction process in the Model 300 System includes the deflection versus time history of the impact event. Therefore, the deflection required to cause incipient damage and peak load is immediately available from the evaluation of the thru penetration test. Shims can then be placed in the drop tower support posts to limit panel deflection to predetermined levels so that damage mechanisms corresponding to specific features of the load/time histories can be studied. For each type of fabrication method examined in this program the four impact tests corresponded to: 1) thru penetration, 2) incipient damage, 3) peak load and 4) between peak load and thru penetration. In this manner, a damage gradient was obtained for each material spanning the entire range of damage mechanisms.

Subsequent to test performance, the panels were visually inspected, front surface indentation measured and photographs taken of the post test condition of the panels. From the load and energy histories, the following parameters were obtained: 1) load at incipient damage, P_I, 2) energy absorbed to incipient damage, E_I, 3) maximum load, P_{MAX}, 4) energy absorbed to maximum load, E_{MAX} and 5) total absorbed energy, E_T.

Results and Evaluation

The traces obtained from the thru penetration tests on the four different types of panels are shown in Figure 3. The load history shown for panel 1487 is typical of the response of 2D laminated graphite epoxy panels. At the incipient damage point, there is a brief but distinctive discontinuity in the load trace. The load then continues to increase until P_{MAX} is reached. At that point there is a sudden and major drop in the load carrying ability of the panel. Subsequent to peak load, there is continued fiber breakage in the panel as evidenced by the high frequency oscillations in the load trace. Finally the impactor penetrates the entire panel and the load trace returns to zero. The energy values corresponding to any feature in the load trace are easily determined by directly reading the value on the energy scale.

The characteristics of the load histories for the 3D and 4D fabricated panels were significantly different than the characteristics of the 1487 panels. Each of the materials exhibited an incipient damage point in a similar manner to the 2D panel but the response around the peak load value changed. Instead of a distinct peak and then a sudden drop, these materials really had no distinct peak load value, but instead the load curve had a relatively "flat top" which appears to indicate that the reinforcements in the thickness directions "tie" the panel together and prevent a major loss in load carrying ability at peak load. This region of panel response absorbs a large portion of the total energy imparted to these 3D and 4D fabricated materials.

Visually, the 3D and 4D panels contained the damage much more effectively than the 2D panels. For severe impacts on the 2D panels, the rear surface graphite epoxy plies were split along almost the entire length of unsupported material. The 3D and 4D panels appeared to suffer damage only in a region the size of the impactor diameter. This damage containment was undoubtedly caused by the reinforcements through the thickness directions, which acted as crack arresters during the impact event. Previous

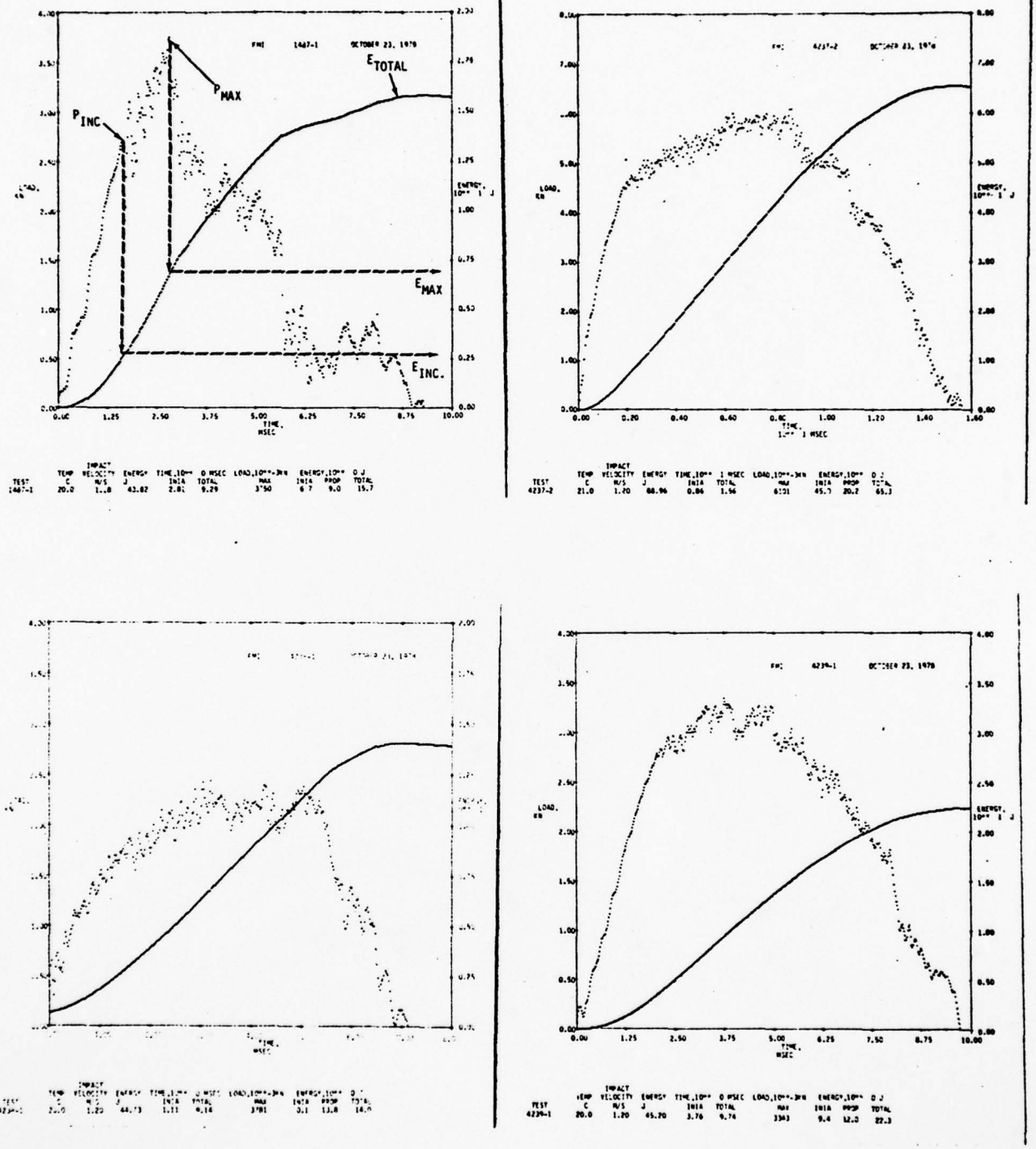

FIGURE 3

DATA TRACES FOR THRU PENETRATION TESTS

testing with woven graphite epoxy panels, in which each ply of the material has reinforcements in perpendicular directions in the plane of the panel also yielded similar damage containment properties. Damage containment is significant for advanced composite materials since it makes field repair simpler and therefore less costly.

The quantitative test results are summarized in Table 1. The table lists for each panel type, the load and energy values corresponding to incipient damage and peak load. Under each column of load (or energy), the average, $\bar{X}$, the standard deviation, σ, and the coefficient of variation, C.V. values are listed. It is apparent from this table that the 3D orthogonal graphite epoxy material possessed, by far, the best impact resistance of any of the materials tested. In addition, the energy required for thru penetration, E_T, was three to four times greater than for the other materials. However, this material was approximately twice the thickness of the other panels and material thickness is very important for impact response. Additional comments and evaluation of the thickness effect are included in subsequent paragraphs.

Other observations which can be made by examination of Table 1 include:

1. The load at incipient damage for the 2D and 4D materials are within 10% of each other. The energy required to initiate damage for the 4D panels was 50% to 80% greater than for the 2D panel. This combination of greater energy for equal load levels implies that the 4D panels were not as stiff as the 2D panels under impact conditions.

2. The C.V. values for incipient damage are greater than those corresponding to peak load. It is hypothesized that since the incipient damage mode is associated with matrix response, there should be more variation in incipient damage values since processing variables primarily affect the matrix properties.

TABLE 1

RESULTS OF IMPACT TESTS

PANEL NO.	P_{INC} $\bar{X}$ LBS.	P_{INC} σ LBS.	P_{INC} C.V. (%)	E_{INC} $\bar{X}$ FT. LBS.	E_{INC} σ FT. LBS.	E_{INC} C.V. (%)	P_{MAX} $\bar{X}$ LBS.	P_{MAX} LBS.	P_{MAX} C.V. (%)	E_{MAX} $\bar{X}$ FT. LBS.	E_{MAX} σ FT. LBS.	E_{MAX} C.V. (%)
1487 (2D Gr/Ep)	500	90	18	1.43	0.39	27	830	17	2.0	4.73	0.15	3.2
4237 (3D Orthog. Gr/Ep)	1050	19	1.8	5.35	0.70	13	1358	54	4.0	28	5.34	19
4238 (4D Gr/Ep)	498	77	15	1.93	0.40	21	596	82	14	5.37	0.64	12
4239 (4D Gr/Ep, Kev/Ep)	566	51	9.0	2.57	0.25	9.7	710	39	5.5	6.87	1.27	18

3. The C.V. values for P_{MAX} are quite low and are probably associated with the fact that fiber properties are very reproducible within a single batch of material

4. The C.V. value for E_{MAX} for panels 1487 is much lower than the E_{MAX} C.V. values for the 3D and 4D panels. This was probably caused by the "flat topped" nature of the load curve for these panels. That is, peak load could occur at any point along the flat top and therefore the energy at peak load could vary substantially even though the P_{MAX} value is quite consistent.

Since panel thickness is known to be an important parameter affecting impact performance, an attempt was made to normalize the thickness effect out of the test results. Data presented in the previously cited reference includes the energy to cause incipient damage as a function of panel thickness for AS3501-5 graphite epoxy. Evaluation of that data shows that the energy required to initiate damage in A53501-5 can be represented by the following equation

$$E_{INC} = 48t^{1.29}$$

where E_{INC} is the incipient damage energy in ft. lbs. and t the panel thickness in inches. It was assumed that the energy parameters evaluated in the current program are thickness dependent in the same manner; that is, by knowing an energy value of a material with a thickness t_a, the energy value of similar material with thickness t_B, may be found from the relation,

$$E_{t=t_B} = \left(\frac{t_B}{t_a}\right)^{1.29} E_{t=t_a}$$

This relation was used to normalize all the energy values obtained in the current testing program. Table 2 lists the "corrected" energy values using the average thickness of the 1487 panels as the baseline. The "corrected" values were then normalized by dividing the 3D and 4D panel energy levels by the values of the baseline 2D panel (1487).

The table shows that the 3D orthogonal panel (4237) was still the most impact resistant material, but the differences are not as great as they were before correcting for thickness effects. In fact, panel 4238 made from 4D graphi-e epoxy is now equal to the baseline material for incipient damage energy and is worse for the other energy parameters (E_{MAX} and E_T). The 4D panel with Kevlar epoxy reinforcement in the thickness direction (4239) requires 50% more energy to cause incipient damage, and 20% more energy at peak load and thru penetration than the 1487 material.

TABLE 2

COMPARISON OF FMI DATA USING
THICKNESS CORRECTION ($t^{1.29}$)
(Panel 1487 Used as Baseline)

PANEL NO.	ENERGY VALUES WITH THICKNESS CORRECTION			NORMALIZED VALUES		
	$E_{I_{AVG.}}$ (FT. LBS.)	$E_{MAX_{AVG.}}$ (FT. LBS.)	E_T (FT. LBS.)	E_I	E_{MAX}	E_T
1487 (2D Gr/Ep)	1.43	4.73	11.6	1.0	1.0	1.0
4237 (3D Orthog. Gr/Ep)	2.27	12.0	20.5	1.6	2.5	1.8
4238 (4D Gr/Ep)	1.38	3.85	7.4	1.0	0.81	0.64
4239 (4D Gr/Ep, Kev/Ep)	2.10	5.64	14.2	1.5	1.2	1.2

AD-A068 517 FIBER MATERIALS INC BIDDEFORD MAINE F/G 11/4
ADVANCED IMPACT RESISTANT MULTIDIMENSIONAL COMPOSITES.(U)
JAN 79 J W HERRICK N00019-77-C-0430
UNCLASSIFIED FR-79-1-3 NL

2 OF 2
AD
A068517

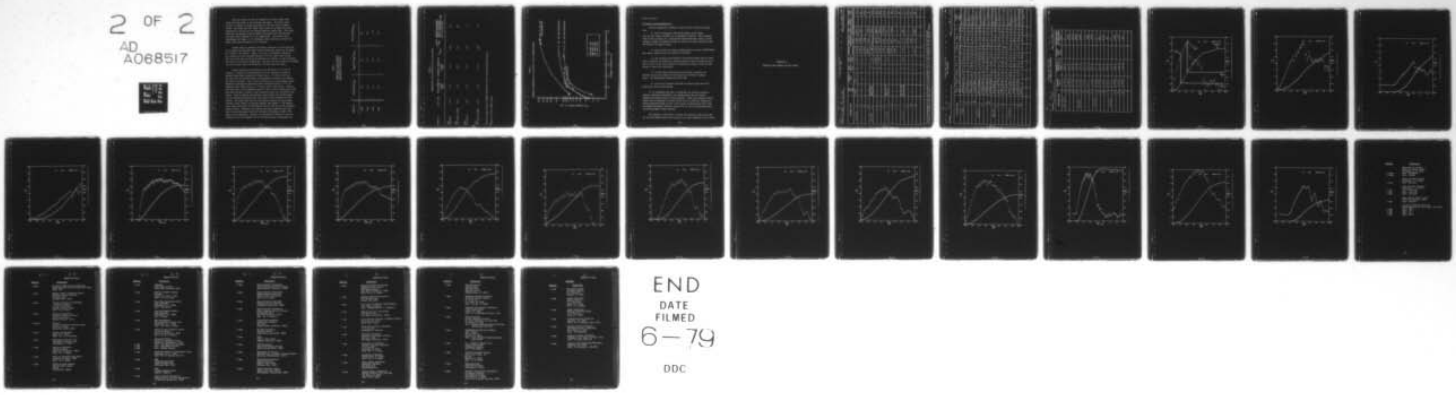

END
DATE
FILMED
6-79
DDC

The test results can also be compared on an equal weight basis (equal thickness basis if the densities are equal). The values shown in Table 3 compare the energy parameters for the four types of panels tested. The energy per unit weight values shown in the table have been normalized to the data for the baseline material, panels 1487. This table shows the same general trends as Table 2 but panels 4237 and 4239 seem even better when compared on a unit weight basis. This results from normalizing with respect to the thickness (since densities are about the same) rather than thickness to the 1.29 power.

Another means of comparing the impact resistance of these materials is to compare the permanent front surface indentation induced in the panels as a result of the impact. Figure 4 is a plot of permanent indentation as a function of total absorbed energy for the four panel types tested. The curves show that the 3D and 4D materials are superior to the 2D material with respect to permanent indentation. The data for the two types of 4D panels are quite similar while the 3D material is better than all others.

Besides comparing the materials among themselves, it is also of interest to compare all these materials with the existing data base on graphite epoxy panels subjected to impact tests. In order to do this, not only must the thickness effect be evaluated but specimen size effects must also be included. Most of the existing data on 16 ply graphite epoxy (AS3501-5) materials was generated with a specimen having a 5" x 5" unsupported area, rather than a 3" x 3" area, used in this series. However, data does exist on 8 ply graphite epoxy for both 3" and 5" unsupported areas. This data was used to obtain a size correction factor for the present test series. Table 4 compares the incipient energy levels for the FMI panels with the existing data base after accounting for both thickness and size effects. The table shows that all the present materials are more impact resistant (with respect to incipient damage) than AS3501-5. The improvements range from 13% for the 4D graphite epoxy to 86% for the 3D orthogonal graphite epoxy. Obviously, the scaling laws used to generate this data have not been thoroughly tested and therefore differences of 10% or 20% might not be significant. However, the improvements indicated in the performance of the 3D orthogonal and 4D with Kevlar epoxy reinforcement are

TABLE 3

COMPARISON OF FMI MATERIALS
ON AN EQUAL WEIGHT BASIS
(Normalized to 1487 Panel)

PANEL NO.	$(E_I/W)/(E_I/W)_{1487}$	$(E_{MAX}/W)/(E_{MAX}/W)_{1487}$	$(E_T/W)/(E_T/W)_{1487}$
1487	1.0	1.0	1.0
4237	2.1	3.3	2.3
4238	1.1	1.0	.75
4239	1.7	1.4	1.4

TABLE 4

COMPARISON OF FMI MATERIALS WITH 16 PLY AS3501

PANEL NO.	E_I ~FT. LBS.	SIZE CORRECTION FACTOR* (SCF)	THICKNESS CORRECTION FACTOR** (TCF)	$E_{I_{CORR.}} = \frac{E_I * SCF}{TCF}$	PERCENT IMPROVEMENT OVER 16 PLY AS3501 WITH 5" UNSUPPORTED AREA E_I = 2.24 FT. LBS.
1487 (2DGr/Ep)	1.43	1.74	.94	2.65	18
4237 (3D Orthog. Gr/Ep)	5.35	1.74	2.21	4.21	88
4238 (4D Gr/Ep)	1.93	1.74	1.32	2.54	13
4239 (4D Gr/Ep, Kev/Ep)	2.57	1.74	1.15	3.89	74

*Based on impact tests on AS3501 Gr/Ep with 3" and 5" Square Unsupported Areas

**Based on 16 Ply (.088") Gr/Ep

FIGURE 4

PERMANENT DEFORMATION AS A FUNCTION OF TOTAL ABSORBED ENERGY

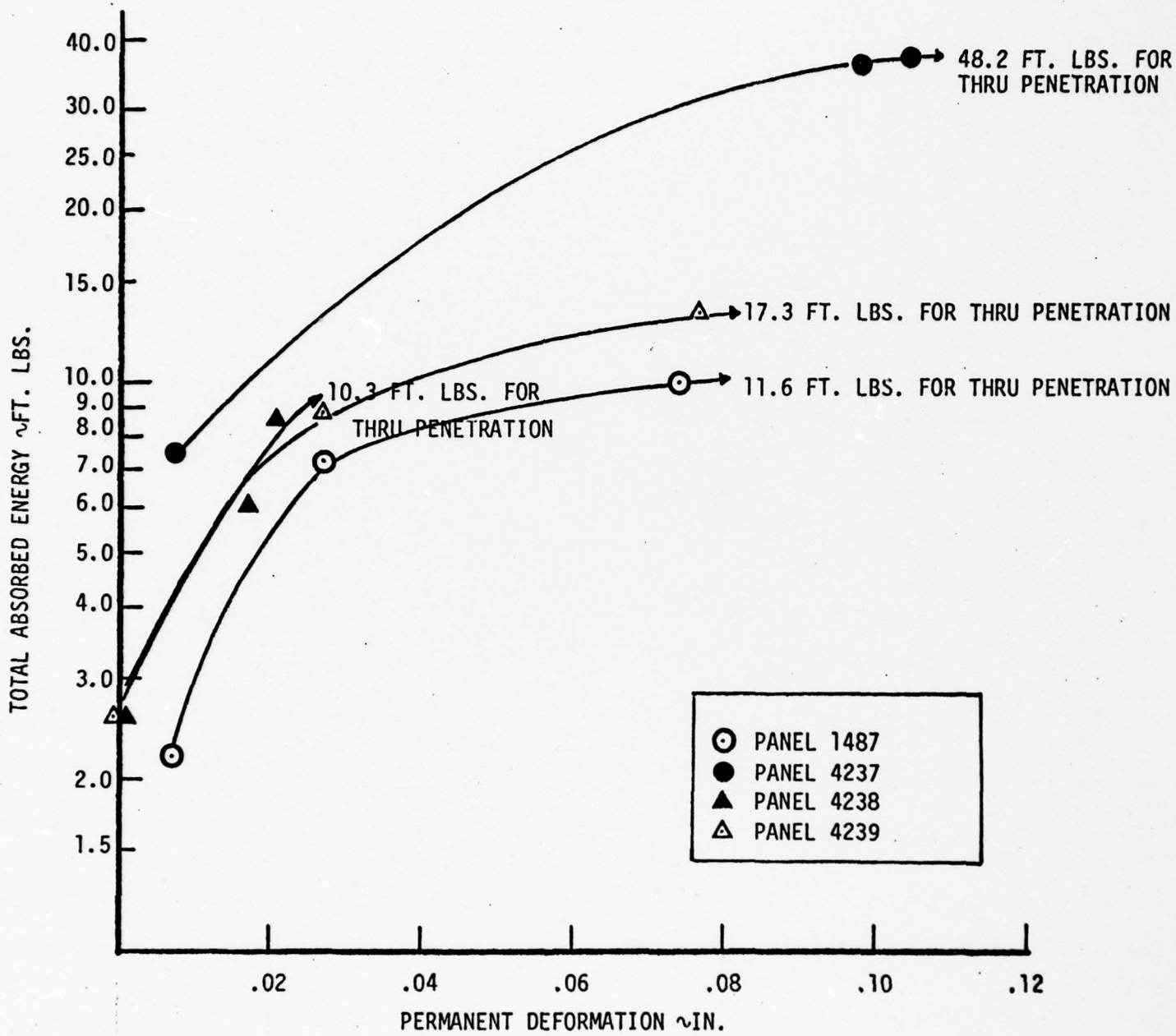

felt to be real.

Conclusions and Recommendations

The most significant findings in this test and evaluation program were:

1) The 3D orthogonally fabricated graphite epoxy panels were the most impact resistant of all materials evaluated. When thickness effects were accounted for, these panels required 60% more energy to cause incipient damage, and 80% more energy to cause total panel penetration than the baseline 2D graphite epoxy.

2) The 4D panels with Kevlar reinforcements were also significantly more impact resistant than the baseline 2D material.

3) The 4D panels with graphite fiber-reinforcements were not more impact resistant (as measured by energy parameters) than the baseline material, in fact, it was less resistant as measured by energy to peak load and energy to cause thru penetration.

4) All FMI panels displayed improved impact resistance (as measured by E_I) when compared to existing data on AS3501-5 graphite epoxy. The improvements ranged from 13% to 86%.

5) All 3D and 4D panels contained the damage region much more effectively than the 2D material.

It is recommended that NDI, fractography and residual mechanical property testing be performed on the damaged panels and the results compared with similar data on virgin material. Other environmental effects should also be addressed in future efforts (such as moisture, fatigue and thermal preconditioning) as well as the issues concerning life cycle costs and weight/performance penalties involved in the use of multidimensionally reinforced graphite epoxy materials.

The appendix of this report contains the laboratory data sheets and the load and energy versus time curves for all tests conducted in this study.

APPENDIX B-1

LABORATORY DATA SHEETS AND TEST TRACES

FRACTURE LAB DATA SHEET
TEST PARAMETERS

CUSTOMER FIBER MAT'LS, INC. DATE 20 OCT. 1983

SPECIMEN CODE	TYPE OF TEST	INDENTER TYPE	DROP HEIGHT (in)	DROP WEIGHT (lbs)	VELOCITY (ft/sec)	DEPTH OF * PENETRATION (mils)	LOAD SETTING (lbs/div)	ENERGY SETTING (ft-lbs/D)	SWEEP TIME (msec/D)
14-87 -1	GR/EP	5/8 BLUNT	3	137	3.87	636	8KN	---	20
-2	"	"	"	"	3.90	258	8KN		8
-3	"	"	"	"	3.90	193	"		20
-4	"	"	"	"	3.90	130	4KN		4
4237 -1	ORTHOG. 3D Gr/EP	"	3	137	3.94	REBOUND	8KN		20
-2	"	"	3	270	3.94	603	8KN		40
-3	"	"	3	137	3.94	417	8KN		40
-4	"	"	"	"	3.94	121	8KN		20
4238 -1	4D OFF AXIS Gr/EP	"	3	137	3.94	588	8KN		20
-2	"	"	"	"	3.94	215	4KN		20
-3	"	"	"	"	3.94	193	"		20
-4	"	"	"	"	"	111	"		8
4239 -1	4D OFF AXIS KEV-Gr/EP	"	3	137	3.94	644	8KN		20
-2	"	"	"	"	"	316	"		20
-3	"	"	"	"	"	230	"		20
-4	"	"	"	"	3.94	109	4KN.		8

*Pre-test measurement of the total travel of the indenter after it makes contact with the specimen. It includes crushing of the stop blocks in the drop tower, but not any compliance in the indenter itself.

FRACTURE LAB DATA SHEET
TEST ANALYSIS

CUSTOMER FMI

DATE 20 Oct. 1978

SPECIMEN CODE	P_{max} (lbs)	$P_{Incip.}$ (lbs)	$E_{Incip.}$ (ft-lbs)	$E_{Max.}$ (ft-lbs)	E_T (ft-lbs)	$t_{Incip.}$ (msec)	t_{max} (msec)	t_T (msec)	DEGREE OF DAMAGE
1487 -1	843	607	1.8	4.9	11.6	1.7	2.8	9.3	THRU PENETRATION R.S BADLY SPLIT
-2	810	521	1.6	4.7	10.0	1.7	3.0	7.0	ALMOST THRU PEN R.S BADLY SPLIT
-3	836	390	0.9	4.6	7.3	1.4	3.1	4.7	F.S. DENT R.S SPLIT
-4	594	480	1.4	2.2	2.2	1.6	2.2	2.2	NO VISIBLE F.S DAM R.S CRAZING
4237 -1	1403	1064	5.2	29.0	37.9	2.1	9.0	16.4	F.S. DENT R.S ⊥ CRACKS
-2	1372	1068	6.3	33.2	48.2	2.4	8.6	15.6	THRU PENETRATION DAMAGE COMBINED
-3	1298	1027	5.3	22.6	35.9	2.3	7.1	13.6	F.S. DENT R.S ⊥ CRACKS
-4	1056	1042	4.6	5.2	7.5	1.8	2.1	2.9	SLIGHT F.S DENT SLIGHT CRAZE R.S
4238 -1	550	418	1.9	5.0	10.3	1.8	4.0	7.0	THRU PENETRATION DAMAGE COMBINED
-2	691	599	2.5	6.1	8.5	2.2	3.6	5.3	F.S. DENT R.S BULGE-CRAZING
-3	546	466	1.6	5.0	6.1	1.7	3.5	4.6	F.S DENT SLIGHT R.S BULGE
-4	579	510	1.7	2.4	2.6	1.9	2.3	2.7	NO VISIBLE F.S DAM SLIGHT CRAZE R.S.
4239- 1	752	622	2.6	7.1	17.3	2.0	3.8	9.7	THRU PENETRATION DAMAGE COMBINED
-2	704	523	2.3	8.0	13.3	2.1	4.5	7.7	F.S DENT R.S BULGE & CRACK
-3	674	554	2.8	5.5	8.8	2.4	4.8	6.7	F.S. DENT R.S INCIPIENT CR.
-4	487	—	—	2.6	2.6	—	2.1	2.7	NO VISIBLE F.S DAM. SLIGHT DISCOLORATION R.S.

FRACTURE LAB DATA SHEET
TEST PARAMETERS (CONTINUED)

Customer FMI

DATE 20 Oct. 1978

SPECIMEN CODE	THICKNESS (in.)	~~RESIDUAL~~ LENGTH ~~(in.)~~ (gms)	RESIDUAL WIDTH (in.)	RESIDUAL DEPTH OF PENETRATION (in.)
14-87 -1	0.093	55.5		—
-2	0.085	52.8		.079
-3	0.077	51.3		.027
-4	0.080	51.8		.007
4237 -1	0.165	96.6		.104
-2	0.165	95.5		—
-3	0.163	95.4		.098
-4	0.162	96.7		.007
4238 -1	0.103	59.0		—
-2	0.108	61.0		.021
-3	0.108	63.0		.017
-4	0.116	66.2		0
4239 -1	0.101	56.3		—
-2	0.098	56.2		.077
-3	0.097	54.0		.027
-4	0.096	55.6		0

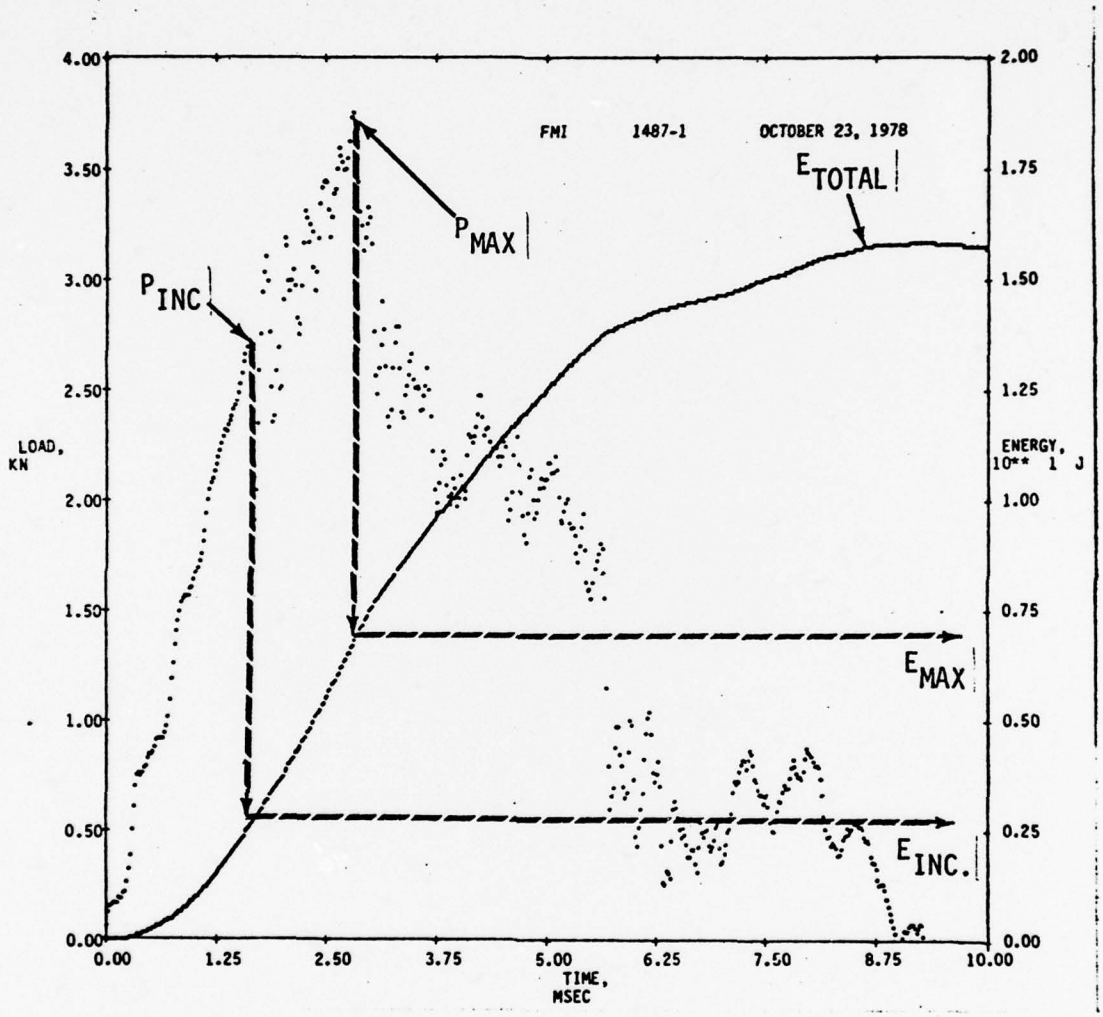
FMI 1487-1 OCTOBER 23, 1978
P_{MAX}
P_{INC}
E_{TOTAL}
E_{MAX}
E_{INC}
LOAD, KN
ENERGY, 10** 1 J
TIME, MSEC
4.00
3.50
3.00
2.50
2.00
1.50
1.00
0.50
0.00
2.00
1.75
1.50
1.25
1.00
0.75
0.50
0.25
0.00
0.00
1.25
2.50
3.75
5.00
6.25
7.50
8.75
10.00

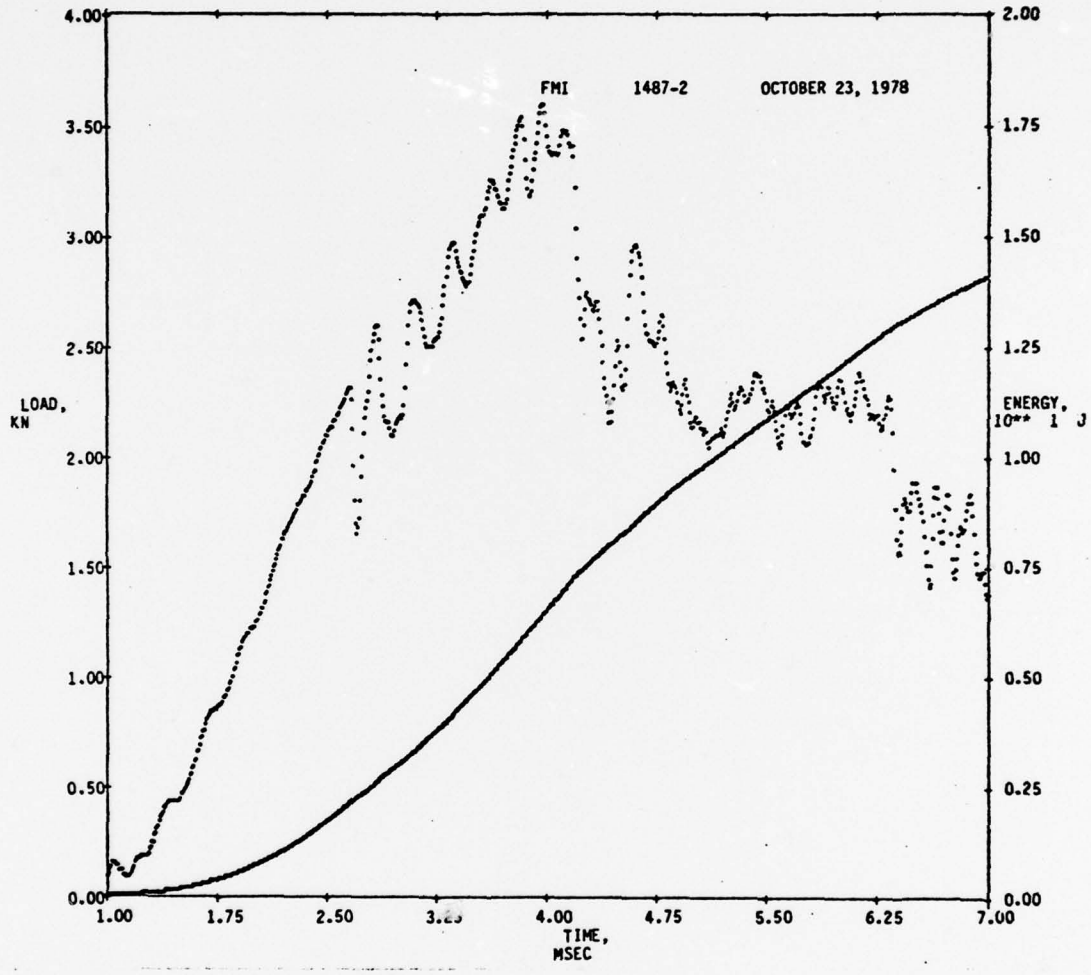
FMI 1487-2 OCTOBER 23, 1978
LOAD, KN
ENERGY, 10** 1 J
TIME, MSEC
4.00
3.50
3.00
2.50
2.00
1.50
1.00
0.50
0.00
2.00
1.75
1.50
1.25
1.00
0.75
0.50
0.25
0.00
1.00
1.75
2.50
4.00
4.75
5.50
6.25
7.00

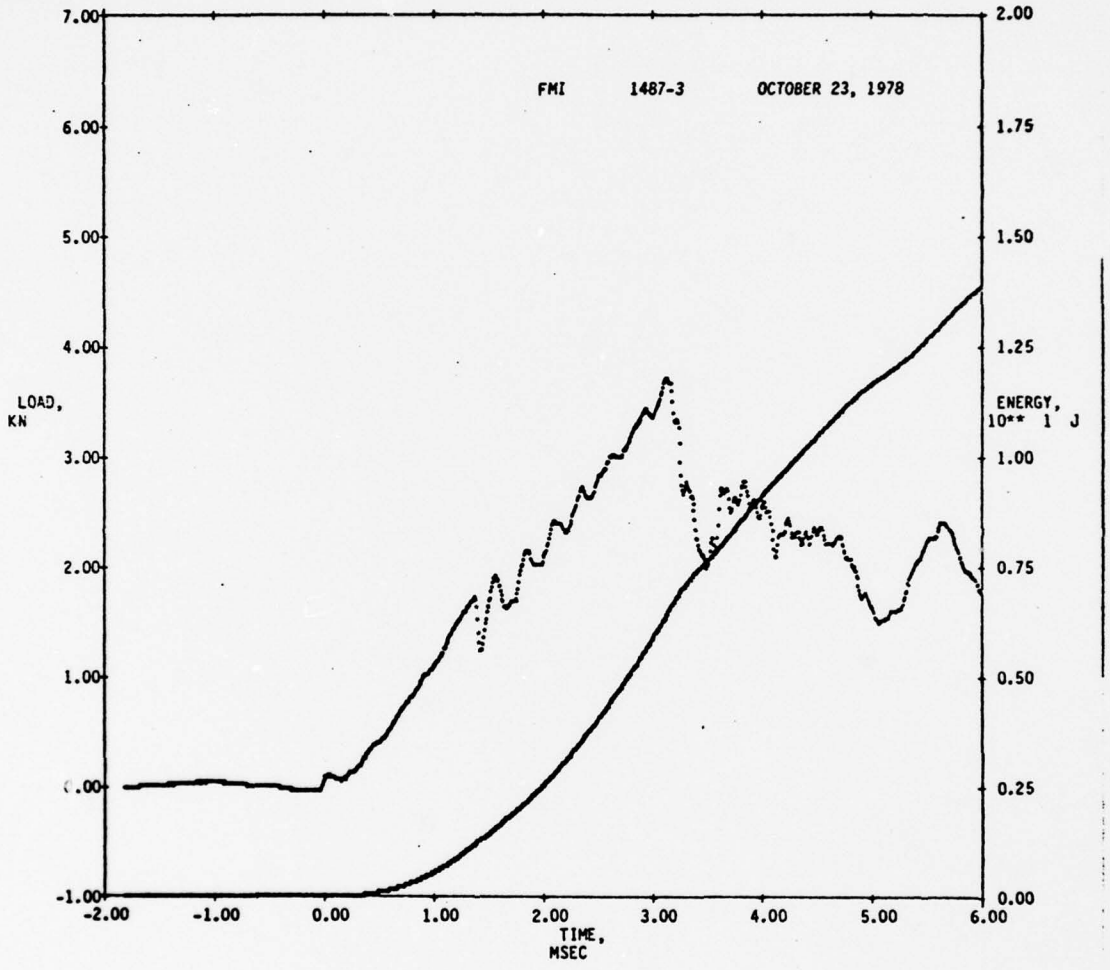
FMI 1487-3 OCTOBER 23, 1978
LOAD, KN
ENERGY, 10** 1 J
TIME, MSEC
7.00
6.00
5.00
4.00
3.00
2.00
1.00
0.00
-1.00
2.00
1.75
1.50
1.25
1.00
0.75
0.50
0.25
0.00
-2.00
-1.00
0.00
1.00
2.00
3.00
4.00
5.00
6.00

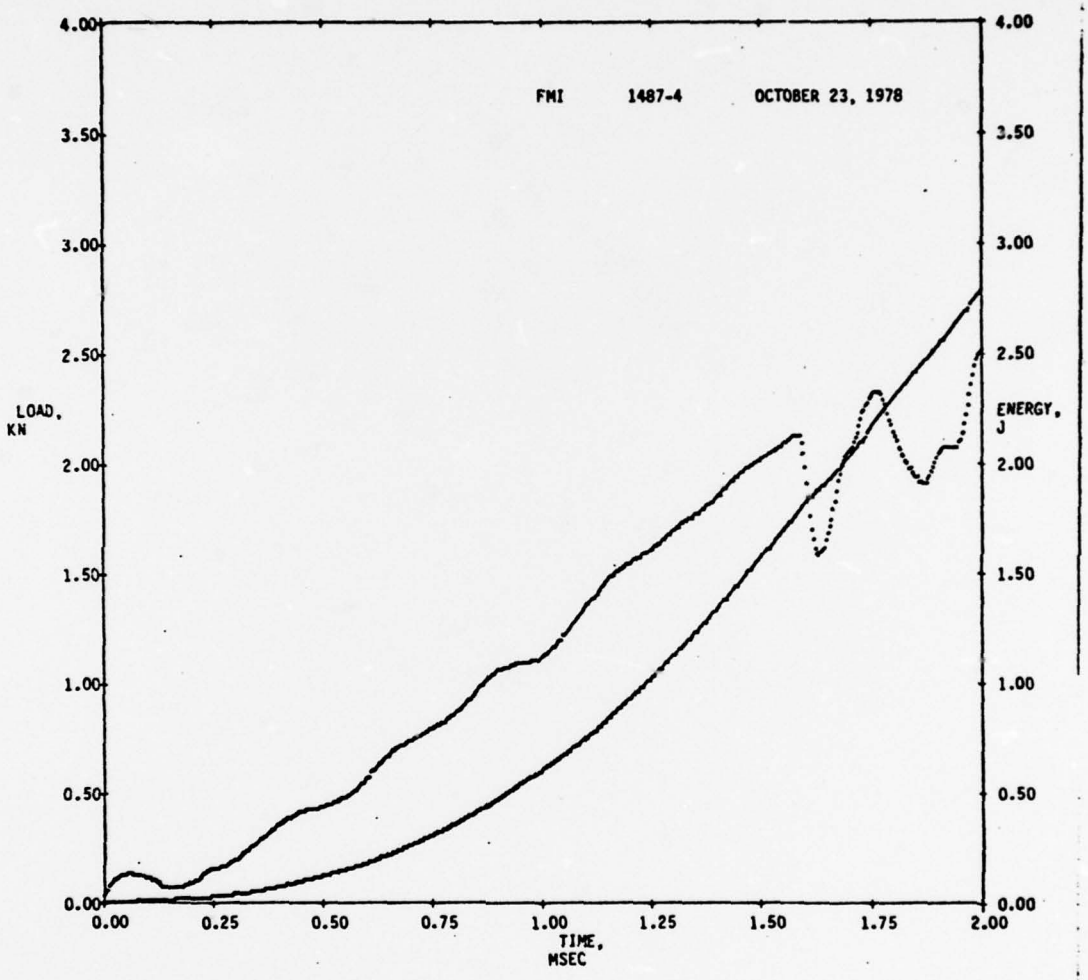
FMI 1487-4 OCTOBER 23, 1978
LOAD, KN
ENERGY, J
TIME, MSEC
4.00
3.50
3.00
2.50
2.00
1.50
1.00
0.50
0.00
0.00
0.25
0.50
0.75
1.00
1.25
1.50
1.75
2.00

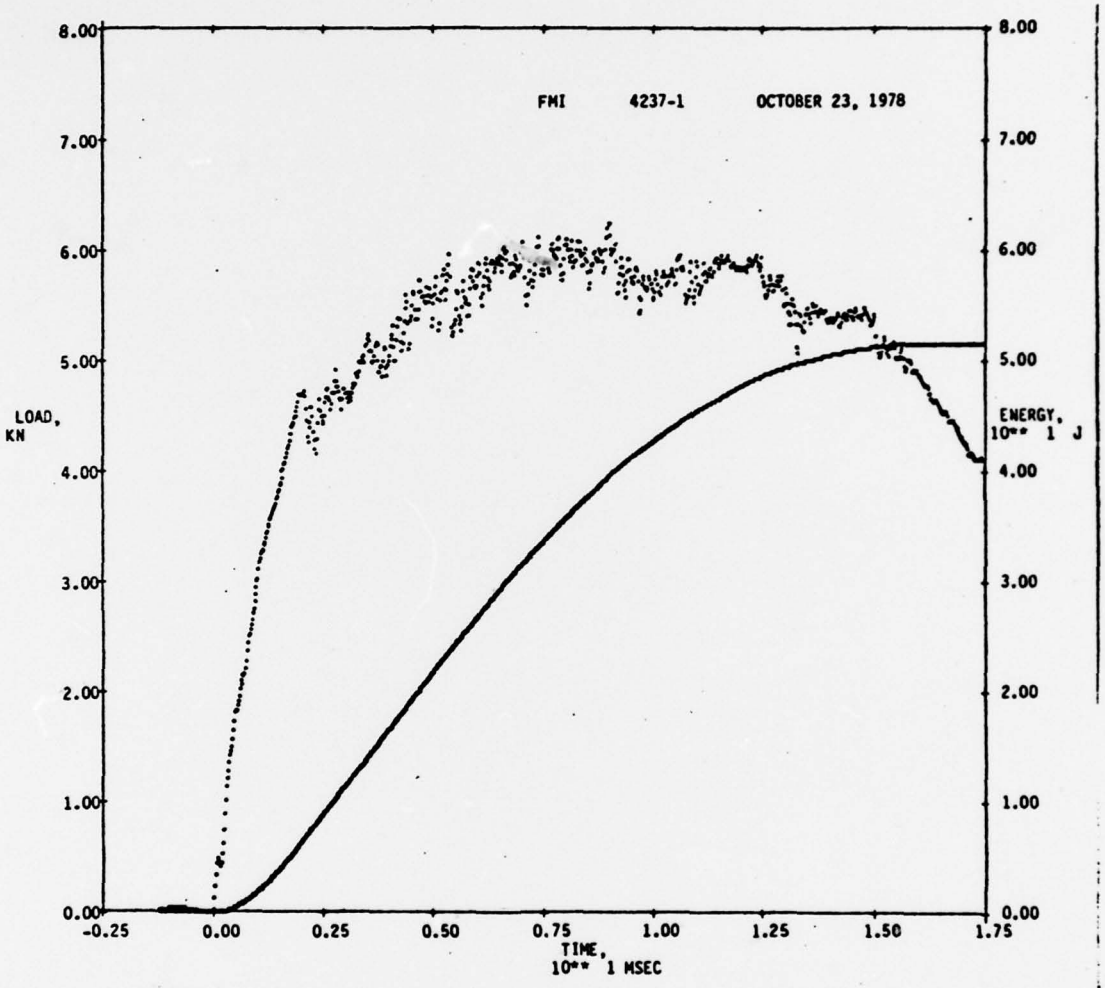
FMI 4237-1 OCTOBER 23, 1978
LOAD, KN
ENERGY, 10** 1 J
TIME, 10** 1 MSEC
8.00
7.00
6.00
5.00
4.00
3.00
2.00
1.00
0.00
-0.25
0.00
0.25
0.50
0.75
1.00
1.25
1.50
1.75

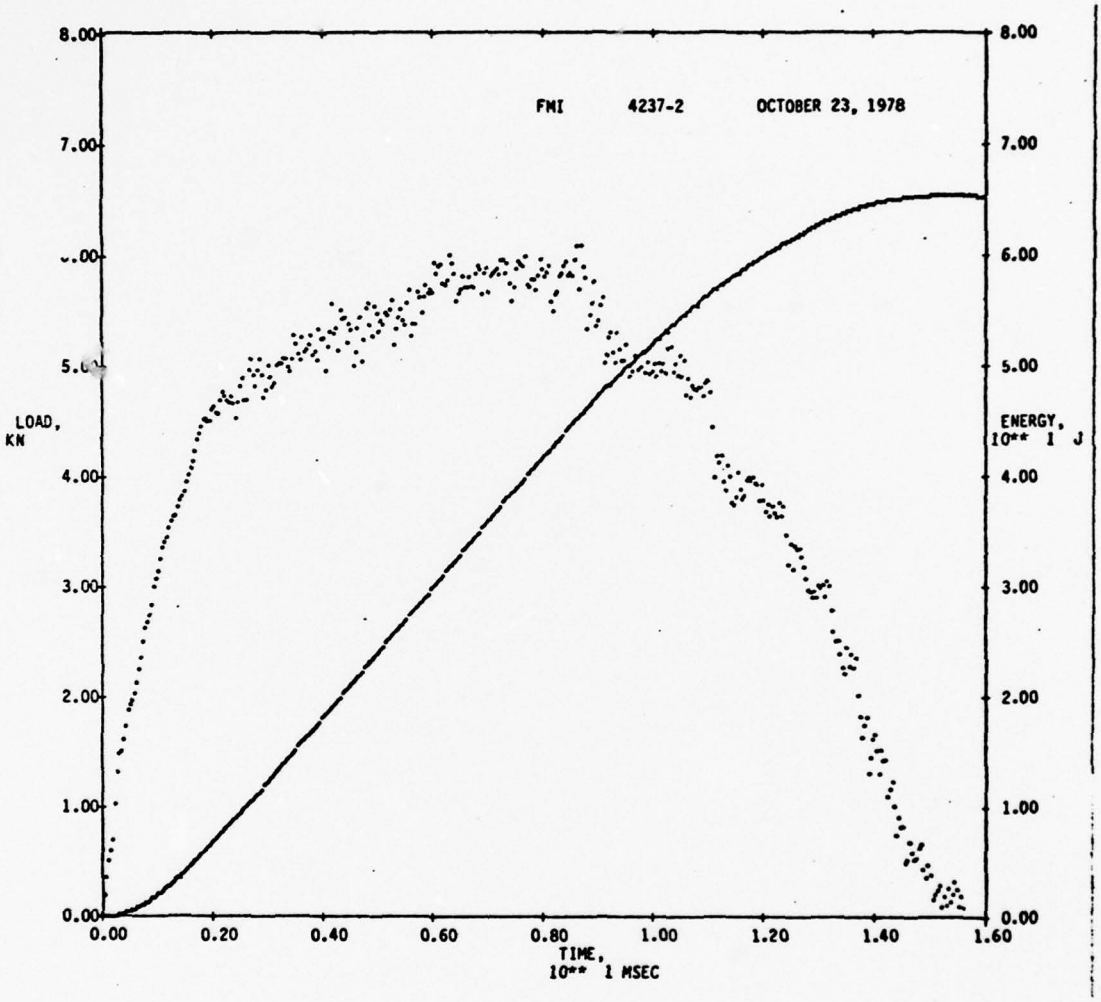
FMI 4237-2 OCTOBER 23, 1978
LOAD, KN
ENERGY, 10** 1 J
TIME, 10** 1 MSEC
8.00
7.00
6.00
5.00
4.00
3.00
2.00
1.00
0.00
0.00
0.20
0.40
0.60
0.80
1.00
1.20
1.40
1.60

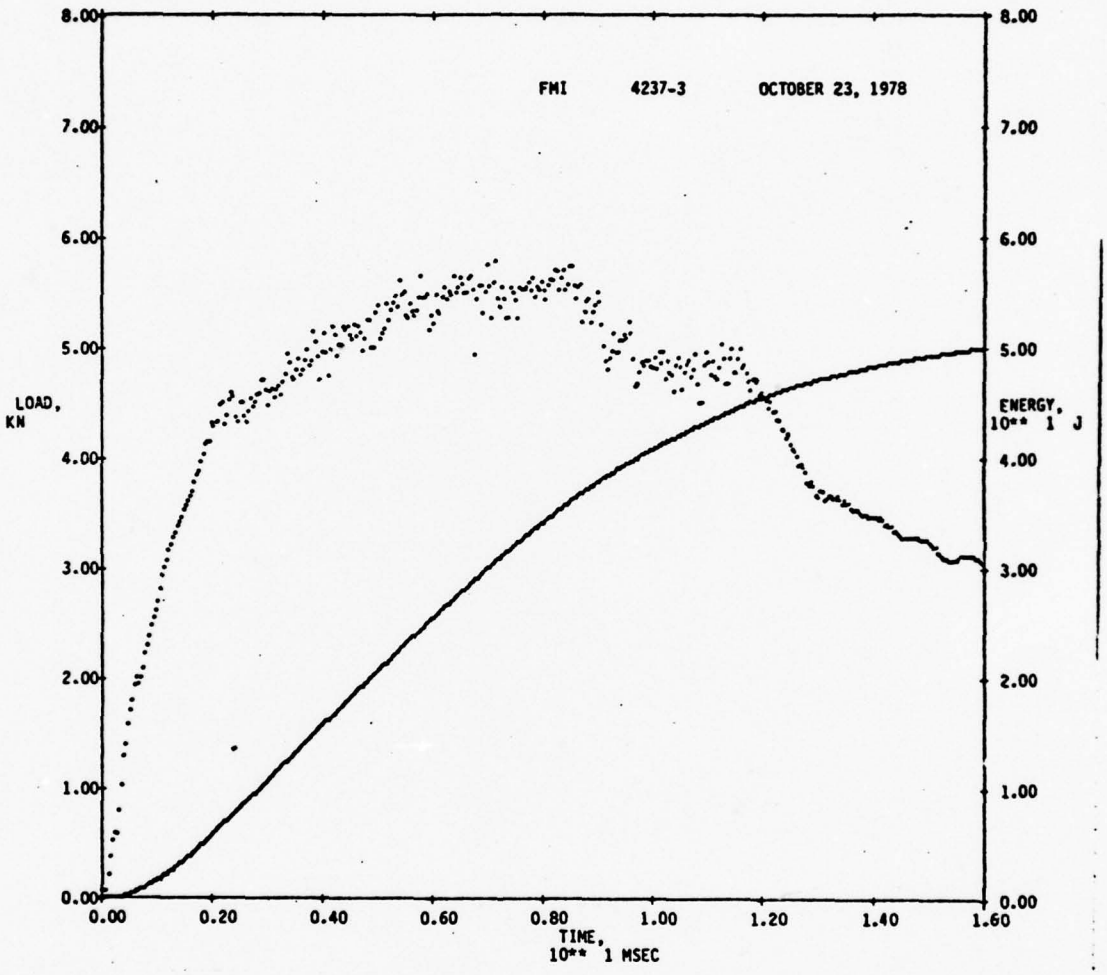
FMI 4237-3 OCTOBER 23, 1978
LOAD, KN
ENERGY, 10** 1 J
TIME, 10** 1 MSEC
8.00
7.00
6.00
5.00
4.00
3.00
2.00
1.00
0.00
0.00
0.20
0.40
0.60
0.80
1.00
1.20
1.40
1.60

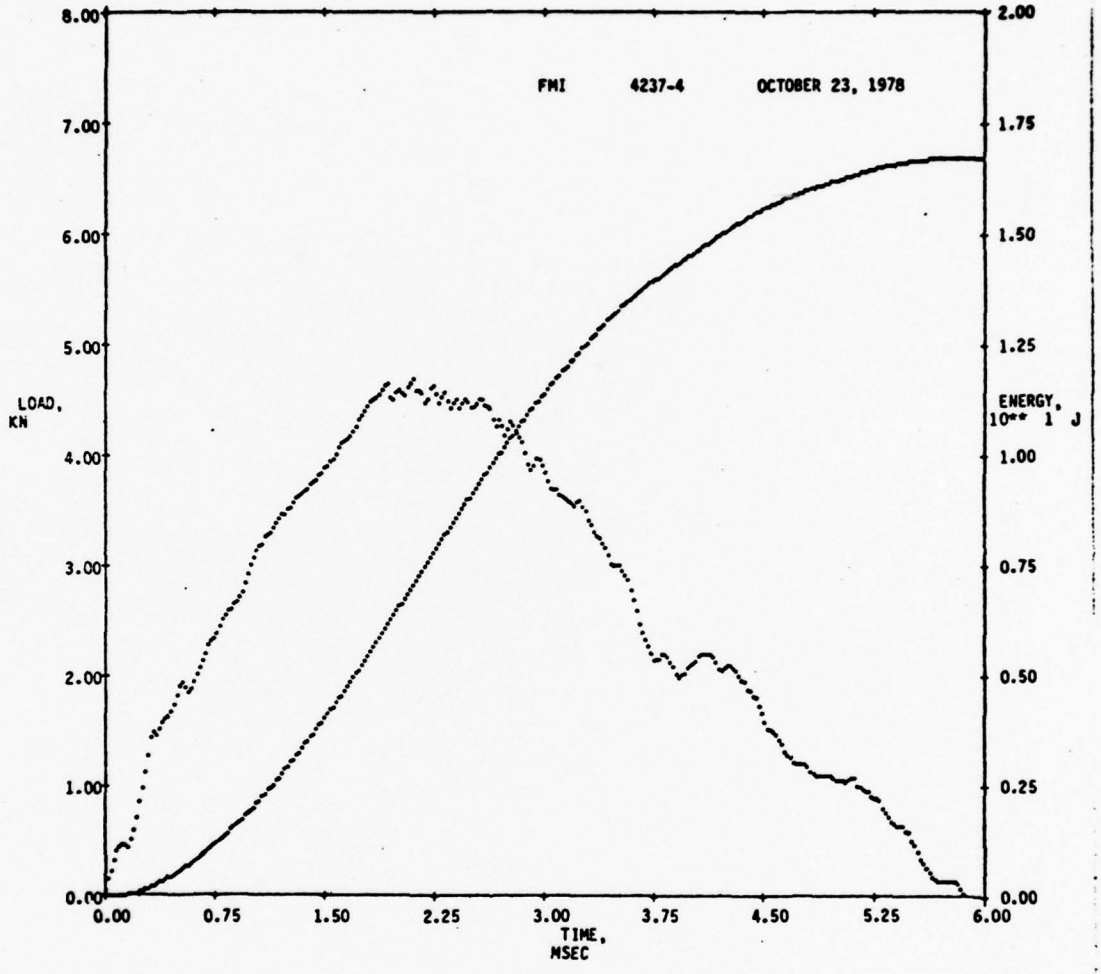
FMI 4237-4 OCTOBER 23, 1978
LOAD, KN
ENERGY, 10** 1 J
TIME, MSEC
8.00
7.00
6.00
5.00
4.00
3.00
2.00
1.00
0.00
2.00
1.75
1.50
1.25
1.00
0.75
0.50
0.25
0.00
0.00
0.75
1.50
2.25
3.00
3.75
4.50
5.25
6.00

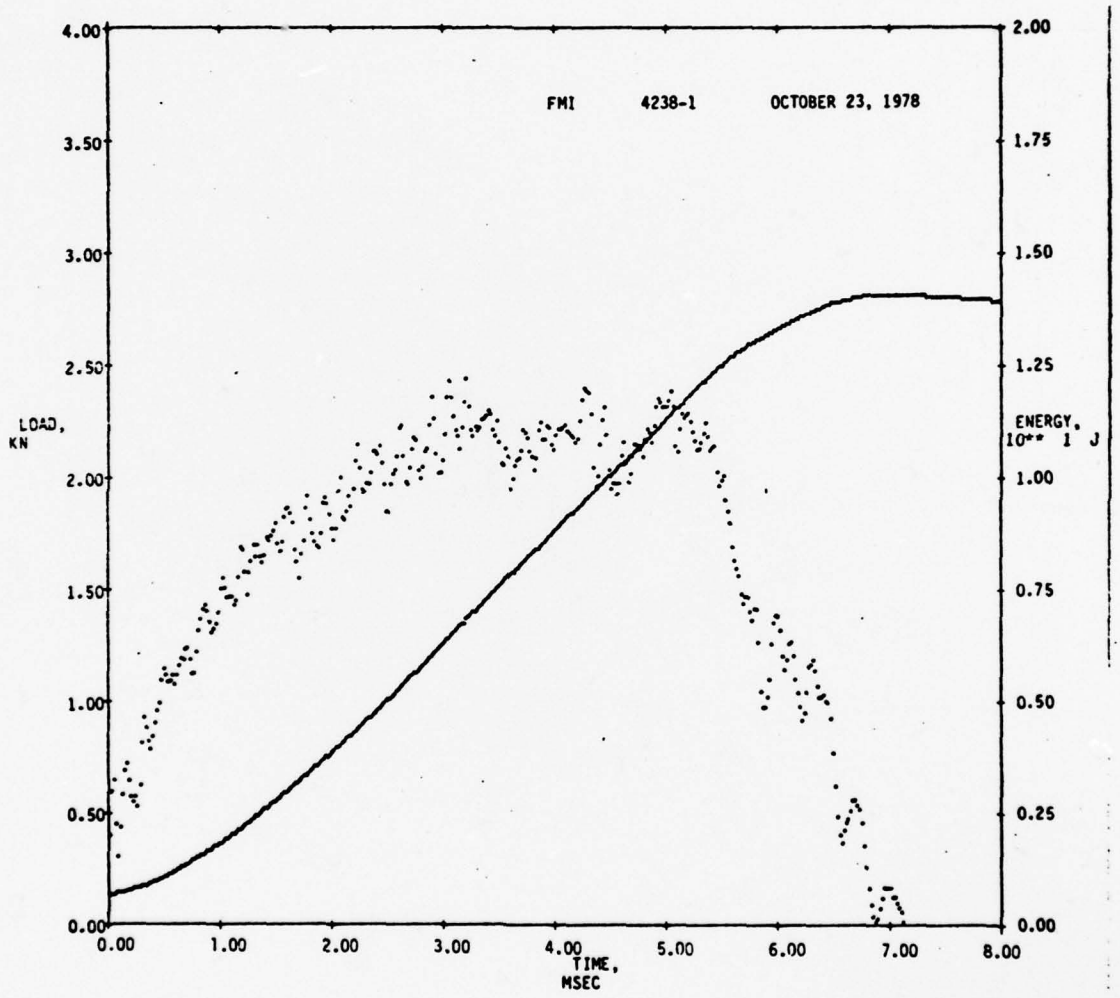
FMI 4238-1 OCTOBER 23, 1978
LOAD, KN
ENERGY, 10** 1 J
TIME, MSEC
4.00
3.50
3.00
2.50
2.00
1.50
1.00
0.50
0.00
2.00
1.75
1.50
1.25
1.00
0.75
0.50
0.25
0.00
0.00
1.00
2.00
3.00
4.00
5.00
6.00
7.00
8.00

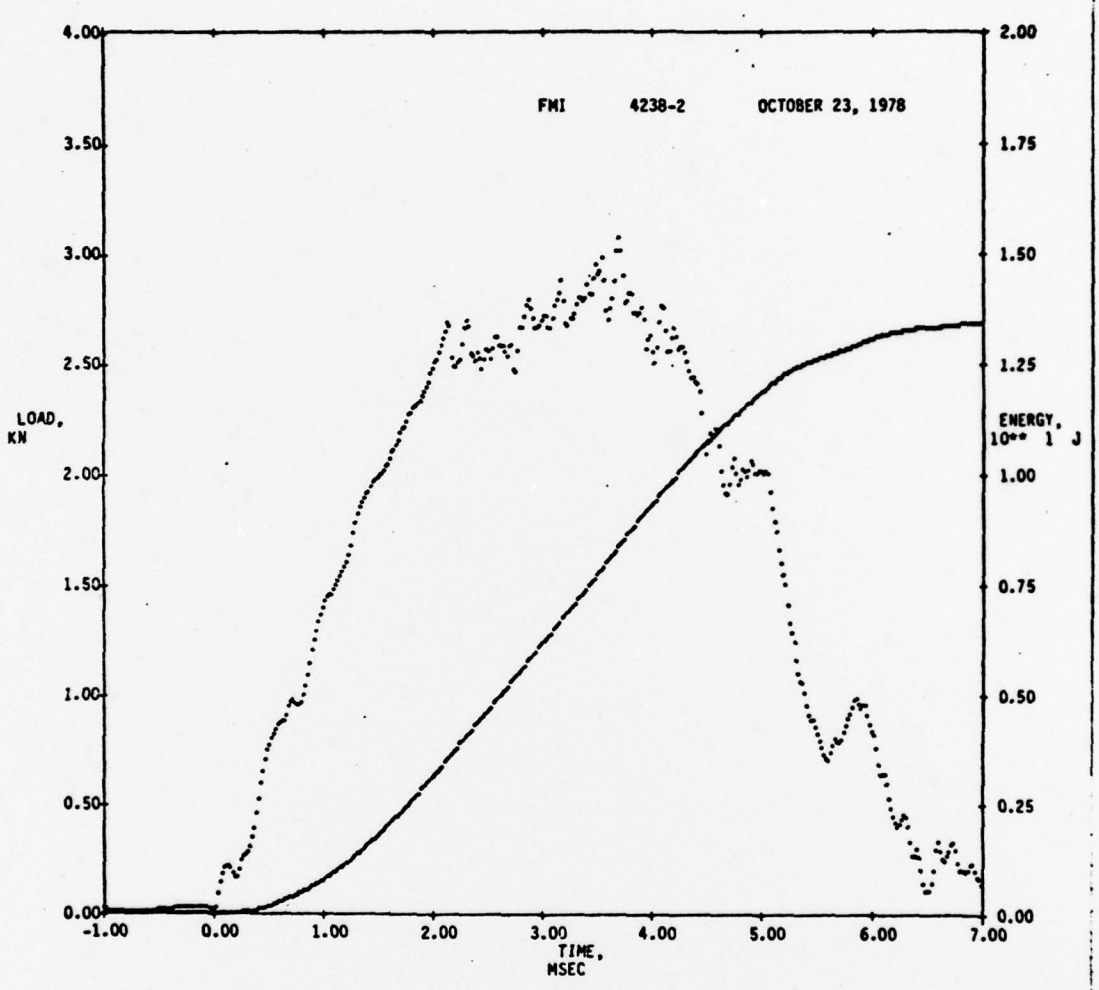
FMI 4238-2 OCTOBER 23, 1978
LOAD, KN
ENERGY, 10** 1 J
TIME, MSEC
4.00
3.50
3.00
2.50
2.00
1.50
1.00
0.50
0.00
2.00
1.75
1.50
1.25
1.00
0.75
0.50
0.25
0.00
-1.00
0.00
1.00
2.00
3.00
4.00
5.00
6.00
7.00

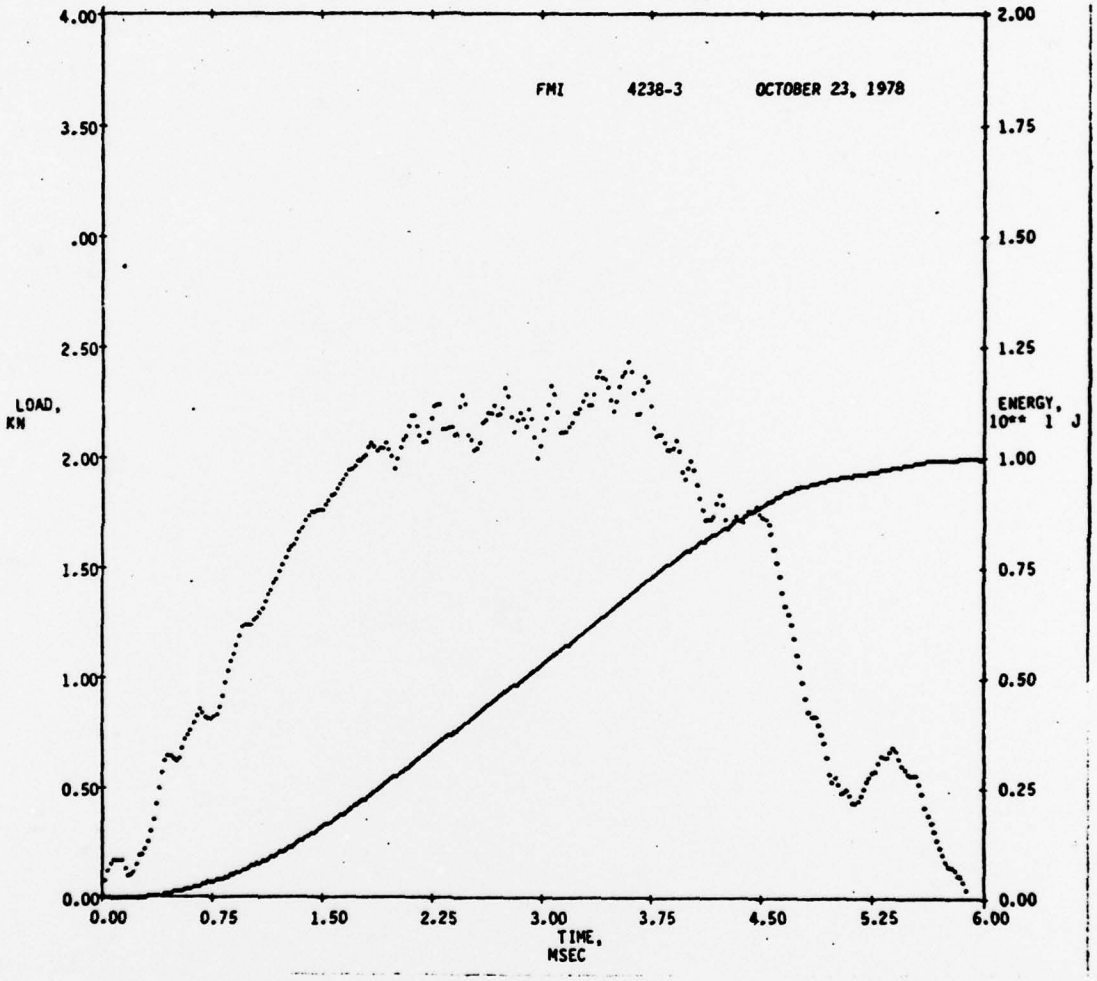
FMI 4238-3 OCTOBER 23, 1978
LOAD, KN
ENERGY, 10** 1 J
TIME, MSEC
4.00
3.50
.00
2.50
2.00
1.50
1.00
0.50
0.00
2.00
1.75
1.50
1.25
1.00
0.75
0.50
0.25
0.00
0.00
0.75
1.50
2.25
3.00
3.75
4.50
5.25
6.00

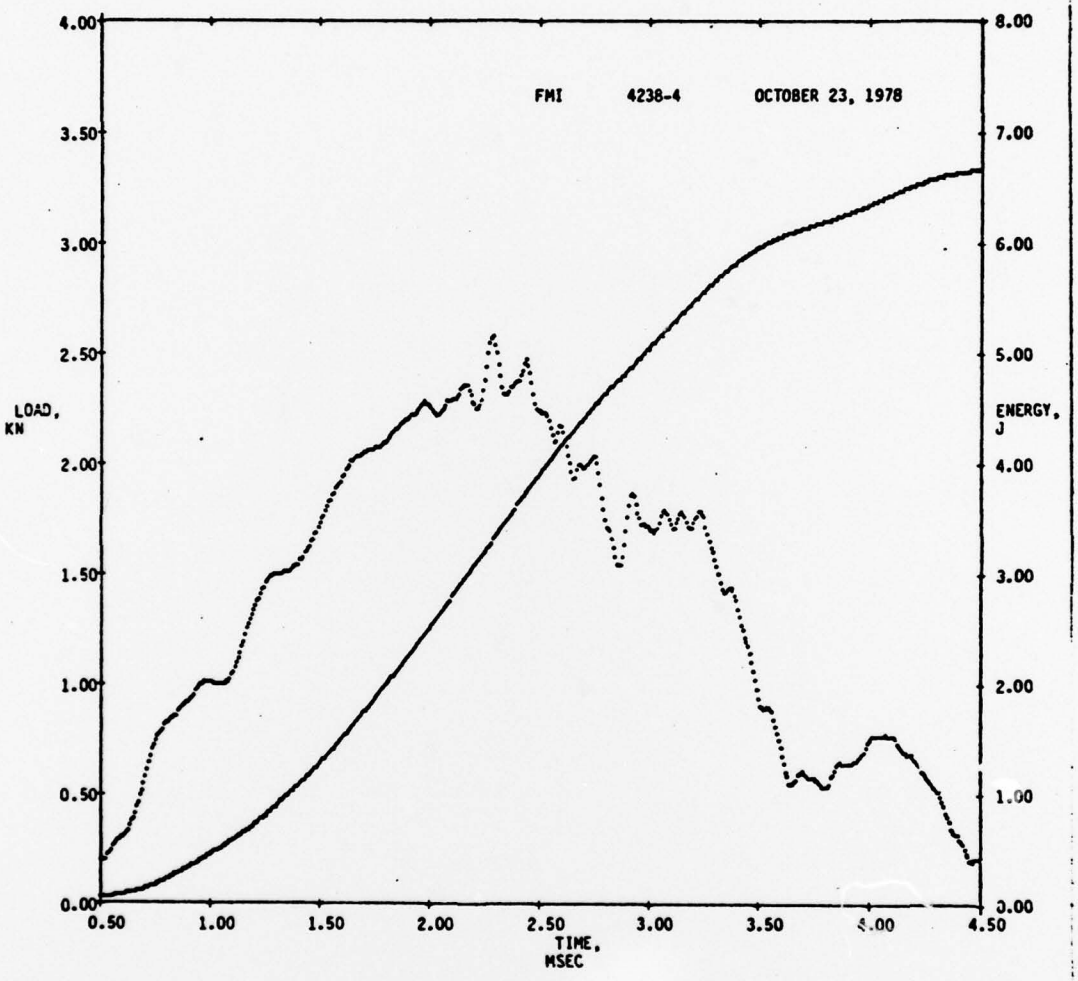
FMI 4238-4 OCTOBER 23, 1978
LOAD, KN
ENERGY, J
TIME, MSEC
4.00
3.50
3.00
2.50
2.00
1.50
1.00
0.50
0.00
8.00
7.00
6.00
5.00
4.00
3.00
2.00
1.00
0.00
0.50
1.00
1.50
2.00
2.50
3.00
3.50
4.00
4.50

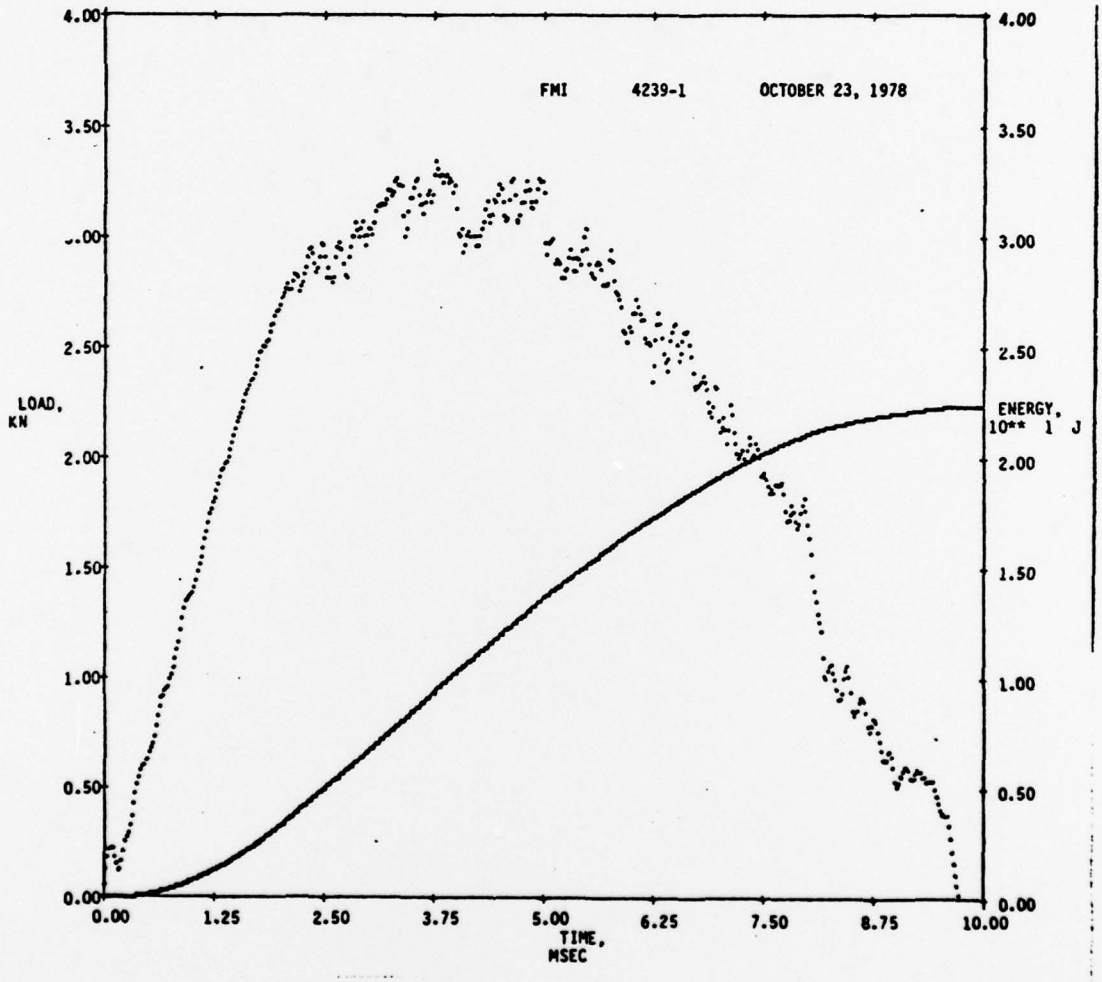
FMI 4239-1 OCTOBER 23, 1978
LOAD, KN
ENERGY, 10** 1 J
TIME, MSEC
4.00
3.50
3.00
2.50
2.00
1.50
1.00
0.50
0.00
0.00
1.25
2.50
3.75
5.00
6.25
7.50
8.75
10.00

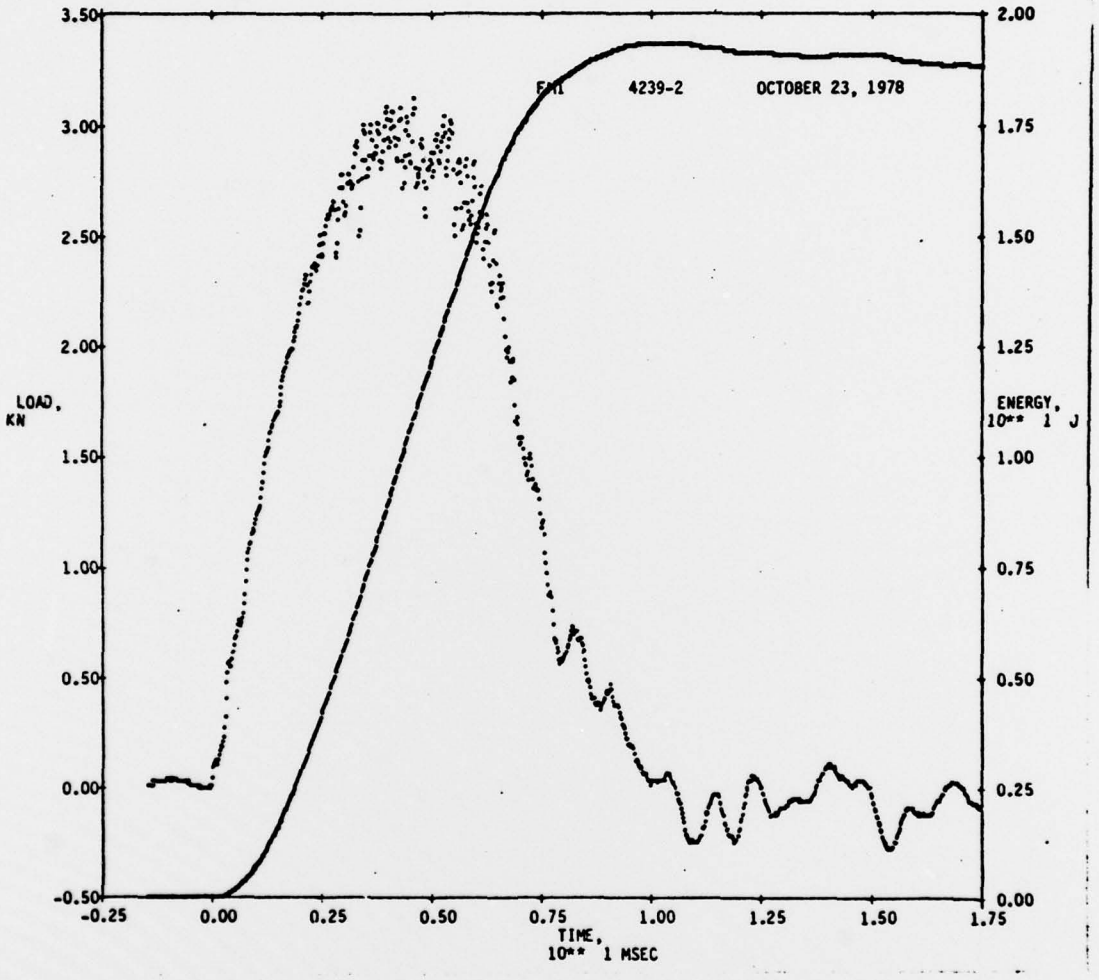
FMI 4239-2 OCTOBER 23, 1978
LOAD, KN
ENERGY, 10** 1 J
TIME, 10** 1 MSEC
3.50
3.00
2.50
2.00
1.50
1.00
0.50
0.00
-0.50
2.00
1.75
1.50
1.25
1.00
0.75
0.50
0.25
0.00
-0.25
0.00
0.25
0.50
0.75
1.00
1.25
1.50
1.75

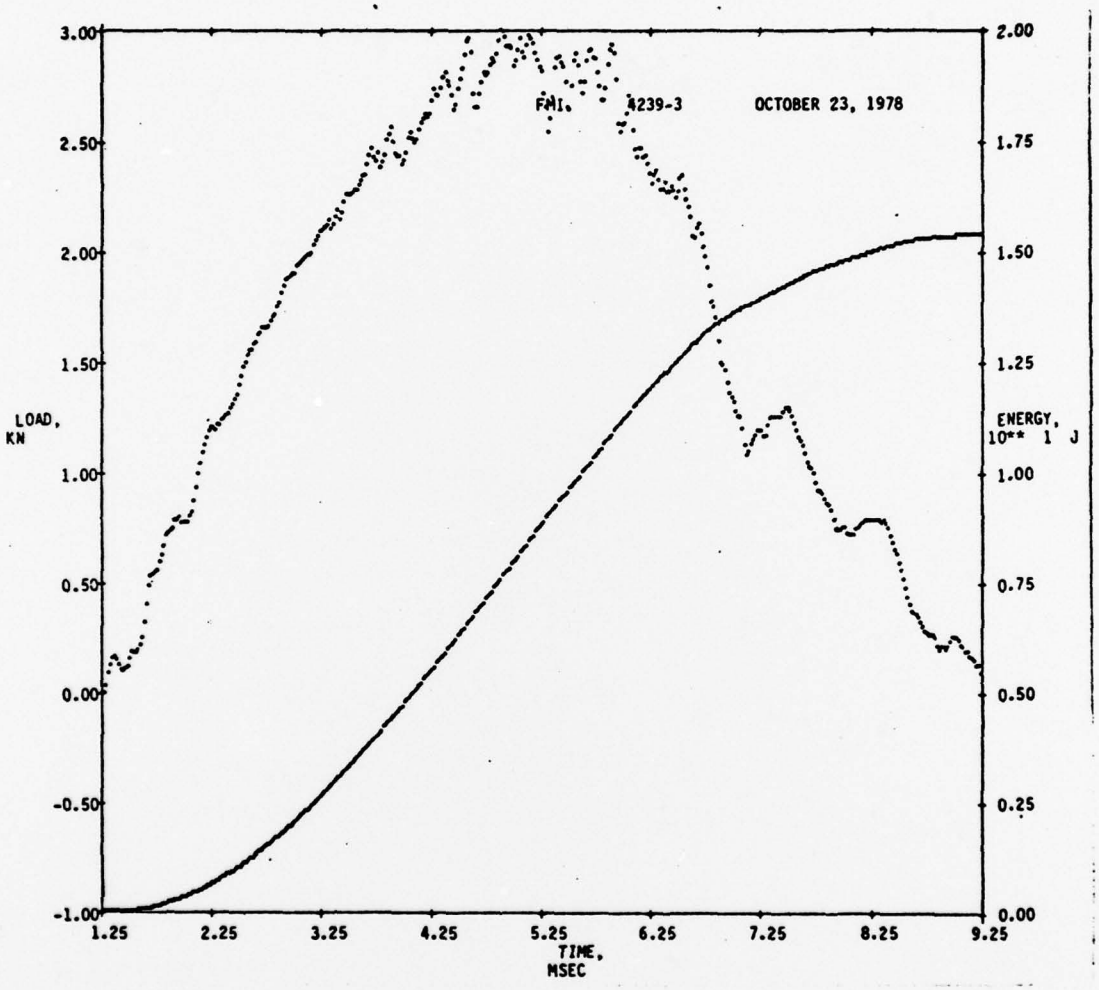
FMI. 4239-3
OCTOBER 23, 1978
LOAD, KN
ENERGY, 10** 1 J
TIME, MSEC
3.00
2.50
2.00
1.50
1.00
0.50
0.00
-0.50
-1.00
2.00
1.75
1.50
1.25
1.00
0.75
0.50
0.25
0.00
1.25
2.25
3.25
4.25
5.25
6.25
7.25
8.25
9.25

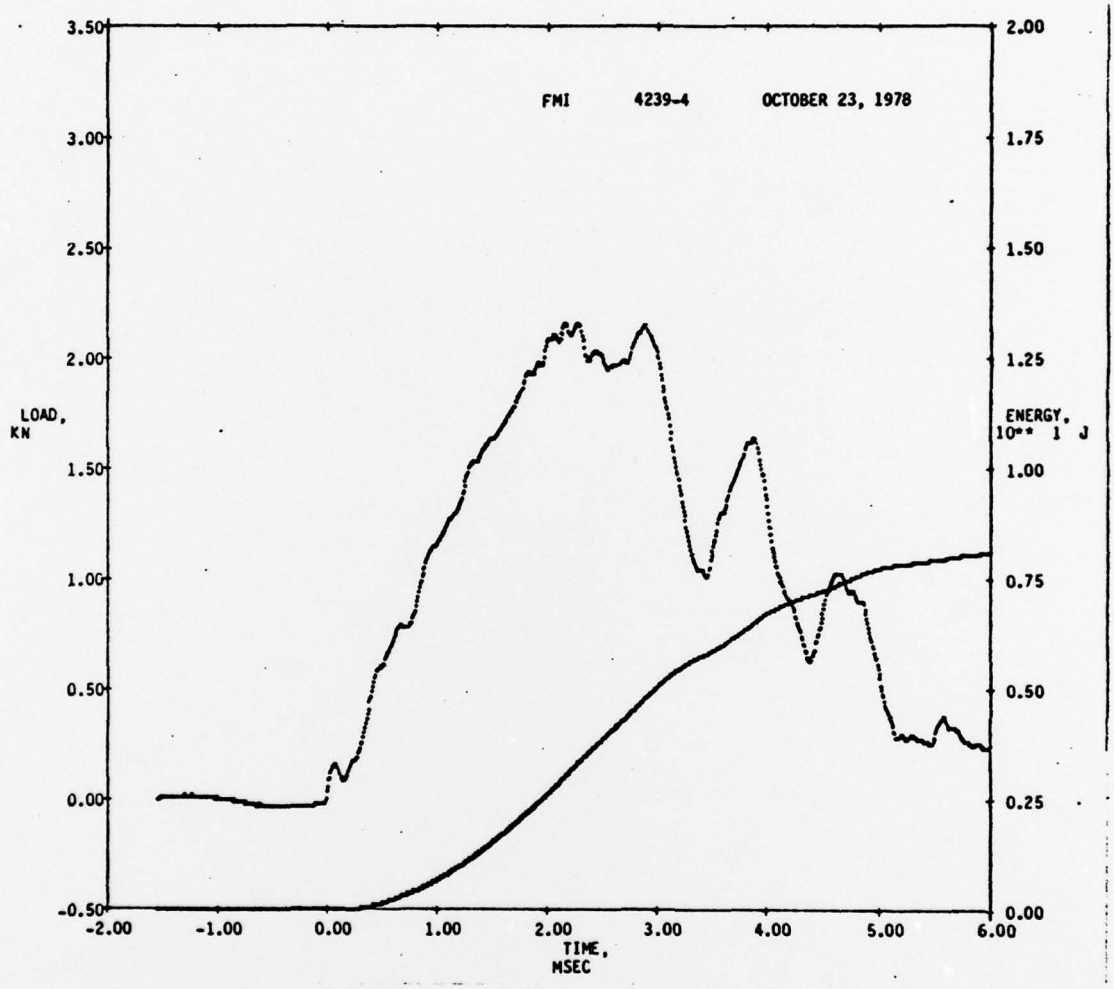
FMI 4239-4 OCTOBER 23, 1978
LOAD, KN
ENERGY, 10** 1 J
TIME, MSEC
3.50
3.00
2.50
2.00
1.50
1.00
0.50
0.00
-0.50
2.00
1.75
1.50
1.25
1.00
0.75
0.50
0.25
0.00
-2.00
-1.00
0.00
1.00
2.00
3.00
4.00
5.00
6.00

Quantity	Destination
	Department of the Navy Naval Air Systems Command Washington, D. C. 20361
3 copies	Attn: AIR-52032D
6 copies	Attn: AIR-954
	Office of Naval Research Washington, D. C. 20350
1 copy	Attn: Code 472
	Naval Research Laboratory Washington, D. C. 20350
1 copy	Attn: Code 6306
1 copy	Attn: Code 6120
1 copy	Attn: Code 8433
	Naval Surface Weapons Center White Oak, Maryland 20910
1 copy	Attn: Code 234
	Air Force Materials Laboratory Wright-Patterson Air Force Base, Ohio 45433
1 copy	Attn: MBC 1
1 copy	Attn: LN 1
1 copy	Attn: LT 1
1 copy	Attn: LAM 1

Quantity	Destination
1 copy	Air Force Flight Dynamics Laboratory Wright-Patterson Air Force Base, Ohio 45433 Attn: FBC
1 copy	Defense Ceramic Information Center Battelle Memorial Institute 505 King Avenue Columbus, Ohio 43201
1 copy	Illinois Institute of Technology Research Institute 10 West 35th Street Chicago, Illinois 60616 Attn: Dr. K. Hofer
1 copy	Brunswick Corporation Technical Products Division 325 Brunswick Lane Marion, Virginia 24354
2 copies	Director Plastics Technical Evaluation Center Picatinny Arsenal Dover, New Jersey 07801
1 copy	Hercules Incorporated Magna, Utah 84044 Attn: Mr. E. G. Crossland
1 copy	Westinghouse Electric Corp Westinghouse Research Labs Pittsburgh, PA 15235
1 copy	Northrop Corporation 3901 W. Broadway Hawthorne, California 90250 Attn: Mr. J. Damman
1 copy	Naval Air Propulsion Test Center Trenton, New Jersey 08628 Attn: Mr. J. Glatz
1 copy	Office of Naval Research Branch Office, London Box 39 FPO New York 09510

Quantity	Destination
1 copy	Commander Naval Weapons Center China Lake, California 92555
1 copy	Celanese Research Company Box 1000 Summit, New Jersey 07901 Attn: Mr. R. J. Leal
1 copy	Naval Ship Engineering Center Navy Department Washington, D. C. 20360 Attn: Code 6101E
1 copy	Naval Sea Systems Command Navy Department Washington, D. C. 20360 Attn: SEA-035
1 copy	NASA Headquarters 600 Independence Avenue, S.W. Washington, D. C. 20546 Attn: RV-2 (Mr. N. Mayer)
1 copy	Office of Naval Research, Boston 495 Summer Street Boston, Massachusetts 02210 Attn: Dr. L. H. Peebles
	Commanding Officer Naval Air Development Center Warminster, Pennsylvania 18974
1 copy	Attn: Aero Materials Laboratory
1 copy	Attn: Structures Division
1 copy	Attn: Radomes Section
1 copy	Naval Ship Research & Development Center Washington, D. C. 20360 Attn: Mr. M. Krenzke, Code 727
1 copy	NASA Lewis Research Center 21000 Brookpark Road Cleveland, Ohio 44135
1 copy	NASA Langley Research Center Hampton, Virginia
1 copy	United Aircraft Corporation United Aircraft Research Laboratories E. Hartford, Connecticut 06108

Quantity	Destination
1 copy	United Aircraft Corporation Pratt & Whitney Aircraft Division East Hartford, Connecticut 06108
1 copy	United Aircraft Corporation Hamilton-Standard Division Windsor Locks, Connecticut Attn: Mr. T. Zajac
1 copy	United Aircraft Corporation Sikorsky Aircraft Division Stratford, Connecticut 06602
1 copy	United Aircraft Corporation Pratt & Whitney Aircraft Division Florida R&D Center West Palm Beach, FL 33402 Attn: Dr. J. Winfree
1 copy	Philco-Ford Corporation Aeronutronic Division Ford Road Newport Beach, California 92663
1 copy	The Rand Corporation 1700 Main Street Santa Monica, California 90406
1 copy	HITCO 1600 W. 135th Street Gardena, California 90406
1 copy	AVCO Corporation Applied Technology Division Lowell, Massachusetts 01851
1 copy	Department of the Army Army Materials & Mechanics Research Center Watertown, Massachusetts 02172
1 copy	North American Aviation Columbus Division 4300 E. Fifth Avenue Columbus, Ohio 43216
1 copy	General Electric Company Valley Forge Space Center Philadelphia, Pennsylvania 19101

Quantity	Destination
1 copy	McDonnell-Douglas Corporation Douglas Aircraft Company 3855 Lakewood Blvd. Long Beach, California 90801 Attn: Mr. R. J. Palmer
1 copy	Monsanto Research Corporation 1515 Nicholas Road Dayton, Ohio 45407
1 copy	U. S. Army Air Mobility R&D Laboratory Fort Eustis, Virginia Attn: SAVDL-EU-SS (Mr. J. Robinson)
1 copy	Material Sciences Corporation 1777 Walton Road Blue Bell, Pennsylvania 19422
1 copy	B. F. Goodrich Aerospace & Defense Products 500 South Main Street Akron, Ohio 44318
1 copy	Great Lakes Research Corporation P. O. Box 1031 Elizabethton, Tennessee
1 copy	Whittaker Corporation Research & Development Division 3540 Aero Court San Diego, California 92123
1 copy	University of California Lawrence Livermore Laboratory P. O. Box 808 Livermore, CA 94550 Attn: Mr. T. T. Chiao
1 copy	University of Maryland College Park, MD 20742 Attn: Dr. W. J. Bailey
1 copy	Union Carbide Corporation Chemicals & Plastics One River Road Bound Brook, N.J.
1 copy	General Dynamic Corporation Convair Division - P.O. Box 1128 San Diego, CA 92138 Attn: W. G. Scheck

Quantity	Destination
1 copy	TRW Incorporated Systems Group One Space Park Bldg 01, Rm 2171 Redondo Beach, CA 90278
1 copy	McDonnell-Douglas Corporation McDonnell Aircraft Company P. O. Box 516 St. Louis, MO 63166 Attn: Mr. Ray J. Jurgens
1 copy	Rockwell International Corporation 12214 Lakewood Blvd. Downey, CA 90241 Attn: C. R. Rousseau Mail Stop AB70
1 copy	General Dynamics Convair Aerospace Division Ft. Worth Operation; P. O. Box 748 Ft. Worth,,TX 76101 Attn: Manufacturing Engineering Technical Library Mail Zone 6212
1 copy	AIRESEARCH Manufacturing Company Dept. 93-39M 402 S. 36th St. Phoenix, AZ 85034 Attn: Chief Materials Engineering Dept. Dept 93-39M
1 copy	E. I. Dupont de Nemours & Co. Textile Fibers Dept Wilmington, Delaware Attn: Carl Zweben
1 copy	Lockheed California Company Dept. 74-54, Bldg. 63 Box 551 Burbank, CA 91503 Attn: J. H. Wooley
1 copy	TRW Incorporated 23555 Euclid Avenue Cleveland, OH 44117
1 copy	Rockwell International Corporation Los Angeles Division International Airport Los Angeles, CA 90009 Attn: Mr. E. Jaffe; Mail Stop AB-61

SCHEDULE

Quantity	Destination
1 copy	The Boeing Company Aerospace Division P. O. Box 3707 Seattle, WA 98124
1 copy	Vought Corporation Systems Division P. O. Box 5907 Dallas, TX 75222 Attn: A. E. Hohman
1 copy	Vought Corporation Advanced Technology Center P. O. Box 6144 Dallas, TX 75222
1 copy	Lockheed Missiles & Space Co. Sunnyvale, CA 94088 Attn: H. F. Armstrong, Dept. 62-60
1 copy	Standard Research Institute 383 Ravenswood Ave - Bldg 102B Marlo Park, CA 94025 Attn: M. Maxomovich
1 copy	Grumman Aerospace Corporation Bethpage, Long Island, New York 11714 Attn: G. Luben, Plant #12
1 copy	David W. Taylor Naval Ship R&D Center Annapolis, MD 21402 Attn: M. Silvergleit, Code 2823